U.PORTO
FEUP FACULDADE DE ENGENHARIA
UNIVERSIDADE DO PORTO

U.PORTO
INSTITUTO DE CIÊNCIAS BIOMÉDICAS ABEL SALAZAR
UNIVERSIDADE DO PORTO

Application of lipid nanoparticles for the delivery of methotrexate for dermal treatment of psoriasis

Maria Filipa Sanches Pinto

Master Thesis

developed in the course of Dissertation

Supervisor: Maria de La Salette de Freitas Fernandes Hipólito Reis Dias Rodrigues

Co-Supervisor: Sofia Antunes Costa Lima

Faculdade de Farmácia da Universidade do Porto

Integrated Master in Bioengineering – Molecular Biotechnology

2013/2014

Porto, July 2014

Abstract

Psoriasis is a chronic inflammatory skin disease that affects 1% to 2-3% of the world population. Several comorbidities on top of considerable social and financial effects on health-care systems and on society in general are associated with this disease, as well as clinical complications that arise from it. While the specific trigger for the development of psoriasis is still unknown, a combination of genetic, immunologic and environmental factors is thought to be in the heart of the pathogenesis of this illness. Even though psoriasis remains an incurable disease, progress regarding the understanding of the genetics and pathophysiology underlying this illness has made it possible for the development of management and treatment strategies at a remarkable rate, for the past 20 to 30 years. Thus, current and emerging treatments include topical and systemic therapies, as well as phototherapy. In the scope of future treatments, the application of nanomedicine through the use of nanoparticles holds the key to the future of psoriasis management and treatment, as it will prospectively allow the enhancement of current and emerging therapies, as well as favour the creation of newer ones.

Methotrexate (MTX) is a folate antagonist of high importance in the treatment of multiple pathologies; in the context of dermatology, it constitutes the current gold standard for the treatment of severe psoriasis. Even though its efficacy has been documented, systemic administration of this drug is plagued by a multitude of side-effects, which potentially limit the extent to which it can be used. Thus, this work documents the creation of a pharmaceutical formulation that not only aims to circumvent this hurdle but also enhance treatment of psoriasis, focusing on patients with mild-to-moderate cases through a topical route of administration (since it is associated with plenty of advantages such as increased patient compliance, avoidance of systemic toxicity and first-pass metabolism, minimization of pain and the possibility of using smaller amounts of drugs). The use of nanoscaled drug-delivery systems was explored to this intent, considering their prominence in the present and future treatment of psoriasis, particularly by the use of Nanostructured Lipid Carriers (NLCs). These lipid nanoparticles are colloidal lipid nanocarriers obtained by mixing solid and lipid liquids together with emulsifiers (such as surfactants). They present benefits in the context of topical administration, such as controlled occlusion and skin hydration resulting in increased permeability, enhancement in bioavailability, physical stability and potential modulation of drug release.

Two NLCs formulations (differing in the type of surfactant in their composition) were obtained as a result of an optimization process where several parameters were tested, namely type and ratios of solid/liquid lipids and surfactant, drug ratios, as well as parameters associated with the methodology of NLCs production. The excipients providing the best compromise between the characterization parameters of the NLCs were found to be Witespol S51 as the solid lipid, oleic acid as the liquid lipid (also regarding its value in topical formulations) and polysorbate 60

and polysorbate 80 as the chosen surfactants for each obtained NLCs formulation (with a solid to lipid liquid to surfactant ratio of 7:3:2, together with 0.5% of MTX of the total mass of excipient used). Mean particle size ranged from 290 to 300 nm with PDI values lower than 0.2 (thus indicating the presence of fairly monomodal size distributions) and absolute zeta potential values higher than 30 mV (indicative of good physical stability during storage), accompanied by encapsulation efficiency levels of over 60%. Stability overtime was observed for these formulations when stored at room temperature, but not at 4ºC for the formulation containing polysorbate 60 as the surfactant. Cryo-Scanning Electron Microscopy analysis revealed an almost spherical shape and smooth surfaces for both types of formulation, with or without encapsulated drug.

MTX encapsulation was confirmed by application of Fourier Transform Infrared (FTIR) spectroscopy, by identification of an absorbance peak at approximately 1640 cm^{-1} (corresponding to the vibration of –COOH groups present in the MTX molecular structure) in the infrared spectra of MTX-loaded NLCs formulations, in comparison to the observed for drug-free NLCs and free MTX.

Three different methods were tested for the separation of unincorporated drug from the obtained NLCs formulations, namely gel filtration (by Sephadex), centrifugation through filter units and dialysis. Ultimately, dialysis of 1 mL of formulation in a receptor medium comprised of PBS pH 7.4 at room temperature during 15 minutes proved to offer the best separation between the NLCs and unincorporated drug, offering the advantage of resuspending particles in this buffer and thus making them adequate for subsequent studies.

In vitro release profiles obtained (in a simulated physiological environment at 37ºC and pH 7.4) showed a biphasic drug release profile for both types of NLCs formulation. This pattern was characterized by the quick release (burst release) of 70-80% of the incorporated drug in the first 3-4 hours, with subsequent gradual and prolonged release of the remaining drug for a period of time up to 24h. While it wasn't possible to obtain a more slow and gradual drug release profile, this release pattern still proved to be of interest in the scope of topical application (due to the potential removal of the formulation after its application to the skin of psoriasis patients caused by daily activities and physiological responses, such as sweating).

In vitro permeation assays performed for free MTX showed that this drug can permeate the skin (using pig ear skin as the model barrier, as it is similar in morphology and function to human skin), despite its low partition coefficient (indicative of low lipophilic character); nevertheless, release of this drug from the produced NLCs would most likely show an improvement in its permeation, given the beneficial properties of NLCs to that end, as well as through the use of additional penetration enhancers. Thus, further testing is needed in this context.

Cytotoxicity testing was performed using the MTT reduction assay in a human THP1 monocyte cell line, for both drug-loaded and drug-free NLCs formulations. These preliminary

results indicated that the IC_{50} values for both types of formulation will be in the range of 1.56 μg/mL to 6.25 μg/mL of incorporated MTX. Nevertheless, it was found that drug-free NLCs formulations are potentially characterized by high cytotoxicity (higher for the formulation containing polysorbate 80 as the surfactant). Additional testing is needed to support these results and confirm their reproducibility.

Overall, the evaluation of the proposed NLCs formulations shows that they possess good properties that make them pertinent vehicles for the topical administration of MTX in the context of psoriasis. Further improvement of these formulations would be possible through the execution of additional works including the optimization of their properties, their inclusion in adequate pharmaceutical formulations, as well as through potential functionalization with pertinent molecular components, such as the monoclonal antibodies used in the context of biological therapies of psoriasis (thus allowing for a more targeted action and the acquisition of a combined therapy encompassing the advantages of both non-biologic and biologic therapies in the context of psoriasis).

Acknowledgements

Ever since I started learning about drug-carrying nanosystems I was fascinated by them and their potential uses, be it in the present day or in the (near) future. Thereby, I naturally gravitated towards this type of work when I had to choose what I wanted to do for my dissertation. Consequently, this project allowed me to further extend my knowledge and interest about this subject, and all the work produced could have not been possible without the crucial support provided by importance people I would like to thank in this section.

I would like to thank my supervisor Prof. Dr. Salette Reis, for providing me the opportunity to work on this project, as well as for valuable advice, support and encouragement in scientific and non-scientific matters throughout the duration of this project.

I would also like to express my sincere gratitude to my co-supervisor, Dr. Sofia Lima, for her continued help and guidance throughout these months along with valuable advice and support in scientific and non-scientific matters, as well as motivation. This work wouldn't have been possible without her help.

I would also like to thank everyone in the Laboratório de Química Aplicada at Faculdade de Farmácia da Universidade do Porto for welcoming me in a very warm way into their "family", and all their support throughout these months. I really enjoyed the hard-working yet healthy atmosphere of the work environment and I will miss everyone dearly.

My family and friends (as well as my kitty!) also have my heartfelt thanks, for unconditionally supporting me through everything and never doubting me for a second.

Table of Contents

Table of Figures

Figures

Tables

Table of Abbreviations

AAD	American Academy of Dermatology
AFM	Atomic Force Microscopy
AICAR	Aminoimidazole-carboxamide-ribonucleoside
APC	Antigen-Presenting Cell
Au	Gold
BSA	Body Surface Area
CCHCR1	Coiled-Coil α-Helical Rod Protein
CD	Cluster of Differentiation
CDSN	Corneodesmosin
DC	Dendritic Cell
DHFR	Dihydrofolate Reductase
DLS	Dynamic Light Scattering
DNA	Deoxyribonucleic Acid
DSC	Differential Scanning Calorimetry
EAD	European Academy of Dermatology
ELS	Electrophoretic Light Scattering
FACS	Fluorescence-Activated Cell Sorting
FDA	Food and Drug Administration
FTIR	Fourier Transform Infrared
GAR	Glycinamide Ribonucleotide
GM-CSF	Granulocyte-Macrophage Colony-Stimulating Factor
GRAS	Generally Regarded As Safe
GWAS	Genomewide Linkage and Association Studies
h	Hours
HLA	Human Leukocyte Antigen
HBD	human β-defensin
HPLC	High-Performance Liquid Chromatography
iDC	inflammatory Dendritic Cell
IFN-α	Interferon-α
IFN-γ	Interferon-γ
Ig	Immunoglobulin
IL	Interleukin
iNOS	inducible Nitric Oxide Synthase
JAK-STAT	Janus Kinase-Signal Transducer and Activators of Transcription
LFA-3	Leukocyte Function Antigen-3

mAb	Monoclonal Antibody
MACE	Major Adverse Cardiovascular Events
MAPK	Mitogen-Activated Protein Kinase
mDC	myeloid Dendritic Cell
MHC	Major Histocompatibility Complex
min	Minutes
MTT	3-[4,5-dimethylthiazol-2-yl]-2,5-diphenyl tetrazolium bromide
MTX	Methotrexate
MWCO	Molecular Weight Cut-Off
NF-κB	Nuclear Factor Kappa B
NK	Natural Killer
NLCs	Nanostructured Lipid Carriers
NO	Nitric Oxide
NOD	Nucleotide-binding Oligomerization Domain
PASI	Psoriasis Area and Severity Index
Pd	Palladium
pDC	plasmocytoid Dendritic Cell
PDE	Phosphodiesterase
PDI	Polydispersity Index
PKC	Protein Kinase C
PMA	Phorbol 12-myristate 13-acetate
PMNs	Polymorphonuclear cells
PSORS	Psoriasis Susceptibility
PUVA	UVA plus psoralen
RNA	Ribonucleic Acid
SEM	Scanning Electron Microscopy
SLNs	Solid Lipid Nanoparticles
SNP	Single Nucleotide Polymorphism
TGF-β	Transforming Growth Factor-β
TLR	Toll-like Receptor
TNF-α	Tumour Necrosis Factor-alpha
UVA	Ultraviolet A
UVB	Ultraviolet B
UV-VIS	Ultraviolet-Visible
VEGF	Vascular Endothelial Growth Factor

1. Objectives

The goal of the thesis hereby presented consists in the development of lipid nanoparticles (particularly Nanostructured Lipid Carriers, NLCs) for the encapsulation of methotrexate (MTX), to be delivered by a dermal route (in detriment to its usual systemic administration). Consequently, an overall increase in therapeutic efficacy and decrease in the adverse side effects associated with the systemic administration of MTX is intended. Thereby, several objectives can be outlined for the present work.

With this work, several formulations of NLCs will be tested using pertinent excipient (solid and liquid lipids and surfactants) and drug combinations, as well as production conditions, in order to design a NLCs formulation with the best compromise between its characteristics, considering the intended topical application. Specifically, NLCs formulations will be characterized in terms of mean particle size, polydispersity index (PDI) by Dynamic Light Scattering, and zeta potential by Electrophoretic Light Scattering, morphology by Scanning Electron Microscopy, and encapsulation efficiency using UV-VIS spectroscopy. This characterization will also be done overtime for a period of 4 weeks in order to evaluate physical stability during storage. Fourier Transform Infrared spectroscopy will also be applied to assess the presence of encapsulated drug in the NLCs. The *in vitro* release profile of MTX to be delivered from the NLCs will be evaluated using a dialysis bag diffusion technique, together with its *in vitro* permeation profile using a Franz Cell Assembly with pig ear skin as the model barrier, considering that a dermal application is intended for the developed NLCs formulations. *In vitro* cytotoxicity will be investigated by the MTT reduction assay.

Overall, the present work has the purpose of developing NLCs formulations for a novel dermal application of MTX in the scope of the treatment of psoriasis. With the successive improvement of their characteristics and their detailed study, this work intends to present NLCs formulations that would be pertinent and efficacious for the dermal treatment of psoriasis. This would allow for the innovative dermal use of MTX, a drug that is systemically administrated in the context of psoriasis, providing an increased therapeutic efficacy and bioavailability, as well as safety in its use, through a decrease in the side effects associated with its usual route of administration and a decrease in the administrated dose; prolonged and gradual release of the MTX into the skin would also be possible. The success associated with the use of MTX by dermal application would also be mirrored in increased patient compliance, as topical administration of therapeutic substances constitutes a much less invasive and more comfortable and convenient route of administration.

2. Introduction

Psoriasis is a chronic inflammatory skin disease that affects 1% to 2-3% of the world population, with equal gender distribution [1, 2]. Even so, psoriasis is generally more common in colder northern geographic areas, in comparison to the tropics. Indeed, its prevalence is highest amongst northern Europeans and it is almost completely inexistent in the aboriginal populations of South America [3]. More specifically, in Europe, psoriasis has a prevalence of 0.6% to 6.5% [4]. This disease can emerge at any time of life, but usually peaks between the ages of 30 to 39 and 60 to 69 [5]. Incidence rates vary from 50 to 140 new cases per 100,000 people per year [1]. It is associated with high levels of distress and morbidity, as well as a general decrease in the quality of life of the patient, even though it is not usually life-threatening. Nonetheless, severe psoriasis increases the risk of mortality, in comparison to the general population [3].

Psoriasis is also associated with inflammation in other organ systems such as the musculoskeletal and gastrointestinal systems, the eye [3] and the joints. In this last case, the resultant condition is similar to rheumatoid arthritis (even though it is usually seronegative for rheumatoid factor) and therefore usually referred to as psoriatic arthritis [2]. This additional burden elevates the morbidity of patients who suffer from cutaneous psoriasis, besides increasing their mortality risk [3].

From a clinical perspective, psoriasis shows a wide spectrum of manifestations. These range from epidermal (scaly) and vascular (thickened, erythematous) involvements of the skin, to a malignant form known as generalized erythrodermia. The most common form of cutaneous psoriasis (psoriasis vulgaris, also referred to as plaque-type psoriasis, Figure 1a,b) typically presents itself as well-defined raised red symmetrical patches called plaques, with adherent thick silvery scales (parakeratosis), which may reveal pinpoint bleeding (Auspitz sign), if removed [6]. These lesions frequently occur on the elbows, knees, scalp and buttocks [7]. Psoriasis plaques cause pain and pruritus to the patient, leading to discomfort and persistent insomnia [2]. Plaque-type psoriasis covers about 80% of the cases of this disease; however, cutaneous psoriasis can also manifest itself in other forms. These include guttate psoriasis, psoriasis of the palms and soles, pustular psoriasis (Figure 1c), flexural psoriasis, erythrodermic psoriasis and infantile psoriasis [6].

Figure 1. (a,b) Examples of cases of plaque-type psoriasis (more common form of psoriasis, consisting in 80% of the cases) affecting the skin in (a) the ear and (b) the scalp; (c) Example of a case of pustular psoriasis (a less common form of psoriasis) [5, 6].

Taking into account the fact that psoriasis can substantially alter and disfigure the aspect of skin and other portions of the body (such as the nails, as reviewed in Oram & Akkaya [8]), the quality of life of the patient lowers extensively [9]. Indeed, psoriasis patients are often embarrassed by their appearance [3] which, in turn, leads to the disruption of their social life and interactions, psychological stress, lowered self-esteem and the impression of social ostracism [2]. Even though psoriasis is not contagious, patients are sometimes stigmatized [5, 6], which can manifest in the form of reduced levels of employment and income [3, 5].

Psoriasis patients are often afflicted by certain patterns of medical comorbidities, particularly in severe cases with a long history of the disease. Such comorbidities can be, in part, responsible for a significant reduction in the life expectancy of these patients [2, 10]. The fact that there is a strong association between psoriasis and numerous components present in metabolic syndromes can explain these comorbidities [2]. Other than psoriatic arthritis, comorbidities such as cardiovascular implications [11], as well as higher rates of obesity, type 2 diabetes mellitus, depression, lymphoma and inflammatory bowel disease (such as Crohn's disease) have been documented in the published literature concerning the subject [2, 12]. Drug-related side effects can also be a cause of the development of the referred comorbidities [7].

Overall, psoriasis and clinical complications that arise from it have a major social and financial impact on health-care systems and on society in general [3, 9], which makes it an important subject of study on many levels, be it from a scientific or social point of view.

The literature revision presented on this section will focus on the state-of-the-art regarding psoriasis and its treatment. Special attention will be given to the pathophysiology of this disease and how the existing and emerging treatments exploit it in order to control its progression and symptoms. Considering the main objectives underlying the work further presented in this document, large emphasis will be given to the use of drug-carrying nanosystems, due to their multiple advantages over the more traditionally used formulations, and how they can be used in the context of psoriasis and topical administration of therapeutic substances of interest (such as MTX, which will also be approached).

2.1. Pathophysiology of Psoriasis

In the early 1970's, psoriasis was mostly thought to be a disease merely associated with dysfunctional proliferation and differentiation of epidermal keratinocytes, with no major involvement of the immune system [5, 13]. Even in the present day, the precise cause underlying the emergence of psoriasis is still unknown [14]; nevertheless, decades of work and published literature concerning this subject show that a combination of genetic, immunologic and environmental factors contribute to the pathogenesis of psoriasis (which will be detailed further) [15]. Indeed, in genetic predisposed individuals, environmental triggers promote the activation of an exaggerated and poorly controlled immuno-inflammatory response in the skin, which leads to the development of this disorder [7]. This phenomena involves abnormalities in infiltrating lymphocytes, neutrophils and lesional cytokines, in addition to epidermal keratinocytes [15].

2.1.1. Genetics of Psoriasis

The role of genetic factors in the emergence of psoriasis has been confirmed by family and twin studies [13]. Numerous population-based epidemiological studies have also confirmed the genetic basis of this disease [16]. Indeed, even though segregation analysis show no clear pattern of inheritance, first- and second-degree relatives of psoriatic patients are more likely to develop this illness, in comparison to the general population, as shown by family studies [5], in which the recurrence risk ratio was analysed. This analysis also allowed for the prediction of a multilocus model of genetic susceptibility for psoriasis. Moreover, the heritability (a measure of the proportion of variability of a trait that is due to genetic factors) for this disorder was estimated to range between 60% and 90% for the Caucasian population [4, 16]. In addition, twin studies have shown that disease concordances are two to three times more likely in monozygotic (identical) than in dizygotic (non-identical) twins [5], specifically 62% and 70% for monozygotic twins, compared to 21-23% for dizygotic twins [4].

Indeed, it is thought that environmental triggers (e.g. trauma, stress, chronic infections, low humidity, smoking, obesity and drugs such as beta-blockers, lithium and antimalarial agents [14]) activate, in polygenic predisposed individuals, an exaggerated inflammatory response in the skin, which leads to the emergence of psoriasis [5]. Further investigation concerning this genetic predisposition involved candidate-driven gene-specific tests and genomewide linkage and association studies (GWAS) [14]. Linkage studies have identified at least nine chromosomal loci linked to psoriasis, referred to as PSORS 1-9 (psoriasis susceptibility 1-9) [5]. The genome regions most strongly associated with the development of psoriasis are areas related to the immune system [14]. In this context, the PSORS1 locus can be highlighted, as it presents the strongest association to psoriasis [4], which accounts for 35-50% of the genetic predisposition of this disorder (in Caucasian populations). In fact, the PSORS1 locus is located on the major histocompatibility complex (MHC) region of the chromosome 6 (specifically 6p21) and several

genes contained in this region have been found to be associated with psoriasis, amongst which HLA-Cw6, *CCHCR1* (coiled-coil α-helical rod protein) and *CDSN* (corneodesmosin) can be highlighted [5, 7]. HLA-Cw6 encodes a class I MHC protein and is associated with early-onset chronic plaque psoriasis [5]. Meta-analysis have shown that there is a 20-fold increased risk of developing psoriasis in individuals carrying specifically the HLA-Cw*0602 allele, which is present in 10-15% of the general population [17]. *CCHCR1*, on the other hand, encodes a protein that is highly expressed in the epidermis of psoriatic lesions and regulates keratinocyte proliferation. *CDSN* encodes a late differentiation epidermal glycoprotein that is overexpressed in the granular and cornified layers of the epidermis, being involved in keratinocyte adhesion [5]. The PSORS 1-9 loci (including a documented PSORS 10 locus), and gene candidates associated with psoriasis contained within them, are summed up on Table 1.

Table 1. Psoriasis susceptibility loci as indicated by mapping through traditional linkage studies [4].

Loci	Genome Location	Gene candidates
PSORS1	6p21.3	HLA-Cw06, *CDSN, HCR, HERV-K, HCG22, PSORS1C3, POU5F1, TCF19, CCHCR1, LMP, SEEK1, SPR1*
PSORS2	17q	*RUNX1, RAPTOR, SLC9A3R1, NAT9, TBCD*
PSORS3	4q	*IRF2*
PSORS4	1q21.3	Loricrin, Filaggrin, Pglyrp, S100, LCE [17] genes within epidermal differentiation complex
PSORS5	3q21	*SLC12A8*, cystatin A, Zn finger protein 148
PSORS6	19p	*JunB*
PSORS7	1p	*PTPN22, IL23R*
PSORS8	16q	*CX3CL1, CX3R1, NOD2/CARD15*
PSORS9	4q28-32	*IL15*
PSORS10	18p11	-

However, it should be noted that, while whole-genome linkage screens of psoriasis have identified many potential susceptibility loci, their fine mapping did not reveal convincing evidence for disease susceptibility genes, with the exception of PSORS1. Many of the aforementioned linkages were, most likely, false positives. In this context, candidate-driven gene-specific tests and GWAS are more robust and fruitful tests. The latter, in particular, is a valuable systematic tool of high throughput single nucleotide polymorphism (SNP) analysis [16], useful in the investigation of the genetic predisposition to a complex disease, such as psoriasis. Indeed, numerous studies have recognized the importance of SNPs in many of the genes associated with psoriasis (as well as their pharmacogenetic implications), where it is possible to highlight, for instance, the importance of SNPs in the promoter region of the tumour necrosis factor gene (*TNFα*), in the context of psoriasis and its treatment [14]. The usage of GWAS allowed for the identification of other genes associated with psoriasis (as well as the validation of previously identified genes, such as HLA-Cw6), namely *IL23R*, contained in the PSORS7 locus (chromosome 1p), which

encodes for the Interleukin-23 (IL-23) receptor [14], and the genes encoding for IL-12B (*IL12B*), IL-23A (*IL23A*), IL-4 (*IL4*) and IL-13 (*IL13*), including others, which are involved in the major signalling pathways associated with psoriasis (documented in more detail in the next section concerning pathogenesis) [4].

2.1.2. Pathogenesis of Psoriasis

Psoriatic lesions are characterized by an assortment of histological modifications driven by a complex network of cellular and molecular events. In this context, the chief role of T cells in the pathogenesis of psoriasis started to become clear in the late 1970's, when T-cell-targeted immunosuppressants were inadvertently found to be successful in the treatment of psoriasis. Indeed, the most indicative evidence was found when T cell proliferation was blocked in different murine models, resulting in reduced development of this disease [5]. This has also been corroborated by the improvement of psoriasis in patients that underwent allogeneic bone marrow transplantation from psoriasis-free donors [17] as well as the emergence of psoriasis in patients who experienced the same type of transplantation in which the donor had this disorder [7].

In early psoriatic lesions, macrophages are present in the epidermis, followed by monocytes, lymphocytes, and granulocytes, with the formation of spongiform micro abscesses called Munro abscesses. These become more pronounced with disease activity, constituting a hallmark of psoriasis [2]. Accentuated dilation of blood vessels in the papillary dermis [18] allows for cell infiltration, leading to the formation of dense clusters of inflammatory cells composed of $CD4^+$ T cells [7] and dendritic cells (DCs) in the dermis, and $CD8^+$ T cells and neutrophils in the epidermis [18].

The inflammatory process associated with psoriasis is mediated by unknown antigens through binding and specific activation and co-stimulation of T cells by antigen-presenting cells (APCs), namely DCs and macrophages, in the epidermis and dermis, by the establishment of an immunological synapse [2]. More specifically, naïve T cells in lesional psoriatic skin can be activated by resident APCs in the dermis and keratinocytes in the epidermis. On the other hand, T cells in the epidermis exhibit the phenotype of effector memory T cells [7]. The previously mentioned HLA-Cw6 gene encodes a HLA-C molecule that is expressed on APCs, such as DCs, and even though its functional role in psoriasis pathogenesis is unclear, it could be involved by affecting the adaptive immune responses by the presentation of processed antigens to $CD8^+$ T cells [17], hence its high association with psoriasis.

The referred autoantigen or immunogen that constitutes the core of the aforementioned activation of naïve T cells still hasn't been identified. Nevertheless, the primary antigen proposed to be involved in this process is from *Streptococci* bacteria. A number of observations corroborate this proposition, such as the fact that psoriasis can become exacerbated after streptococcal throat infection, as well as improve with tonsillectomy [19]. In addition, circulating T cells of

psoriatic patients respond to such antigens with enhanced production of Interferon-γ (IFN-γ). Streptococcal antigens do not appear to persist within psoriatic lesions, which leads to the proposition that psoriasis may be initiated by T cells primed against streptococcal proteins existing in the palatine tonsils, which then respond to cross-reacting keratin antigens after diapedesis into the skin [5]. Moreover, psoriatic plaque T cells are oligoclonal, i.e. a few different clones undergo expansion; therefore, these are able to recognize various determinants which are similar to streptococcal M-protein (namely keratin 16 and keratin 17). T cells might also be able to recognize peptidoglycan, a component of bacterial cell wall, which could, in turn, interact with various receptors of innate immunity, including Toll-like receptors (TLRs), nucleotide-binding oligomerization domain 1 (NOD1) and NOD2. This being said, it is also relevant to note that there might not be an autoantigen in psoriasis [7]. Summing up, T cells in psoriatic lesions may be reacting to a group of antigens or, alternatively, they might be a proliferative response of the abovementioned memory T cells, proliferating in response to cytokines in an antigen-independent manner [5].

Another important histological change that characterizes psoriatic lesions is the result of epidermal keratinocyte rapid proliferation and aberrant differentiation, which leads to the formation of a thickened epidermis. In addition, a reduced or absent granular layer is also characteristic of psoriatic skin [18]. In this sense, it is possible to further highlight the key role of effector T cells, together with DCs, in the development of psoriatic lesions, as the cytokines produced by these cells stimulate keratinocytes to proliferate and increase the migration of inflammatory cells into the skin, thus promoting inflammation and epidermal hyperplasia [2].

2.1.2.1. Cytokine networks in the core of psoriasis

An intricate network of cellular signalling and differentiation together with molecular factors, namely cytokines, lies at the core of the pathogenesis of psoriasis, involving both the innate and adaptive portions of the immune system [17, 20].

Although psoriasis was initially classified as a Th1 disease and therefore associated with Th1 cytokines such as IFN-γ, IL-2 and IL-12 (which predominate in psoriatic lesions), recent discoveries from studies of cytokine expression strongly indicate that a specific $CD4^+$ T cell subtype is an important modulator in the immunopathogenesis of this disorder, namely the Th17 cell subset [5, 17]. Cells from this subset are found at increased levels in the dermis of psoriatic lesions (validated by fluorescence-activated cell sorting (FACS) of single-cell suspensions from skin tissue samples). Likewise, Th17 cells produce several cytokines that have been found to be overexpressed in psoriatic plaques, such as IL-17A, IL-17F, IL-21 and IL-22 [5]. Differentiation of precursor $CD4^+$ T cells into the Th17 subset is stimulated by transforming growth factor-β (TGF-β) and IL-6, which induce the expression of IL-17A and the IL-23 receptor (IL-23R) [20]. It is interesting to note that this type of cells has also emerged as a key aspect in the development of

other inflammatory and autoimmune diseases, such as multiple sclerosis, rheumatoid arthritis, systemic lupus erythematosus and inflammatory bowel diseases, in addition to psoriasis [17].

In this molecular perspective, a specific cytokine signalling pathway stands out from the rest, namely the IL-23/Th17 cytokine axis. It seems to be central in the pathogenesis of this disease, since it is differentially increased in psoriatic lesions [17, 21]. IL-23 plays a key role and contributes to the pathophysiology of psoriasis since it alters T cell polarization in the skin of psoriasis patients [17]. It is produced by stimulated DCs, macrophages and other APCs [5]. While IL-23 does not seem to be needed for the early stages of Th17 development, it is required for maintenance, terminal differentiation, as well as for promoting Th17 effector responses (by their amplification) [17]. Indeed, when this cytokine is intradermally administered to mice, it induces the formation of psoriatic lesions [5]. Additionally to IL-23, other cytokines belong to this cytokine axis, acting at different steps to regulate Th17 cell differentiation from naïve T cells. IL-12, IL-1β and IL-6 can be highlighted in this context, as well as IL-21 (required for cell amplification) and the aforementioned IL-23 (which is essential for the stabilization and terminal differentiation of this cell lineage) [17]. Also, IL-23 enhances the Th17 expression of cytokines (namely the aforementioned IL-17A, IL-17F, IL-21 and IL-22).

Amongst the abovementioned assortment of cytokines, the role of IL-17 in the pathogenesis of psoriasis can be emphasized. Besides Th17 cells, other cell types are able to produce it, such as $CD8^+$ T cells (in psoriatic lesions), γ:δ-T cells and Natural Killer (NK) T cells. The IL-17 signalling pathway encompasses a family of six cytokines (IL-17A to IL-17F) and five receptors (IL-17RA to IL-17RE) [17]. A specific member of this family of cytokines, namely IL-17A, is suggested to have a notable role in the pathogenesis of psoriasis. In fact, it is involved in Th17 cell recruitment, neutrophil chemoattraction, induction of expression of antimicrobial peptides and cytokines on keratinocytes, skin barrier disruption (through the downregulation of fillagrin in keratinocytes as well as genes involved in their adhesion) and stimulation of other diverse cell types (including myeloid DCs (mDCs), macrophages, fibroblasts and endothelial cells) [20]. One other T cell subtype was found to be important in the context of psoriasis, namely the Th22 $CD4^+$ T cell subset, which produces IL-22. This cytokine, in turn, together with IL-17A, coordinates an innate immune response against extracellular pathogens, by inducing expression of antimicrobial peptides and chemokines with the purpose of recruiting neutrophils. These two cytokines have contrasting actions, in the sense that IL-17A produces an inflammatory response, whilst IL-22 has a protective and regenerative role [7].

Additionally, the role of tumour necrosis factor (TNF)-α in the pathogenesis of psoriasis is indisputably important. It induces the secretion of multiple proinflammatory cytokines by activated lymphocytes or keratinocytes [22], as well as increases the action of the Nuclear Factor Kappa B (NF-κB) transcription factor, enhancing the inflammatory response and inhibiting apoptosis of keratinocytes [22, 23]. TNF-α also has a stimulating role in the formation of vascular

endothelial growth factor (VEGF) by increasing the production of nitric oxide (NO). At last, in regard to the aforementioned DCs present in the epidermis, TNF-α can facilitate their migration and infiltration, through the inhibition of the expression of E-caderin, potentially favouring the immune response observed in psoriatic plaques [22].

Naïve T cells can also differentiate into regulatory T cells (T_{regs}). These are able to supress the activity of effector T cells and promote resolution of inflammatory processes. In the context of psoriasis, the regulatory activity of T_{regs} is deficient; in addition, effector T cells appear to be resistant to their suppressant activity. This disequilibrium contributes to the state of exacerbated inflammation observed in psoriasis [7].

2.1.2.2. Innate immune system cells in psoriasis and interaction with the adaptive immune system

The fact that innate immune cells and their products can be found in psoriatic lesions suggests a role for innate immunity in psoriasis pathogenesis. Cells of the innate immune system include DCs, macrophages and NKT cells, among others [5].

DCs, as professional APCs, play an essential role in regulating the balance between immunity and immunological tolerance, acting as sentinels. Recently published studies have shown that DCs might be the primary cell type that drives Th17 differentiation in psoriasis, through the production of IL-6 and IL-23. Studies in animal models and in humans document that distinct subsets of DCs, such as plasmocytoid DCs (pDCs), mDCs and inflammatory DCs (iDCs), are involved in psoriasis [17]. Indeed, pDC numbers are elevated in psoriatic skin, in comparison to normal skin. This subset of DCs expresses TLR9 receptor which, when activated by the microbial cathelicidin LL37 bound to self-DNA fragments released from stress or dying cells in the skin, induces the production of large amounts of IFN-α in the cell. These cells also express TLR8 and TLR7, which also induce the production of IFN-α when stimulated with self-RNA-LL37 complexes. IFN-α is an important mediator for the development of psoriasis through the action of T cells. Indeed, IFN-α therapy on psoriasis patients worsens their pathological condition by exacerbating psoriatic lesions [7]. In addition, mDCs also express TLR8 and can, therefore, be stimulated by self-RNA-LL37 complexes, which induces their differentiation into mature cells, besides the production of IFN-α and IL-6 [7], as well as IL-12, IL-23, and inducible Nitric Oxide Synthase (iNOS) [5]. In a general way, the immune environment and the DC cell subsets promote Th17 cell abnormalities in the skin, thus contributing actively to psoriasis pathogenesis. This has been corroborated by *ex vivo* studies that revealed that DCs obtained from psoriatic lesions activated T cells to produce IL-17, in contrast to the observed for DCs from normal skin [17].

Concerning macrophages, these cells are present in great numbers within psoriasis lesions. They are able to secret IL-7, IL-12, IL-23, TNF-α [5] and iNOS. While their specific function in the context of psoriasis pathogenesis is yet unknown, studies in mice indicate that

macrophages are the major source of TNF-α needed to trigger the inflammatory process that results in the development of psoriasis [7].

Keratinocytes can be considered as an integrated entity within the skin-resident immune system. Indeed, they can act as APCs, produce innate immune mediators and contribute to the skin homing and local activation of immune cells [7]. In this context, it is noteworthy to analyse one of the links established between the adaptive and innate immune system, through the action of keratinocytes. More specifically, IL-21 and IL-22 produced by Th17 cells induce keratinocyte hyperplasia [20], while IL-17 synergises with IFN-γ, thereby increasing the production of proinflammatory cytokines (IL-6 and IL-8) as well as granulocyte-macrophage colony-stimulating factor (GM-CSF) by keratinocytes [5]. In that way, these epithelial cells are an important source of relevant mediators for the establishment of psoriatic lesions and emergence of vicious cycles that perpetuate their own existence. They may play an active role in sustaining and amplifying inflammatory responses, also being responsible for the production of chemokines, inducing the recruitment, retention and activation of immune cells in the skin [20] (e.g. CCL20, which has been suggested as a mechanism that maintains Th17 cells within psoriatic lesions [17]). Keratinocytes may also respond to cytokines through the increase in the expression of antimicrobial peptides (such as human β-defensin (HBD)-2, HBD-3 and the aforementioned LL37 [7]), to further direct immune cells to the skin [20].

NKT cells are a subset of T cells which express typical NK cell markers ($CD161^+$ and $CD94^+$), but only utilize a restricted assortment of T cell receptors. They have immunoregulatory functions in the recognition of self and foreign antigens, having already been associated to the pathogenesis of several autoimmume inflammatory diseases, such as psoriasis. However, their role in this disease is not yet understood. Nonetheless, psoriatic plaques overexpress CD1d, an antigen-presenting molecule which presents glycolipid antigens that activate this subset of cells. Upon activation, NKT cells quickly secrete IFN-γ and IL-4, [7], further aggravating the inflammatory response leading to the development of psoriatic lesions [5]. Psoriatic keratinocytes can also activate this type of cells [7].

Innate immune cells like neutrophils, γδ-T cells and mast cells are also related to the pathogenesis of psoriasis, although their exact roles have not yet been found [5, 7]. All the same, another linkage between the innate and adaptive immune systems can be recognized through the function of neutrophils. Indeed, the increased expression of IL-17 in the skin can induce pathogenesis by inducing the production of key cytokines and chemokines that recruit and activate neutrophils that, as previously mentioned, participate in this pathogenic chain of events [17].

From a general perspective, it is possible to ascertain that both the innate and adaptive portions of the immune system are of the utmost importance in the pathogenesis of psoriasis [5], in which the important role of the IL-17 cytokine and the IL-23/Th17 cytokine axis, together with

their integration with the remaining cell types and signalling pathways present in psoriatic lesions, can be emphasized. Figure 2 shows an overall scheme of the main cellular and molecular events underlying the pathogenesis of psoriasis and formation of psoriatic plaques.

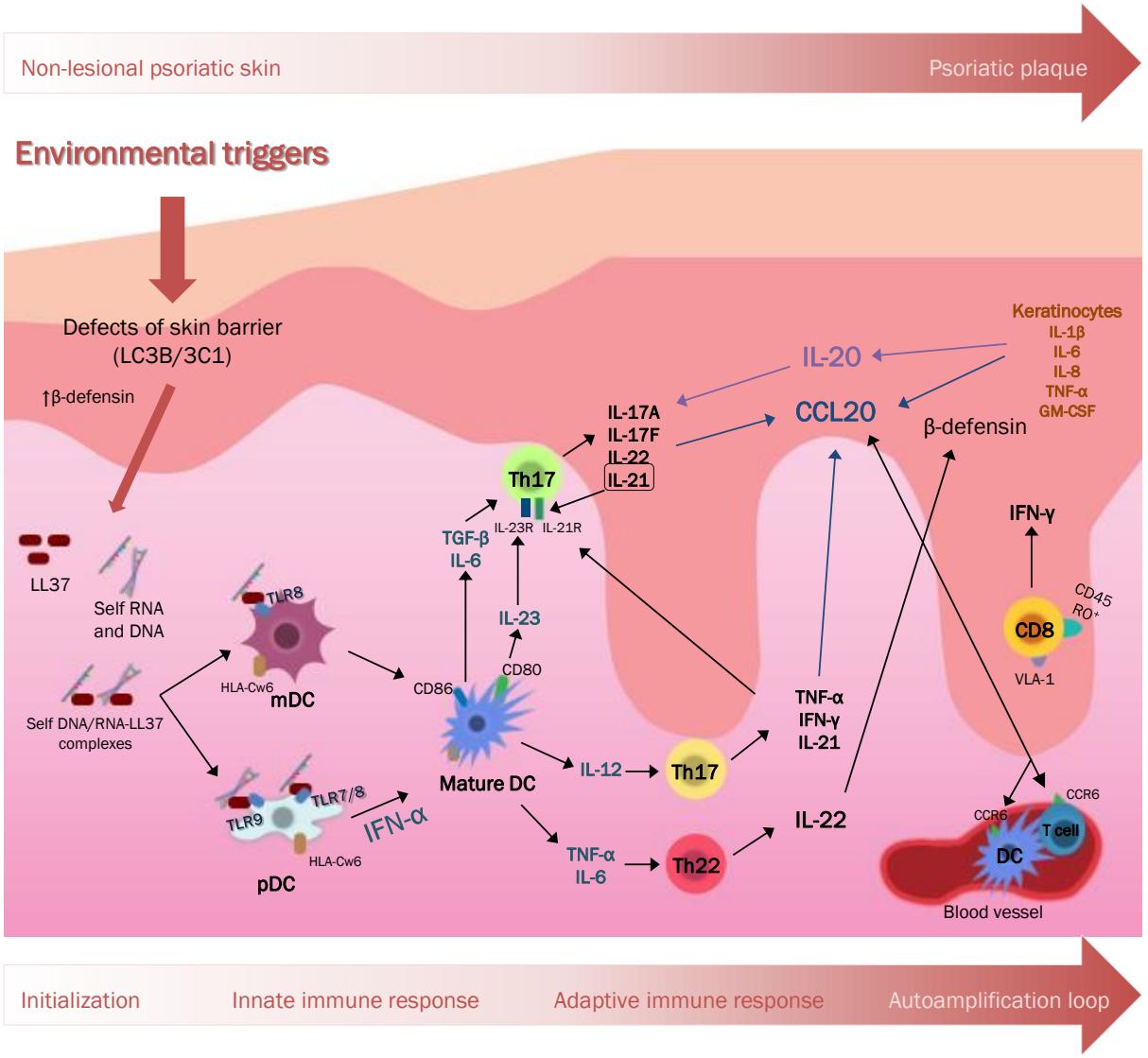

Figure 2. Schematic view of the cytokine network and cells involved in the pathogenesis of psoriasis, in regard to the formation of psoriatic plaques. Adapted from [7].

2.2. Management and Treatment of Psoriasis

Progress regarding the understanding of the genetics and pathophysiology underlying psoriasis has made it possible for the development of the management and treatment of psoriasis at a remarkable rate, for the past 20 to 30 years [24]. Complete clearance of psoriasis is most likely not yet achievable by the use of the current treatments, so the main goal of the existing therapy methodologies is to rapidly control the severity of this disease and prevent relapses [5].

In this section, a summarized view of the literature published concerning the existing treatment landscape for psoriasis will be presented. It will focus on the most important aspects of

both current and emerging treatments (including topical treatments, phototherapy and systemic therapies), with special emphasis on MTX, considering the goal of the work presented in this document.

2.2.1. Current and Emerging treatments

The different methodologies employed for the management and treatment of psoriasis are different depending on the severity of the disease. More aggressive treatments are used only in more serious cases, should treatments with fewer adverse side effects fail, in a therapeutic ladder of increasingly efficacious treatments [25]. This severity can be evaluated through the use of the Psoriasis Area and Severity Index (PASI). This clinically-validated index accounts for the Body Surface Area (BSA) affected by this disease (distinguishing between mild, moderate and severe cases of psoriasis, in a clinical perspective), together with erythema, induration and scalping. This index is scored on a scale of 0-72, where higher scores are related with higher severity of the disease. The percent reduction of this index is commonly used in clinical trials of potential psoriasis therapies, in order to indicate an improvement of the severity of this disease, after an intervention. For an example, a PASI75 response means that a 75% or greater reduction in the PASI score was achieved after treatment. Indeed, in this context, a common endpoint in clinical trials is the percentage of patients that achieve this response [12].

As it is a life-long disease, the management of psoriasis starts with the patients themselves. They must be educated about their disease and its environmental triggers, so that they can reduce their disease relapses. Additionally, psoriasis symptoms can be relieved by the use of an adequate soap substitute, in order to reduce skin irritation and to help the retention of moisture in the skin [5].

2.2.1.1. Topical treatment

The subsequent first line of active treatments for psoriasis is the use of topical agents [5]. This type of therapy is typically sufficient in the management of mild to moderate psoriasis [25], namely when this disease affects less than 10% of the BSA [26]. Hence, it constitutes the cornerstone of management for most psoriasis patients [27]. Topical agents comprise coal tar [28] and dithranol [29, 30], corticosteroids [31–33], vitamin D analogues [26, 34, 35], and retinoids [5, 25, 36], as well as keratolytic agents such as salicylic acid [37] and urea [27]. Newer topical agents include calcineurin inhibitors, immunosuppressive drugs (such as tacrolimus and pinecrolimus) and Phosphodiesterase (PDE) 4 inhibitors [26]. These agents can be administrated through various formulations, such as ointments, spray, foam, lotion, shampoo, soap and cream formulations. Overall, these compounds act by diminishing and regulating keratinocyte proliferation and differentiation, and/or through the modulation of the immunological processes that are fundamental to the pathogenesis of psoriasis, with special regard to inflammatory

processes. Some of them can also act in a synergic way by the use of combined therapies [26], which allow for quicker and more efficient therapeutic action, with potentially less side effects.

While topical therapies constitute the first choice of treatment for psoriasis, since most patients suffer from mild to moderate illness [38], when the effects arising from these treatment strategies are suboptimal or when the extent of the disease makes it unfeasible for the use of topical therapy, phototherapy and systemic therapy may need to be considered [24].

2.2.1.2. Phototherapy

Phototherapy has been used as a treatment strategy for psoriasis for more than 50 years until the present date [37]. Indeed, even in the event of biological therapies (detailed further on this document), the role of phototherapy in psoriasis (and dermatology, in general) remains considerably important [39].

The practice of phototherapy as a treatment for psoriasis is based on particular mechanisms of action, namely the alteration of the cytokine profile, induction of T cell apoptosis and promotion of immunosuppression in the treated areas, as well as other potential mechanisms such as cell-cycle arrest, gene expression modification and inhibition of double strand RNA activity [40].

There are several modalities of phototherapy with pertinence as therapeutic strategies for psoriasis. These include the usage of ultraviolet B (UVB), UVA plus psoralen (PUVA), UVA1 and excimer laser/excimer lamp [39], with the first two being the more commonly used in this perspective [40]. UVB and UVA can be distinguished by their wavelength range (311-312 nm and 320-400 nm). While UVB radiation is more biologically active than UVA, UVA radiation can also be used as a treatment together with the administration of psoralens (PUVA), which maximally absorb at particular wavelengths, *in vivo*, including the wavelength interval corresponding to the UVA spectrum. Psoralens are naturally occurring phototoxic compounds with the ability of absorbing photons and subsequently undergoing photochemical reactions, consequently acting on cell function [39].

Even though the control and/or clearance of psoriasis may take several months to be achieved by the use of phototherapy, efficacy and response rates are well known. Indeed, UVB and PUVA produce a PASI75 response in 40% to 80% and more than 80% of treated patients, correspondingly. This efficacy can be further enhanced by the combination of phototherapy with other types of treatment, such as topical therapies and systemic drugs (including biological therapies) [39].

Phototherapy benefits from not usually causing systemic toxicity, due to the lack of pharmacologic interactions. It can also be more appropriate for the treatment of psoriasis in children, given the fewer options concerning Food and Drug Administration (FDA)-approved therapeutic agents [39]. The same can be said referring to the treatment of pregnant women [5].

Nonetheless, skin cancer (such as squamous cell carcinoma and basal cell carcinoma) constitutes a risk in the use of phototherapy, which is significantly higher with PUVA (while it is theoretical and yet to be proven with the use of UVB) [37].

2.2.1.3. Systemic therapy

Currently available systemic therapies (administrated intravenously, subcutaneously or orally, depending on the therapeutic agent) for psoriasis include non-biological and biological therapies. As previously stated, these are commonly used as monotherapies or in combination with other modalities of treatment in patients with graver cases of psoriasis (namely in moderate to severe psoriasis, when the affected BSA is higher than 10%) [5].

Non-biological systemic agents

The most prominently used non-biological systemic agents are MTX, cyclosporine and orally administrated retinoids (such as acitretin) [5, 24] (MTX will be approached bellow). Cyclosporine acts as a calcineurin inhibitor, having immunossupressive action [41] and inhibiting keratinocyte hyperproliferation [42]. It is characterized by a rapid onset of action [43], even in patients with severe unresponsive psoriasis [42]. Cyclosporine use is accompanied by an abundant number of adverse side effects, with hypertension and chronic nephrotoxicity being the most evident ones [44]. Acitretin can be highlighted as a retinoid used in the treatment of psoriasis, affecting epidermal differentiation and proliferation, besides having immunomodulatory effects [45, 46]. Orally administrated retinoids provide a systemic effect that is limited by adverse reactions, such as teratogenicity, mucocutaneous toxicity, serum lipid elevations [5, 46], skeletal changes and hair loss [5], as well as hepatic, metabolic, ophthalmologic, neurological and musculoskeletal effects [45]. Overall, it can be noted that the efficacy of the currently employed non-biological systemic therapies is greatly dampened by their adverse side effects, such as the aforementioned systemic toxicities. Additionally, distinct patients with different stages of psoriasis can produce varied responses to the treatment. Thus, combinational and rotational therapeutic strategies are needed, in order to use these pharmaceutical agents and adequately control their effect and minimize their toxicity, in a long-term perspective [47].

The next sub-section will provide further detail concerning MTX in the context of psoriasis, as it constitutes the therapeutic compound of interest to be used in the work further presented in this document.

Methotrexate (MTX)

MTX (4-amino-N^{10}-methyl pteroyglutamic acid, Figure 3a) is an antimetabolite, namely a folate antagonist [48] (structurally similar to folate acid, Figure 3b) renowned for its use in the context of many different types of pathologies, including acute lymphoblastic leukemia, osteosarcoma, non-Hodgkin's lymphoma, Hodgkin's disease as well as head, neck, lung and

breast cancers [49]. The discovery of MTX as a therapeutic substance of interest in the context of dermatology was made in 1951, when Gubner *et al.* [50] observed that treatment with aminopterin (also a folate antagonist, the first effective treatment to be used for leukemia [51]) to be very effective against psoriasis [50]. Thus, a more stable and less toxic derivative of this drug was subsequently obtained, namely MTX [48, 51]. In the field of dermatology it is mainly used in the context of psoriasis (as well as psoriatic arthritis); even so, it can also be applied in the scope of several other dermatologic diseases such as vasculitic connective tissue, blistering and lymphoproliferative diseases [48], as well as pityriasis rubra pilaris, dermatomyositis, lupus erythematosus, sarcoidosis, systemic sclerosis, morphoea, atopic dermatitis and immunobullous diseases [51].

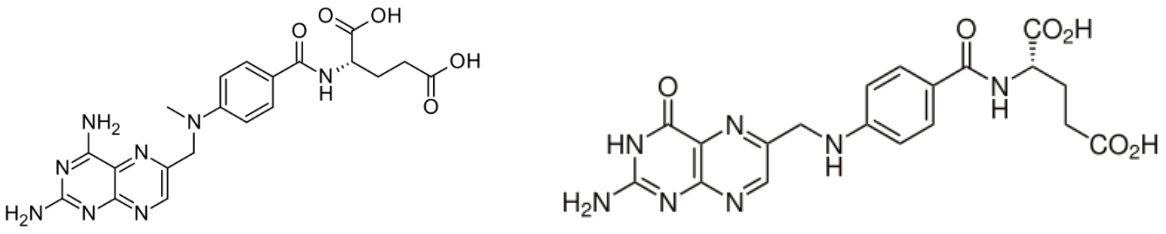

(a) (b)

Figure 3. Chemical structures of (a) MTX and (b) Folic Acid.

Current therapeutic strategies for the treatment of psoriasis generally employ oral and parenteral administration routes for MTX. When administered orally, MTX is relatively well absorbed from the gastrointestinal tract at low doses (< 25 mg/m^2); however, at higher doses, absorption becomes erratic and a parenteral route of administration is preferred. Orally-administrated MTX shows a relative lower bioavailability to the one obtained by parenteral administration, as shown by pharmacokinetic studies, due to the variable intestinal absorption as well as first-pass metabolism in the liver (where approximately 10% of the orally-administrated MTX is converted to 7-hydroxy-MTX; the remaining orally-administrated MTX reaches maximum plasma concentration after 0.75h-2h) [51]. As it reaches blood circulation, approximately 50% of MTX is bound to plasma proteins. MTX clearance is mostly performed by proximal tubular filtration; as significant renal insufficiency can lead to the overall reduction in MTX clearance, the administered dose of MTX need to be adjusted accordingly in order to reduce toxicity associated with its use [51].

From a global perspective, MTX remains the gold standard of systemic treatment in the context of moderate to severe psoriasis, namely when the disease is unresponsive to topical or phototherapy or when other possible therapeutic options are counterindicated for certain patients [51]. Regarding dosage of MTX for the treatment of psoriasis, multiple successive revisions of the guidelines for MTX dosage have been performed from 1972 to 2009 by the American Academy of Dermatology (AAD) as well as by the European Academy of Dermatology (EAD). The current recommended weekly single oral dose of MTX is of 7.5-25 mg. Nonetheless, it should be noted

that there is still a wide variation in MTX dosing due to the absence of a consensus on the optimum dose of MTX for the treatment of psoriasis. The systematic review produced by Montaudié *et al.* (2011) [52] showed that the starting dose of administered MTX should range between 5 and 10 mg/week, for the first week, and thereafter undergo a fast increase so that a therapeutic dose of 15-25 mg/week can be achieved (in the subsequent 4 weeks). This dosage scheme arises from the fact that these authors found therapeutic response to MTX to be apparently dose-dependent; indeed, a PASI75 response was achieved within 16 weeks in 60% of psoriasis patients undergoing treatment with an initial dose of 15 mg/week, which lowered to 40% for an initial dose of 7.5 mg/week [52].

Mechanisms of action

MTX inhibits epidermal cell proliferation [48] and has anti-inflammatory action at low doses [48, 53].

Concerning the inhibition of cell proliferation, MTX acts through the depletion of the intracellular stores of activated folate (i.e. fully reduced folates). More specifically, MTX interferes with the activity of enzymes in the metabolic pathways associated with *de novo* purine and pyrimidine synthesis [51]. The primary metabolite of MTX, namely MTX-polyglutamate (produced after MTX enters a target cell through the reduced folate carrier), competitively inhibits the action of an enzyme designated as dihydrofolate reductase (DHFR), thus preventing the reduction of folate cofactors. Consequently, thymidylate synthase function is inhibited, thus preventing pyrimidine synthesis. Polyglutamate can also inhibit the action of other folate-dependent enzymes, such as aminoimidazole-carboxamide-ribonucleoside (AICAR) transformylase, which subsequently prevents purine synthesis [48]. Transmethylation reactions are also inhibited by MTX [48, 51], namely the methylation of homocysteine to methionine, which interferes in the synthesis of polyamines like spermidine and spermine. It should be underlined that a therapeutic prolonged effect of MTX can be achieved since when this drug enters target cells it cannot be transported back to the extracellular medium, unless it is hydrolysed by the enzyme γ-glutamyl hydrolase, thus being accumulated inside the target cells [51]. As a result, MTX disrupts cell replication, leading to the inhibition of epidermal cell proliferation (by inhibiting DNA synthesis and consequently inducing apoptosis in keratinocytes [51]), which has also been shown to happen, to an even larger degree, in lymphoid and macrophage cell lines [48].

The therapeutic interest of MTX in the context of dermatology also arises from its anti-inflammatory action [51]. For lower therapeutic doses, MTX shows strong anti-inflammatory action not necessarily mediated by the depletion in the intracellular stores of activated folate. Indeed, the inhibition of AICAR transformylase, besides resulting in the inhibition of purine synthesis, has also been associated with the subsequent increase in the levels of AICAR, inducing the release of adenosine (with an increase of both intracellular and extracellular levels of this

molecule) [48, 51]. Adenosine is a purine nucleoside with endogenous anti-inflammatory properties. It can bind to particular cell surface receptors on multiple types of target cells and exert its anti-inflammatory action through different pathways. It can inhibit the production of oxygen free radicals (oxidative burst) by polymorphonuclear cells (PMNs) such as neutrophils and monocytes. Adhesion and chemotaxis of PMNs are also inhibited, as adenosine downregulates the expression of adhesion molecules such as L-selectin, B2-integrin and CD11b [48, 51]. Other actions include the prevention of leukocyte chemotaxis and inhibition of the secretion of multiple cytokines involved in the pathogenesis of psoriasis, such as TNF-α, IL-10 and IL-12 [48].

From an immunomodulatory perspective, besides the already mentioned effects of MTX on PMNs and cytokine expression (arising from the increase in levels of adenosine), it has also been observed that MTX exerts immunosuppressant action on both T and B lymphocytes. This further indicates the immune system as a pertinent target for the treatment of psoriasis mediated by MTX, in addition to its direct action on keratinocytes. Also, it was recently shown by Meephansan *et al.* (2011) [54] that administration of MTX to psoriasis patients leads to a significant decrease in the levels of IL-22 which, as already explained, is a cytokine of considerable importance within the cytokine network associated with the pathogenesis of psoriasis [51].

Figure 4 sums up the overall known mechanisms of action associated with the therapeutic use of MTX.

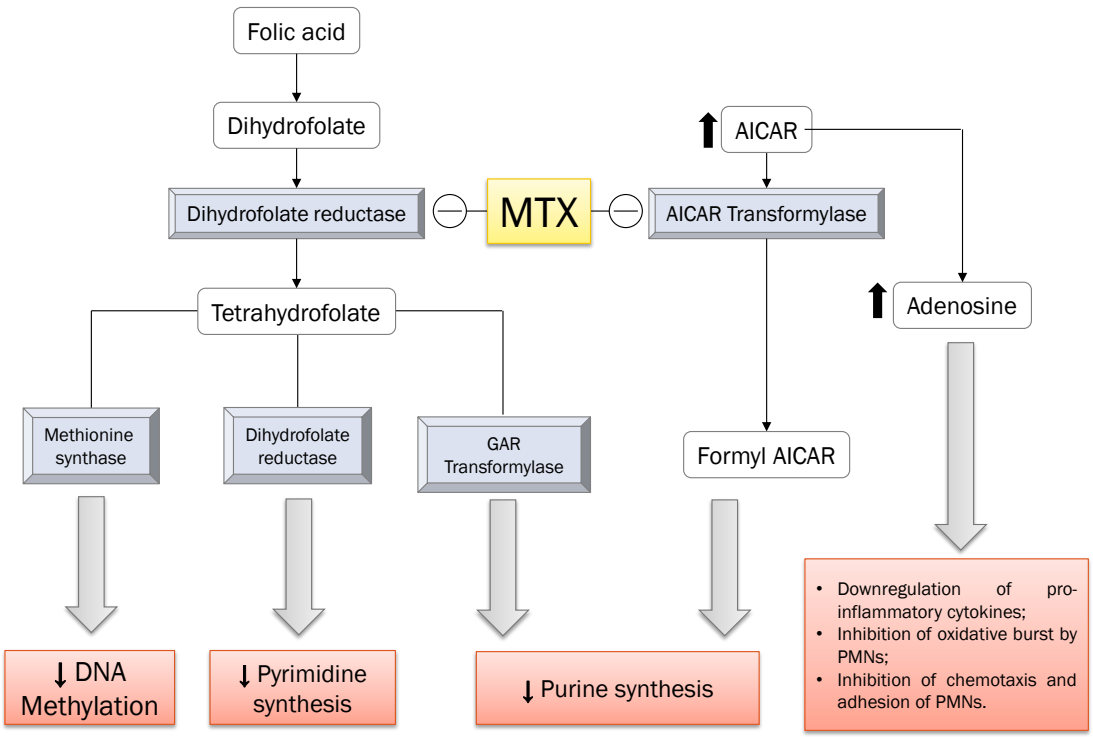

Figure 4. Schematic diagram of the multiple mechanisms of action of MTX that have been described up to the present date. Abbreviations: AICAR, aminoimidazole-carboxamide-ribonucleoside; GAR, glycinamide ribonucleotide. Adapted from [48].

MTX efficacy and side effects

Efficacy associated with the treatment of psoriasis has been found to be linked, at a pharmacogenetic level, with particular polymorphisms in DHFR [51], as well as other polymorphisms associated with the adenosine pathway [48]. On the other hand, resistance to the treatment with psoriasis can also be observed, due to reduced transport of MTX into target cells, decreased capability to synthetize MTX-polyglutamate and increased expression of drug-efflux transporters of the multidrug resistance protein class. Nonetheless, monotherapy employing MTX usually induces a visible response in psoriasis patients in a period of time ranging from 1 to 4 weeks with a reduction of at least 50% in the PASI score in 70-80% of the treated patients [51]. For a more detailed view on MTX efficacy as tested by several studies (as a monotherapy, as well as in combination therapy with other conventional systemic therapies and biological therapies), the reader is directed to Tables 3, 4 and 5 of the review produced by Dogra *et al.* (2013) [51].

It should be noted that there is a large number of adverse effects associated to systemic administration of MTX [48], where liver toxicity can be highlighted as the most important adverse effect for long-term treatment in psoriasis patients. Risk factors associated with this side effect comprise Type 2 diabetes, alcohol consumption, obesity and hepatitis B and C [48]. Nevertheless, some side-effects (such as gastrointestinal side-effects, including nausea, vomiting, diarrhoea and stomatitis) can be minimized by the concomitant supplementation of folate to the patient [48], which was also recommended by Montaudié *et al.* (2011) [52] as part of their suggested dosing regimen [52]. A summary of the side-effects associated with MTX administration is presented on Table 2.

Table 2. Side effects of MTX administration.

Constitutional	Nausea, fatigue, malaise, anorexia (dose-dependent; can be minimized by folic acid administration);
Gastrointestinal	Nausea, diarrhoea, stomatitis (dose-dependent; can be minimized by folic acid administration), hepatotoxicity;
Haematological	Cytopenia (rare event in the absence of potential risk factors; improvement is usually achieved after dose reduction or therapy withdrawal);
Pulmonary	Pneumonitis, pulmonary fibrosis;
Reproductive	Teratogenicity, oligospermia and potential mutagenesis;
Oncogenic potential	Epstein-related lymphoma, Squamous cell carcinoma;
Mucocutaneous	Mucositis, photosensitivity, radiation-recall reactions, drug hypersensitivity reactions, diffuse non-inflammatory alopecia;
Infections	Oportunistic, tuberculosis reactivation, hepatitis;
Neurological	Headache, dizziness, fatigue, mood alterations (dose-dependent, but can also result from chronic use)
Others	Development of stress fractures of long bone (low-dose administration), anaphylactoid reactions (during initial exposure of a low-dose administration);

Adapted from Shen et al. (2012) [48].

The increased risk of multiple types of toxicity associated with systemic administration of MTX constitutes one of the main driving forces of the work presented in the present document, as

defended further on, regarding the novel incorporation of this drug in nanoparticulate drug-delivery systems for a safer treatment of psoriasis by topical administration (and also more effective, due to the beneficial properties of the mentioned nanoparticulate drug-delivery systems, which will be discussed later on this document), with a larger focus on mild to moderate psoriasis (with the concomitant employment of lower doses of MTX, thus also limiting toxicity).

Small molecules

As far as future non-biological systemic treatments are concerned, the importance of small molecules (< 800 Da) with therapeutic action can be underlined [24]. These molecules target and inhibit particular enzymes within signalling pathways related to the pathogenesis of a disease, thereby modulating intracellular signalling with therapeutic intent. Indeed, many of the small molecules currently being developed for the treatment of psoriasis (and other inflammatory diseases) target cell-signalling components associated with inflammatory processes, which have been identified through genetic research (as documented earlier) [55].

The main advantages concerning the use of small molecules are the fact that they are usually inexpensive to produce as well as appropriate for oral administration (contrary to most biological therapies). Small therapeutic molecules in development range from PDE inhibitors, kinase inhibitors (e.g. affecting pathways including Mitogen-Activated Protein Kinase, MAPK; Janus Kinase-Signal Transducer and Activators of Transcription, JAK-STAT; Protein Kinase C, PKC), lipids [55], sphingosine 1-phosphate receptor agonists and chaperonin 10 [24]. Two small molecules can be stressed: apremilast, a PDE4 inhibitor [56, 57] and tofacitinib, a JAK3 kinase inhibitor [58, 59], both promising small molecules that are currently undergoing phase III clinical trials [24].

For a more detailed view on other small molecule inhibitors in development for the treatment of psoriasis, the reader is directed to the reviews published by Gudjonsson *et al*. [55] and Laws and Young [24].

Biological therapies

Biological therapies focus on the use of biologic agents such as antibodies, soluble cytokine receptors and fusion proteins that bind to specific antigens and cytokines that are related with the pathogenesis of psoriasis, as triggered and maintained by the immune system. Indeed, these treatment strategies specifically target the immune system (namely precise molecules within it), thereby avoiding an increased number of adverse effects associated with the previously depicted non-biological systemic therapies [47].

Biological agents (also referred to as biologics or biopharmaceuticals) developed in this context can act as TNF-α inhibitors/antagonists, as well as target T cells and interleukin pathways (specifically, the IL-12/23 pathways [47]) and, in the future, the IL-17 and IL-22 pathways [12].

Table 3 sums up the currently FDA-approved biologics for the treatment of psoriasis, as well as other biologics still under development.

Table 3. Summary of biopharmaceuticals for the treatment of psoriasis currently marketed and in development.

Therapeutic Agent	Type	Clinical Trial Phase (Psoriasis)	Mechanism of action
CNTO1959	IL-23 inhibitor (p19)	I	Fully human mAb that binds and inhibits the p19 subunit exclusive to IL-23
SCH900222	IL-23 inhibitor (p19)	II	Fully human mAb that binds and inhibits the p19 subunit exclusive to IL-23
LY252623	IL-23 inhibitor (p19)	II	Fully human mAb that binds and inhibits the p19 subunit exclusive to IL-23
APG2305[1]	IL-12/23 inhibitor	II	Small molecule (short peptide sequence) that inhibits the IL-23 receptor
Ixekizumab	IL-17 inhibitor	III	Fully human IgG4 mAb that inhibits IL-17A
Secukinumab	IL-17 inhibitor	II	Fully human IgG1κ mAb that inhibits human IL-17A
Brodalumab	IL-17 inhibitor	II	Fully human IgG2 mAb that binds to human IL-17RA, blocking IL-17A, 17F, 17A/F and 17E
Fezakinumab	IL-22 inhibitor	I/II	Fully human IgG mAb that inhibits IL-22
Briakinumab	IL-12/23 inhibitor	Withdrawn	Fully human IgG1 mAb binds the common p40 subunit of IL-12 and IL-23
Certolizumab pegol	TNF-α inhibitor	III	mAb fragment that binds to TNF-α
Golimumab	TNF-α inhibitor	Not registered	Fully human IgG Ab that binds to soluble and membrane-bound TNF-α
Infliximab	TNF-α inhibitor	Marketed	Chimeric (75% human/25% mouse) IgG1 mAb that targets soluble and membrane-bound TNF-α
Adalimumab	TNF-α inhibitor	Marketed	Recombinant fully human IgG1 mAb that binds to soluble and membrane-bound TNF-α
Etanercept	TNF-α inhibitor	Marketed	Soluble dimeric fusion protein consisting of TNF-α receptor component bound to Fc portion of IgG that binds to soluble TNF-α and lymphotoxin
Alefacept	T cell modulator	Marketed	Human fusion protein (obtained by recombinant technology) that binds to CD2 on memory effector T cells and inhibits activation of T cells
Ustekinumab	IL-12/23 inhibitor	Marketed	Fully human IgG1 mAb that binds the common p40 subunit of IL-12 and IL-23
Aplimod mesylate[1]	IL-12/23 inhibitor	Marketed	Small molecule that inhibits IL-12/Il-23 expression

Adapted from [12, 47, 55]; mAb: monoclonal antibody
[1]The inclusion of APG2305 and apilimod mesylate in this table is due to their pertinence in treatment in the context of anti-cytokine action, even though they are orally administrated small molecules and not exactly biopharmaceuticals.

TNF-α inhibitors

TNF-α inhibitors constitute the largest and most studied group of biological therapies to the present date, having been approved for the treatment of psoriasis for more than 10 years (and before that, they had already been approved by the FDA to treat rheumatoid arthritis) [47]. TNF-α is an inflammatory cytokine that plays a key role in the pathogenesis of psoriasis, being produced by T cells and keratinocytes alike [24]. It generally acts by inducing the production of chemokines and the expression of adhesion molecules by keratinocytes and vascular endothelial cells, further amplifying the inflammatory process within psoriatic plaques by recruiting inflammatory cells [60]. TNF-α can bind to its receptor, after being cleaved from a transmembrane-bound precursor. Blockade of TNF-α can lead to the inhibition of the corresponding inflammatory cascade and thereby conduce to a clinical improvement of psoriasis [24].

The usage of TNF-α inhibitors is associated with several side effects. These include injection site reactions, palmoplantar pustulosis [24], as well as an increased risk of skin and upper respiratory tract infections. Indeed, the use of TNF-α inhibitors is not recommended for

patients with a personal or strong family history of malignancy or chronic infection (such as tuberculosis and hepatitis B or C), as they are immunossupressive [24]. Rarer adverse effects comprise drug-induced lupus (from autoantibody formation) and exacerbation of demyelinating disorders, as well as worsening of moderate-to-severe congestive heart failure [12, 24, 47]. Other adverse effects have also been pointed out, for which causality has not yet been determined, namely risk for development of lymphoma and non-melanoma skin cancer [47], due to role of TNF-α in the context of cancer. Indeed, there is also substantial evidence that the chronic inflammation inherent in conditions such as psoriasis is itself associated with an increased risk for malignancy [61]. Nevertheless, psoriasis patients can still potentially benefit from treatment with TNF-α, in comparison to other treatments (namely topical and non-biological systemic therapies), due to the reduction in the risk of developing cardiovascular disease and diabetes [12].

Infliximab, adalimumab and etanercept constitute the three FDA-approved existing TNF-α inhibitor molecules for psoriasis treatment [12]. Adalimumab and etanercept are adequate in the treatment of moderate to severe plaque psoriasis, while infliximab is indicated for severe plaque psoriasis [60].

Infliximab is a chimeric monoclonal antibody (75% human, 25% murine) in which the Fc portion (constant region) is human immunoglobulin G1 (IgG1) and the Fab portion (variable regions) is essentially of murine origin. It was the first biologic drug to be used in the treatment of psoriasis (along with psoriatic arthritis). Infliximab can bind both to soluble and membrane-bound TNF-α [12, 47] with high affinity and specificity, being able to bind about 100% of TNF-α molecules after infusion, as verified by pharmacodynamics studies [62]. A phase III clinical trial showed that infliximab was highly effective and rapid in its therapeutic action, resulting in long-term remission of skin and nail psoriatic lesions; indeed, a PASI75 response was attained by 80% of the treated patients after 10 weeks of treatment [63]. However, it should be noted that anti-infliximab antibodies are frequently produced after prolonged therapy, decreasing its efficacy, as well as potentially causing an anaphylaxis-like infusion reaction (that occurs in less than 1% of the patients) [12, 47].

Adalimumab is a recombinant fully humanized monoclonal antibody (IgG1) which binds with high affinity to soluble and membrane-bound TNF-α [24, 47], thus being indicated for the treatment of various immune-mediated inflammatory diseases, including psoriasis and psoriatic arthritis [61]. A *post hoc* analysis of patient data from three phase III clinical trials of adalimumab in patients with moderate to severe psoriasis was produced by Mrowietz *et al*. [64]. These authors evaluated the efficacy of adalimumab based on the European Consensus Programme (ECP) treatment goals, which include consideration for patient quality of life. Their analysis revealed consistent results between the three trials, having found that treatment with adalimumab rapidly induced efficacious responses in moderate to severe psoriasis patients. A PASI75 response was

achieved by more than 93% of patients who reached ECP treatment goals [64]. Nevertheless, even though adalimumab is a fully humanized antibody, response to the treatment can be hampered by the development of anti-adalimumab antibodies that can occur in up to 20% of treated patients [13]. In addition, loss of efficacy has been reported for intermittent therapy, so continuous treatment with adalimumab is recommended [24].

Etanercept is a dimeric soluble recombinant fusion protein containing a TNF-α receptor (p75) fused to the Fc portion of a human IgG1. It acts by binding to soluble TNF-α and, as a result, lowers its free concentration in the serum and impedes its interaction with TNF-α cell-surface receptors, thus preventing subsequent activation of inflammatory cascades [12, 60]. The dimeric nature of etanercept renders it capable of binding TNF-α with an affinity that is 50 to 1000 times greater than naturally occurring TNF-α receptors. Etanercept is approved for use in psoriasis, in addition to other inflammatory-mediated illnesses [60]. A particular advantage of etanercept, in comparison to its monoclonal antibody TNF-α binding counterparts, is the fact that it is associated with a lower risk of reactivation of latent infections with mycobacteria, including tuberculosis. This is due to its poor penetration in granulomas (as shown in a mouse model of lung inflammation) [65]. A phase III clinical trial for etanercept showed that, for the highest tested dose, a PASI75 response was attained by 49% of the patients and this efficacy was maintained even after dose reduction [66].

Regarding TNF-α inhibitors that are presently being developed, certolizumab pegol and golimumab can be stressed [24]. Certolizumab pegol is a humanized monoclonal antibody fragment bound to a polyethylene glycol moiety, which increases its half-life in the blood circulation. Unlike the aforementioned TNF-α inhibitors, it does not possess a Fc portion, and therefore cannot bind Fc receptors and induce apoptosis of inflammatory cells [55]. It is currently in phase III clinical trials for the treatment of psoriasis and psoriatic arthritis, and has already been approved by the FDA for the treatment of Crohn's disease and rheumatoid arthritis [47]. Alternatively, Golimumab is a fully human IgG antibody that can bind both soluble and transmembrane TNF-α with high-affinity [67]. It is already licenced for use in psoriatic arthritis. No clinical trials are currently registered concerning golimumab for the specific treatment of plaque psoriasis [24].

T cell targeting

In the context of T cell targeting, alefacept can be highlighted. This molecule is a recombinant human dimeric fusion protein, comprising an extracellular portion of the leukocyte function antigen-3 (LFA-3) fused to the Fc portion of a IgG1 [68]. It is able to selectively inhibit T cell activation through the binding of LFA-3 to the CD2 molecules present in the surface of memory T cells (in general, since these have higher expression of CD2 than naïve T cells) [47, 68], potentially leading to long periods of remission in some patients. It is used in both moderate and

severe psoriasis cases [47]. A phase III clinical trial showed that, after a 12-week course of treatment, 28% of patients treated with alefacept reached a PASI75 response, maintaining at least a PASI50 response for a median of 7 months after treatment [69]. Even so, given its immunosuppressive action, alefacept is not recommended for the treatment of individuals with a personal or strong family history of malignancy or chronic infection, as analogously mentioned for TNF-α inhibitors [24].

IL-12/23 targeting

The development of biological therapies with the IL-12 pathway as a target, specifically its p40 subunit, was based on the fact that psoriasis was firstly thought to be a Th1 disease, as already mentioned. In opposition, subsequent studies revealed the more prominent role of Th17 cells in the pathogenesis of psoriasis and the involvement of IL-23, which also possesses a p40 subunit, since there is significantly more of this cytokine than IL-12 in psoriatic lesions. As a consequence, growing evidence corroborated that the efficacy of p40-targetting biologics was due to their action via IL-23, in detriment of IL-12 [70]. As a result, new biologics have begun to be developed with the intent of targeting the p19 subunit that is unique to IL-23 [12], which will be approached further on.

Concerning p40-targeting agents, ustekinumab and apilimod can be emphasized.

Ustekinumab is a fully human monoclonal antibody (IgG1) that is FDA-approved for the treatment of mild to severe psoriasis, [12, 71]. By binding to the p40 subunit of IL-12 and IL-23 [71, 72], it prevents the interaction between these cytokines and their corresponding receptors. This subsequently leads to a reduction in the expression of cell surface markers associated with skin homing as well as the activation and inhibition of the secretion of anti-inflammatory and proinflammatory cytokines, respectively. A single dose of ustekinumab is able to lower the numbers of $CD4^+$ Th cells and NK cells in psoriatic lesions [71]. Its approval for treatment of psoriasis was based on two phase III clinical trials, which showed that approximately 70% and 80% of the patients (corresponding to each study), treated with the highest dose of ustekinumab, reached a PASI75 response after 12 weeks of treatment [73, 74]. Still, it should be taken into account that ustekinumab pharmacokinetics are strongly affected by body weight [71, 72].

Apilimod mesylate, on the other hand, is not exactly a biological therapy (by definition) but an orally administered small molecule that is still pertinent to discuss in this context. It was discovered by high-throughput screening for IL-12 inhibitors [75] and suppresses the expression of IL-12 and IL-23 in psoriatic lesions, by hampering the accumulation of c-Rel in the nucleus. c-Rel is a pivotal transcription factor in the expression of the p40 and p19 subunits, as well as the p35 subunit of IL-12 [12]. Also, apilimod simultaneous enhances the action of IL-10, an anti-inflammatory cytokine [75]. An open-label study performed by Wada *et al*. [75] showed its efficacy, in which approximately half of the patients with the highest dosing regimens showed a 50% or

greater improvement in their psoriasis severity, accompanied by a decrease in epidermal thickness and in the number of infiltrating T cells and DCs [75].

As mentioned, IL-23 antagonists that specifically target this cytokine are currently being developed and undergoing clinical trials. These include humanized monoclonal antibodies to the p19 subunit unique to IL-23, such as CNTO1959, SCH900222 (which are currently being submitted to phase II clinical trials) [24] and LY2525623 [21]. Indeed, CNTO1959 is seemingly promising, in the sense that a phase I clinical trial showed that administration of this drug in individuals with moderate to severe psoriasis led to a PASI75 response in all of the patients treated with 300 mg, in a single dose [76]. Additionally, in this context, APG2305 can also be underlined. While it is not a biologic, being (by definition) a small molecule therapeutic agent, it comprises a short sequence of peptides with the ability of inhibiting the IL-23 receptor. This drug is also currently being submitted to phase II clinical trials [55].

Some side effects associated with the inhibition of the IL-12/23 pathways have been reported, with increased risk of major adverse cardiovascular events (MACEs) being the most conspicuously suggested by existing data [12]. A palpable example in this perspective is briakinumab, a recombinant fully human IgG1 monoclonal antibody that binds to the p40 subunit of IL-12 and IL-23. While it showed remarkable therapeutic efficacy (as indicated by a phase II clinical trial where 90-93% of the subjects were able to reach a response of PASI75, together with other studies) [13], a pooled study regarding safety results (where five parent studies and an open label extension were analysed) suggested increased rates of infections, malignancies and MACEs in patients treated with brianukinab [77]. Indeed, during a phase III clinical trial evaluating this drug, MACEs were observed in 5 out of 981 treated patients [24]. Ultimately, it was withdrawn from further investigation and application for licencing because of the abovementioned reasons [12, 24].

IL-17/Th17 and IL-22 targeting

The importance of IL-17 (more specifically, IL-17A) together with IL-22 in the pathogenesis of psoriasis, as documented earlier, constitutes the fundamental rationale for the development of psoriasis biological treatments that target these cytokines (or corresponding receptors).

In this perspective, three main drugs can be enumerated, specifically ixekizumab, secukinumab and brodalumab [12].

Ixekizumab and secukinumab are both humanized monoclonal antibodies (IgG4 and IgG1, respectively) that selectively bind and neutralize IL-17A [78, 79]. Concerning ixekizumab, this drug is currently undergoing phase III clinical trials. A previously published phase II clinical trial showed that approximately 80% of the patients treated with different doses of ixekizumab were able to reach PASI75 responses, 12 weeks after initiating treatment. PASI90 responses were also obtained for around 70% of the patients treated with the highest dose [80]. Regarding

secukinumab, two phase II clinical trials showed its potential as an efficacious treatment option for patients with moderate to severe psoriasis [79, 81]; indeed, in the study conducted by K. A. Papp *et al*. [81], PASI75 responses were attained in 80% of the patients, 12 weeks after the beginning of the treatment. At last, brodalumab also targets the Th17 pathway, being a fully human IgG2 monoclonal antibody that binds with high affinity to one of the IL-17 signalling pathway receptors, namely IL-17RA [82]. By doing so, it blocks the action of IL-17A, as well as IL-17F, IL-17A/F heterodimer and IL-17E [12]. A phase II clinical trial conducted by K. A. Papp *et al*. [82] proposed brodalumab as a potentially interesting treatment for moderate to severe psoriasis, as PASI75 responses were obtained in 70% to 80% of the patients receiving different treatment doses, 12 weeks after the beginning of treatment [82].

Bearing in mind that, at present, not many patients have already been treated with the aforementioned experimental drugs, it is not yet possible to accurately determine the risk of rare side effects associated with them, such as cardiovascular events or serious infections. In addition, though not observed in preliminary studies, a theoretical risk of impaired resistance to fungal infection is also a possibility [13], due to the importance of the Th17 pathway in host defense against extracellular bacteria and fungi [20].

At last, in view of the contribution of IL-22 to the pathogenesis of psoriasis (especially in the scope of epidermal proliferation), it is also possible to highlight fezakinumab, a monoclonal antibody that binds human IL-22, that is currently undergoing phase I clinical trials for the treatment of this disease [12, 55].

Overall, biological therapies revolutionized the management and treatment of psoriasis [5] by allowing the progression of broad strategies of immunosuppression into novel targeted therapies [12], as a result of the progressing knowledge concerning the immunopathophysiology of this complex illness.

Even though prescription of biological agents is associated with expensive costs [5], their elevated efficacy might reflect itself in the decrease of expenses related with the need or the length of hospitalization associated with other therapies (namely non-biological treatments). Additionally, greater improvement is generally achieved in the condition of psoriasis patients that have been treated with biological therapies, in comparison to topical therapies, phototherapy and non-biological systemic therapy. Indeed, increased patient satisfaction has been reported for biological therapies, whilst the other depicted treatments are commonly associated with patient frustration and low compliance due to their unsatisfactory outcomes [78].

Nevertheless, the complexity surrounding the cytokine networks that embody the pathogenesis of psoriasis is not yet completely understood. Consequently, disturbances in the homeostasis of the immune system can have adverse unexpected consequences such as unwanted suppression of other important immune pathways [5], on top of infections and cardiovascular events, for an example [12]. Also, the long-term use of immunomodulatory drugs

also raises concern over long-time side effects, even though short-term safety data has provided encouraging results [24]. Taking these facts into consideration, a global view of the present treatment landscape shows that further work, and efficacy and safety studies concerning biological drugs is needed. This is so that more highly selective and safe targeted therapies can be obtained [12] and used in a more cost-efficient way, with emphasis on the necessity for continuous pharmacovigilance [24].

Combination treatment in psoriasis

The relevance of combination therapy should be highlighted, as it is a very common therapeutic strategy in clinical practice in the management and treatment of mild, moderate and severe psoriasis. Indeed, while clinical trials are mostly dominated by investigation of monotherapies, there is a growing number of randomized controlled trials with the purpose of evaluating combination therapy, in which all the previously detailed treatment modalities can be considered [36]. Indeed, this allows the creation of multiple therapeutic strategies that not only have the objective of decreasing the amount of adverse side effects, but also increase the efficacy of current treatments, and treat even the most serious refractory cases of psoriasis [83]. Table 4 presents a few notable examples of combination therapy in the treatment of psoriasis, with different types of treatments, according to a systematic review and meta-analysis performed by Bailey *et al*. [84].

Table 4. A summary of combination treatments for moderate to severe psoriasis vulgaris from a systematic review and meta-analysis produced by Bailey *et al*. [84] (taken from [5]).

Therapeutic Agents	Outcomes
Topical vitamin D analogues and corticosteroids	Patients had a 22% (95% CI: 12%–33%) increased likelihood of clearance than did patients receiving vitamin D derivative monotherapy
Topical vitamin D analogues and UV-B phototherapy	Patients had no statistically significant increase (11%; 95% CI: 2%–24%) in the likelihood of clearance than did patients receiving UV-B monotherapy
Topical retinoids and vitamin D analogues	Patients had a 33% (95% CI: 22%–44%) increased likelihood clearance than did patients receiving topical retinoids monotherapy
Topical corticosteroids and salicylic acid	Patients had no statistically significant increase (3%; 95% CI: 0%–7%) in the likelihood of clearance than did patients receiving UV-B monotherapy
Topical corticosteroids and UV-B phototherapy	Patients had no statistically significant increase (−6%; 95% CI:−24%–12%) in the likelihood of clearance than did patients receiving UV-B monotherapy
Topical retinoids and corticosteroids	Patients had a 19% (95% CI: 11%–27%) increased likelihood of clearance than did patients receiving vitamin A derivative monotherapy
Topical retinoids and UV-B phototherapy	Patients had a 21% (95% CI: 5%–36%) increased likelihood of clearance than did patients receiving UV-B monotherapy
UV-B phototherapy and biological agents	Patients had a 68% (95% CI: 51%–85%) increased likelihood of clearance than did patients receiving alefacept monotherapy
UV-B phototherapy and methotrexate	Patients had a 36% (95% CI: 10%–63%) increased likelihood clearance than did patients receiving UV-B-methotrexate monotherapy

95% CI: 95% Confidence interval.

2.3. Drug-carrying Nanosystems in Psoriasis: Why & How?

Nanotechnology is an emerging and fast developing and promising technology that holds the key to the future progression of science and engineering alike. This notion was firstly conceptualized by Richard Feynman, in the 1950's. Indeed, in 1959, Feynman gave a lecture called "There's Plenty of Room at the Bottom" in which he explored the possibility of the direct manipulation of individual atoms. This lecture would ultimately become a central event in the history of nanotechnology, being the inspiration for the application of these concepts, decades later. Indeed, contemporary nanotechnology focuses on the exploration of the interesting properties of matter on a scale where the dimension of particles is reduced to that of individual molecules or their aggregates, namely particles whose size is 100 nm or less [85, 86]. These properties include electrical conductivity, magnetic characteristics, hardness, increased active surface area and chemical reactivity as well as biologic activity [87]. These features derive, in large part, from the increased surface area-to-volume ratio of such particles [88]. Nanotechnology comprises an ever-growing number of related scientific, engineering and industry areas of work and knowledge, where nanomedicine can be highlighted as one of the most promising. As its designation suggests, nanomedicine comprehends the application of nanotechnology and related research to medicine, with therapeutic and diagnostic purposes [85, 87].

In the scope of the management and treatment of psoriasis, nanodermatology is subsequently emphasized as one of the numerous divisions of nanomedicine, relating to the application of emerging nanomaterials to the skin [87], more precisely, nanoparticles. Without a doubt, the development of nanoparticles for dermatologic applications is an area of increasing magnitude and interest, as it has been possible to observe a recent growth in financial investments and an exponential number of registered patents in this context [86]. The usage of nanoparticles in dermatology allows for the creation of newer and better targeted therapeutic strategies, through surface modification and binding of particular ligands for specific cell targets. Enhancement of the use of already existing (and sometimes discarded) pharmaceutical agents, together with the innovative application of the same drugs but through different administration routes, is also possible by the use of nanoparticles. These drug carriers can provide a sustained drug release over a prolonged period of time, allowing a constant drug level in the target tissue [89]. Encapsulation of bioactives also shields them from chemical degradation [90, 91]. Hence, therapeutic effect can be maximized and toxicological concerns related to drug overdose and clearance can be minimized. Patient compliance is higher, as these therapeutic strategies enable a reduction in the frequency of drug administrations [89].

Thus, the following section will grasp the unmistakable prospective advantages of the use of nanosystems for the controlled and directed release of drugs, consecutively focusing on the context of psoriasis management and treatment, with emphasis on topically administrated

formulations, given the work presented in this document. Nanoparticles toxicity and safety concerns will also be approached.

2.3.1. Drug-releasing nanoparticles and the skin

2.3.1.1. Skin structure and function

Previously on this document, both topical and systemic therapies for the treatment of psoriasis were enumerated. Since dermatology focuses on the treatment and diagnosis of skin illnesses, topical application is still the usually preferred and ideal administration route for the use of therapeutic agents, as it is associated with higher patient compliance and satisfaction (in regard to the administration route itself) [85]. Indeed, the use of topical delivery of drugs allows for avoidance of systemic toxicity, circumvention of first pass metabolism and minimization of pain [91] as well as the possibility of utilizing smaller amounts of drugs [92] amongst other advantages, in comparison to other administration routes. A global perspective of the skin as a functional and physical barrier will be provided (a simplified scheme of a cross-section of skin is presented in Figure 5).

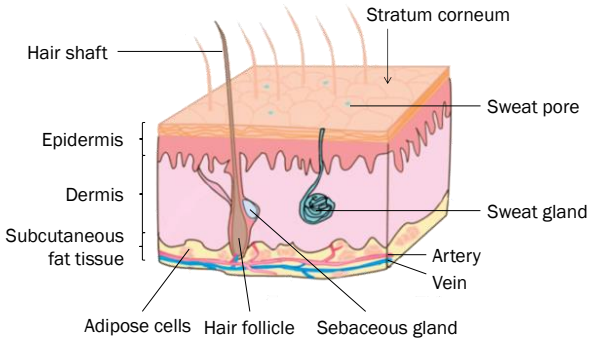

Figure 5. Simplified schematic image of a cross-section of skin. Adapted from [92].

Skin is the largest organ of the human body, having a surface area that ranges between 1.5 and 2 m^2 for adults [92]. Hence it is physical barrier that functions as a first-line defense from the external environment. Indeed, the skin not only provides protection against physical injuries and dehydration, but also confers immunological-, metabolic- and UV-related defences to the organism [86, 90].

In terms of structure, the skin is composed of three main layers. The outermost one is the epidermis, which has a thickness of about 50-150 μm, followed by the dermis, with a thickness of approximately 250 μm and finally, subcutaneous fat tissue.

Focusing on the epidermis, this layer is characterized by the absence of blood vessels, thus obtaining nutrients by diffusion across the five sublayers which it comprises. Of these five layers, the outermost one is a structure called stratum corneum, which has a thickness that

varies between 15 and 20 μm. It is composed of rigid desmosome-linked epithelial cells called corneocytes (terminally differentiated, dead, and dehydrated keratinocytes) [90, 91], which are embedded in a lamellar matrix of intercellular lipids (such as phospholipids, ceramides and cholesterol sulphate [86]). Altogether, this structure is responsible for the barrier function of the skin, namely its inherent permeation resistance. It avidly reduces the passage of molecules, particularly those larger than 500 Da. In addition, depending on the anatomical site and age, the outermost layers of the stratum corneum are regularly subjected to desquamation, in an upward migration, in order to renew this layer and therefore maintain epidermal barrier homeostasis. This also prevents the entrance of pathogens into the organism and provides it with an elimination pathway for cancerous cells or solid particulate matter [90].

The dermis, on the other hand, promotes metabolic exchanges between the skin and the blood and lymphatic networks. It incorporates blood and lymphatic vessels, nerves and elevated concentrations of collagen fibres. Cells of varied functions exist in this structure, such as the aforesaid dermal DCs, together with multiple subsets of T cells and other immune-related cells, which interact and coordinate their actions with epidermal keratinocytes. At last, located under the dermis resides a layer composed of adipocytes interconnected by collagen fibres, which form a thermal barrier, store energy and function as a physical shock/aggression dampener for the body [90]. Furthermore, pilosebaceous units, hair follicles and sweat glands can also be emphasized, as appendages that constitute significant discontinuities in the structure of the skin [91].

2.3.1.2. Nanoparticles for topical delivery

From a global perspective, it is through the exploration of the aforementioned anatomical and functional characteristics of the skin barrier that it becomes possible to develop nanoparticle formulations that are able to penetrate it and adequately deliver drugs for exertion of therapeutic effect [91, 93]. Certainly, appropriate drug penetration through the skin barrier until the therapeutic site of action must be attained, so that therapeutic concentrations can be reached and bioavailability of the drug is assured, in a reasonable time frame [90].

Molecule agents can penetrate the skin through three different pathways: an intercellular pathway, through the abovementioned lipid matrix; a transcellular pathway, through the keratinocytes; and a transappendageal pathway, by the use of the hair follicles, sebaceous glands and sweat glands. While the intercellular pathway was thought to be the most prominent from the three mentioned, the transappendageal pathway, regarding hair follicles, has also gained notable interest. It functions as a shunt for the penetration of hydrophilic compounds or supramolecular structures (e.g. proteins or carrier systems) and/or reservoir for topically administrated agents. In consequence, particular cell populations or structures associated to hair follicles, such as dermal

DCs and other inflammatory-related cells, can become pertinent targets for the action of drug-carrying nanoparticles [89, 91].

In view of these penetration pathways, common ideal physicochemical characteristics of topically administrated drugs include high lipophilicity and poor aqueous solubility (with log octanol/water partition coefficient values higher than 6.0, [log P] > 6.0) [90], as justified by the presence of the lipid matrix in the stratum corneum. The size of drugs and associated drug-carriers is also a factor of key significance, as larger molecules or drug-carriers are unable to efficiently permeate the stratum corneum [86]. Diffusion through the epidermis can also be affected by the interaction between the formulation and the myriad of membrane components, enzymes and transporters comprised in this layer [90]. Diffusion rates can similarly be affected by surface charge, properties of the nanomaterial, drug-loading efficiency, mode of application and hydrogen bonding ability [91].

In this perspective, how this barrier function is altered in diseased skin, such as psoriatic plaques, is likewise critically relevant [94]. Indeed, drug delivery into the epidermis and dermis through an integral skin barrier has shown to be very challenging, as evidenced by the already depicted exceptional barrier functions of the skin [91]. Indeed, in order to circumvent this obstacle, active skin penetration enhancement methods have been developed, including electrical-, mechanical- and other energy-related approaches [92]. Conversely, when this barrier is compromised (because of pathological processes or artificially, through the use of chemical enhancers for that end [91]), nanoparticle penetration might be considerably enhanced. Indeed, the alteration of the stratum corneum associated with inflammation and keratinocyte hyperproliferation could aid in the penetration of nanoparticles in psoriatic lesions, thereby favouring the use of these drug carriers for topical administration of drugs. Nonetheless, it should be noted that the effects of psoriasis (and other important dermatologic diseases) on skin barrier integrity, specifically concerning nanoparticle penetration, have yet to be studied [94].

It is possible to distinguish between some major types of nanoparticles, which include self-assembled lipid systems (including micelles, liposomes, microemulsions, nanoemulsions, solid lipid nanoparticles (SLNs), nanostructured lipid carriers (NLCs)) and polymer systems (polymeric micelles, polymeric nanoparticles and dendrimers) [86], as well as inorganic nanoparticles (e.g. carbon nanotubes, quantum dots, titanium dioxide and zinc oxide-based nanoparticles) [85]. Amongst this variety of nanoparticles, SLNs and NLCs will be further explored in the following sections, as they are reported to be of prodigious interest for dermal applications [90, 93], hence the application of NLCs in the context of the work presented in this document.

Lipid Nanoparticles

Solid Lipid Nanoparticles (SLNs)

SLNs (Figure 6a) are a colloidal system of nanoparticles built with solid lipids as a matrix medium (0.1% (w/w) to 30% (w/w)), which is stabilized in aqueous media, if needed, by the use of surfactants (0.5% (w/w) to 5% (w/w), preferably) [95]. These solid lipids are characterized by not melting at body temperature. They consist of glyceride mixtures, highly purified triglycerides, or waxes. Incorporation of drugs in these nanoparticles occurs in the voids of the solid lipid matrix crystals, where drug loading is dependent of the type of solid lipids in use, solubility of the drug in the lipids, method of production and polymorphic change in lipid crystals in the SLNs. SLNs range in size from 50 to 1000 nm in diameter. There are multiple production techniques for SLNs [96], yet the most imperative ones are high-pressure homogenization and microemulsion-based techniques [97]. Moreover, SLNs can be characterized by numerous techniques. For instance, in terms of size and shape, scanning electron microscopy (SEM), transmission electron microscopy (TEM) and atomic force microscopy (AFM) can be applied [96], as well as Dynamic Light Scattering (DLS) (that also allows for the evaluation of the zeta potential and polydispersity, in addition to size) [95]. Infrared spectroscopy (such as Fourier Transform Infrared spectroscopy, FTIR) is also appropriate in this context, for the evaluation of lipid crystallinity and modifications [98].

Given their composition, SLNs are frequently used to incorporate and deliver lipophilic drugs [96]. Nonetheless, they can also be used for the delivery of hydrophilic agents, being versatile nanoparticles that are compatible with all routes of administration [97].

SLNs present many advantages, in a general perspective as well as for targeted topical administration of drugs. Both the lipids and surfactants employed in the construction of SLNs are generally regarded as safe (GRAS) substances; additionally, organic solvents are not required for the synthesis of these nanoparticles, which allows a demarcated decrease in toxicity associated with their use. SLNs are also characterized by their capability of giving prolonged drug release and more stable formulations, with no issues regarding sterilization [96]. This, together with the fact that SLN synthesis requires low-priced excipients, makes these nanoparticles potentially adequate for scaled-up production in an industrial setting [99]. In the scope of topical administration, SLNs possess features that render them ideal, such as the possibility for small particle size, as well as film forming properties [96]. Indeed, aqueous formulations of SLNs are characterized by their occlusive ability of creating a mono-layered lipid film onto the skin, thereby avoiding water evaporation and increasing skin moisture and hydration and, consequently, drug permeation [90, 96]. As a matter of fact, topical applications in SLNs range from sunscreen, occlusive day cream, anti-aging creams, insect repellents, to creams for the treatment of skin illnesses [96].

As far as shortcomings are concerned, a major problem exists in the use of SLNs. Besides low drug-loading capacity, drug leaking can also occur upon crystallization or cooling of these nanoparticles, not to mention that the ensuing polymorphic change to a low-energy state of its lipid matrix leads to modifications in drug release kinetics (even though more crystalline formulations allow for more stability). As a result, nanostructured lipid carriers (NLCs) were developed, in order to overcome these hurdles [96].

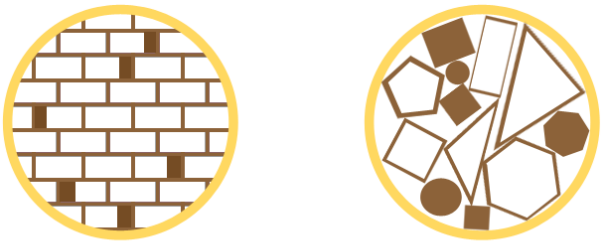

Figure 6. Nanoparticulate structures of (a) SLNs (characterized by a rigid crystalline structure) and (b) NLCs (characterized by an amorphous structure). Dark brown colour indicates the incorporation of drugs in the structure of these nanoparticles. Adapted from [95, 99].

Nanostructured Lipid Carriers (NLCs)

In order to avoid the drug leaking phenomena that occurs in SLNs after a polymorphic transition, lipids that do not give rise to highly ordered crystalline arrangements were employed. This led to the creation of a second generation of colloidal lipid nanocarriers, namely NLCs [99] (Figure 6b). NLCs are produced by using solid lipids mixed with liquid lipids (oils), preferably in a ratio of 70:30 up to 99.9:0.1 [95]. This allows the formation of an overall amorphous nanostructure with many imperfections within its matrix. Thus, it prevents the occurrence of the unwanted polymorphic transitions that characterize SLNs, providing NLCs with higher drug capacity and a lesser degree of drug expulsion during storage [95, 99]. As with SLNs, NLCs can be prepared by many methods, with high pressure homogenization being the most preferred one, given that it can be applied in a large scale. TEM, SEM, DLS and FTIR are also adequate for the characterization of NLCs (in terms of size, shape, zeta potential, polydispersity, lipid crystallinity and modifications), amongst other methods [98].

The inherent advantages of NLCs are essentially those already enumerated for their SLNs counterparts, namely film formation, controlled occlusion and skin hydration resulting in increased permeability, enhancement in bioavailability, physical stability, modulation of drug release, and others. They are also adequate for virtually all administration routes. In a topical application perspective, the fact that non-irritant and non-toxic GRAS lipids are used in NLC production also makes them adequate for use on damaged or inflamed skin. “Intelligent” NLCs (INLCs) may also be of interest, as they consist in NLCs with the capability of releasing incorporated drugs in a controlled way after an adequate stimulus (such as a change in

temperature or loss in water, through an intended polymorphic transition from a state of high energy to low energy) [98].

Overall, SLNs and NLCs are auspicious drug-carrying nanoparticles in the context of topical application of bioactives. An increased and prolonged activity has been consistently reported for these nanoparticles, throughout the existing literature, with a concomitant elevation of the benefit/risk ratio in the administration of many drugs. These formulations display increased performance in comparison to market formulations of many therapeutic agents. Hence, SLNs and NLCs alike will most likely be utilized, in the near future, for the improvement in the use of currently and emerging therapeutic substances of dermatologic interest [95].

2.3.1.3. Current and emerging examples in the scope of psoriasis

Literature concerning the topical administration of drug-carrying nanosystems as therapeutic strategies for psoriasis presents interesting examples of the application of nanoparticles, such as SLNs and NLCs. Some pertinent examples in this context will be approached in the following segments.

The work conducted by Agrawal *et al.* [100] shows that a nanoparticle approach, as well as a change in the administration route, can add considerable value to the use of less significant therapeutic agents (that are, for instance, very limited by systemic toxicity concerns). Indeed, these authors concentrated their study on the use of acitretin. As previously discussed in this document, acitretin is a retinoid that is usually orally administrated. Its strong systemic side effects can be partially avoided by topical application, whilst allowing an increase in drug bioavailability in the skin. Still, this alternative therapeutic approach can still cause erythema, peeling and burning at the application site, as well as increased sensibility to the sunlight, thereby substantially lowering patient compliance. Other disadvantages include issues related with drug stability and inclusion in suitable administration vehicles. Thus, these authors intended to formulate and characterize acitretin loaded NLCs, while studying their corresponding *in vitro* drug release and deposition and clinically evaluating the action of a gel containing these nanoparticles for the topical treatment of psoriasis. Their study employed a 3^2 factorial experimental design that allowed the selection of adequate solid lipid and lipid liquid contents for optimum particle size and maximum loading efficiency of acitretin. Deposition of acitretin, as evaluated by *in vitro* skin deposition studies (in human cadaver skin), was shown to be increased for the gel containing NLC-encapsulated drugs, in detriment to the gel containing plain acitretin. Furthermore, a clinical study performed in 12 psoriasis patients for a period of 4 weeks showed that the NLC containing gel significantly improved their condition (which was evaluated by diverse indexes, including PASI scores), while simultaneously allowing a reduction in the aforementioned side effects [100]. Globally, this study redefines the use a potentially shunned pharmaceutical agent like acitretin, evidently underlining its potential when topically administrated and concomitantly delivered by

NLCs. A similar example to this study is that of Raza *et al*. [101]. Indeed, another retinoid employed for the treatment of psoriasis, namely tretinoin, was the focus of this study, which had the intent of decreasing topical administration-, stability- and lipophilicity-related issues (mostly identical to the ones depicted for acitretin). These authors prepared several tretinoin-loaded lipid nanoparticles, which included liposomes and ethosomes, in addition to NLCs and SLNs. Analogously to the study of Agrawal *et al.*, these authors also developed bioadhesive hydrogels containing these nanosystems. These were evaluated in terms of rheological properties, photostability, *ex vivo* skin permeation and retention (with porcine skin) and anti-psoriatic activity in a mouse tail model. The attained results showed augmented biocompatibility and effectiveness of all the tested nanosystems, in comparison to the marketed version of tretinoin. Still, superiority of NLCs and SLNs was also shown, in detriment to ethosomes and the marketed version of tretinoin (with simillar results for liposomes). Indeed, NLCs and SLNs showed better photostability, skin transport and anti-psoriatic activity [101]. This study demonstrates how the use of nanoparticles can solve administration and stability problems of useful efficacious drugs.

Lin *et al*. [102] evidences how combination therapy in psoriasis can be applied to nanoparticles for topical administration. This study relays the combination of calcipotriol (a vitamin D analogue) and MTX incorporated in NLCs for topical treatment of psoriasis. The creation of this combination had several intents: attainment of a sole therapeutic formulation, in order to increase patient compliance; avoidance of cutaneous irritant reactions associated with calcipotriol topical administration, and circumvention of adverse effects arising from MTX systemic administration. Drug permeation and skin irritation of the carriers were evaluated (along with other endpoints for nanoparticle characterization). Even though MTX and calcipotriol possess very different polarities, the results showed that it is possible to combine them in the same therapeutic formulation by the use of NLCs, allowing enhanced drug permeation (at least for methotrexate) and reduced skin irritation [102]. While studies such as the above mentioned are still scarce, an increase in their numbers is very probable, in the future. Indeed, since combination therapy is of great relevance in the context of psoriasis, as more nanocarrier-based therapeutic strategies are developed, these will most likely take this factor into account.

The work of Agrawal *et al.* [103] also illustrates how the use of nanoparticles can reduce side effects arising from topical administration of drugs. These authors documented the encapsulation of capsaicin in SLNs and NLCs in order to improve its topical delivery. Capsaicin (trans-8-methyl-N-vanillyl-6-nonenamide) can be used with therapeutic intent in the context of psoriasis. It inhibits the cutaneous vasodilation associated with its pathogenesis, being specifically used in moderate to severe cases. Topical administration of capsaicin is linked to significant drawbacks: in addition to the difficulty in skin permeation, topical administration of capsaicin is limited by the induction of erythema accompanied by sting, burning and pain sensations. With regard to the study, as expected, a higher drug loading capacity was reported for

NLCs, in comparison to SLNs. Both types of nanoparticles also caused minimum to no skin irritation. Cumulative amounts of drug that permeated through the skin were also reported as being higher for NLCs, in comparison to SLNs and plain drug solution, which could be explained by the reduced size of NLCs (in comparison to SLNs, thus favouring their skin permeation). Altogether, these results showed that, while both SLNs and NLCs are interesting nanoparticles for the topical application of capsaicin, NLCs are still the most promising nanocarrier type in this context. This is comprehensible, in view of their enhanced properties, in comparison to SLNs [103].

It should be noted that nanocarrier-based approaches other than SLNs and NLCs have been reported for the treatment of psoriasis. Thus, the reader is directed to Pradhan *et al.* [104] for a review concerning lipid and polymeric novel colloidal nanocarriers for the treatment of psoriasis.

2.3.1.4. Toxicity and safety concerns

While the potential of nanoparticle-based therapeutic strategies is incontestable, the unstopping development of new products and applications in this setting is associated with toxicity and safety concerns [86].

One of the relevant issues in this context is the biodegradable vs. persistent nature of the various types of currently existing nanoparticles. A biodegradable nanoparticle is able to disintegrate into molecular species upon application onto the skin (which are soluble and can be eliminated by the organism); persistent nanoparticles, on the other hand, are insoluble. Therefore, the latter are of special concern, particularly if taken up by the skin, translocated/transported and eventually accumulated in secondary target organs (especially after repeated treatments). Thus, they require thorough assessment of risk prior to their use [94]. Still, current research is principally centred on the development of biodegradable nanoparticles, as they are still more interesting from a toxicological, environmental and safety standpoint [89].

One other related aspect in regard to this matter involves public health in general, as well as environmental issues. More specifically, fundamental properties of nanoparticles, such as the fact that they have a higher surface area per unit mass than bulk mass, lead to a substantial increase in the availability of surface area for biologic interactions to occur. This, in turn, could give rise to the emergence of new classes of irritants, allergens, haptens, cross-reactants and unexpected particle-particle interactions. In addition, nanoparticles have the potential to damage DNA and cell membranes as well as cause adverse reactions from the organism (in response to these exogenous materials) [86]. Furthermore, nanoparticles can stay lodged in the environment, thus causing nanopollution [85]. This assortment of facts becomes especially significant if one considers that contemporary society is being increasingly exposed to nanoparticles that are present in the environment, healthcare products and consumer products (such as skin care

products, which include cosmetics, sunscreens, toothpastes, shaving creams and shampoos, that many times are designed with penetration enhancers [86]). Thus, society must be adequately educated about this emerging technology and play an active role in is evaluation. It is likewise imperative that research and development of nanoparticles proceeds with caution, as it is difficult, if not impossible, to accurately determine the hazards associated with the present widespread use and exposure to nanoparticles [85].

3. Materials and Methods

3.1. Materials

For the preparation of NLCs, several different solid lipids, liquid lipids and surfactants were used, obtained from different providers, which are listed on Table 5. MTX was kindly provided by Excella (Germany) as a gift.

All chemicals and solvents were of analytical grade and were therefore used without further purification. Aqueous solutions were prepared with double-deionized Milli-Q water (Arium Pro, Sartorius AG, Göttingen, Germany), which possesses conductivity values lower than 0,1 μS cm^{-1}.

3.2. Preparation of NLCs

MTX-loaded NLCs were prepared by the hot homogenization method for the production of NLCs [99]. Excipients (solid and liquid lipids, and surfactant) and the drug (0.5 to 1% of the total mass of excipients) were heated up to 50ºC or 70ºC (depending on the melting point of the solid lipid used), allowing for lipid melting and consequent drug solubilisation, further aided by manual agitation during 5 minutes. Subsequently, double-deionized Milli-Q water warmed up to the used temperature was added and the combination was immediately mixed by a high-shear homogenizer (YSTRAL GMBH X10/20-E3, Ballrechten-Dottingen, Germany) at Position 3 (12000 rpm/min) for 2 minutes to obtain a microemulsion. This microemulsion was then homogenized with a probe-type sonicator (VCX130, Sonics & Materials, Newtown, CT, USA) for 15 minutes with frequency amplitude of 70% in order to obtain a nanoemulsion. Drug-free NLCs were prepared by an identical protocol which differed only in the absence of the addition of MTX to the initial excipient mixture. Various excipients were tested, which are summed up in Table 5. One replicate of each type of formulation was obtained for the purpose of the optimization of the NLCs formulations (unless stated otherwise).

Concerning the final NLCs formulations chosen for further testing, as a result of their optimization, at least three batches of each formulation were produced in order to evaluate reproducibility, with the excipients being Witepsol S51, Oleic Acid and polysorbate 60 or polysorbate 80 (7:3:2), with drug mass corresponding to 0.5% of the total mass of excipients.

Witepsol S51 comprises a mixture of mono-, di- and triglycerides of hydrogenated coconut oil with ceteareth-25 and glyceryl ricinoleate as additives [105]. Ceteareth-25 refers to a mixture of non-ionic surfactants comprising high molecular mass saturated fatty alcohols with 25 ethylene oxide residues in the corresponding polyoxyethylene chain; glyceril ricinoleate is the monoester of glycerol and ricinoleic acid (constituting is 87-90% of the composition of castor oil) [106].

Table 5. Excipients (solid and liquid lipids, and surfactants) and corresponding providers used for the preparation of NLCs formulations.

Excipients		*Chemical Description/INCI name*	*Providers*
Solid Lipids	Witepsol® H32	Hydrogenated Coco-Glycerides	Cremer Oleo (Germany)
	Witepsol® E85	Hydrogenated Coco-Glycerides	Cremer Oleo (Germany)
	Witepsol® S51	Hydrogenated Coco-Glycerides + Ceteareth-25 + Glyceryl Ricinoleate	Cremer Oleo (Germany)
	Lipocire® CM	Hydrogenated Palm Glycerides, Hydrogenated Palm Kernel Glycerides	Gattefossé (Nanterre, France)
	Cetyl Palmitate	Cetyl Palmitate	Gattefossé (Nanterre, France)
	Precirol® ATO 5	Glycerol distearate	Gattefossé (Nanterre, France)
	Imwitor® 308	Glyceryl Caprylate	Cremer Oleo (Germany)
Liquid Lipids	Oleic Acid	Oleic Acid	MAY & BAKER LTD (Dagenham, England)
	Miglyol® 812	Caprylic/Capric Triglyceride	Acofarma (Spain)
Surfactants	Tween™ 60	Polysorbate 60	Merck (Germany)
	Tween™ 80	Polysorbate 80	Merck (Germany)

Oleic acid (Figure 7) is a monounsaturated fatty acid present in various animal and vegetable sources. Its correspondent saturated counterpart is stearic acid. Besides being part of a normal human diet, oleic acid is important as an excipient for pharmaceutic agents; it can also be used as an emulsifying or solubilizing agent in aerosol products (amongst with other varied uses). It can be found in olive oil (constituting 55-80% of it) as well as pecan oil (59-75%), peanut oil (36-67%), grape oil (15-20%) and sesame oil [107]. Also, fatty acids like oleic acid, besides possessing oily components, function as penetration enhancers for dermal application of therapeutic substances [99].

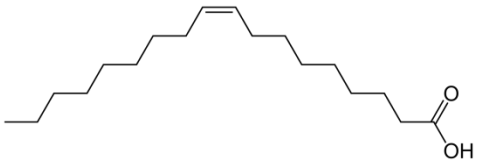

Figure 7. Molecular structure of oleic acid (also referred to as cis-9-octadecenoic acid).

Polysorbate 60 and polysorbate 80 are both non-ionic surfactants comprising mixtures of partial fatty acid esters of sorbitol and its anhydrides, copolymerized with approximately 20 moles of ethylene oxide for each mole of sorbitol and sorbitol anhydride. Particularly, in polysorbate 60, the fatty acid is stearic acid (with the possibility of the inclusion of other fatty acids, especially palmitic acid), whilst the fatty acid in polysorbate 80 is oleic acid. Polysorbate 60 has the appearance of a gelatinous transparent mass (becoming a clear liquid at temperatures higher

than 25ºC), while polysorbate 80 is a yellow/yellowish brown oily liquid [108]. The molecular structures for both polysorbates are present in Figure 8.

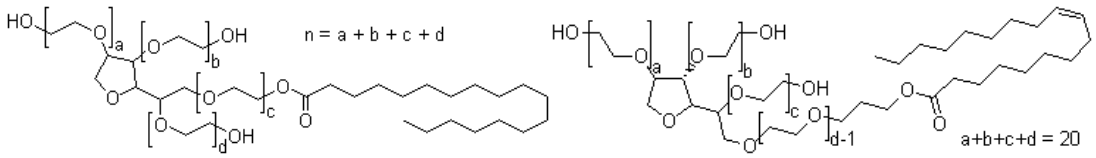

(a) (b)

Figure 8. Molecular structures of (a) Tween 60 (Polysorbate 60, also referred to as Polyoxyethylene 20 sorbitan monostearate; sorbitan monooctadecanoate, poly(oxy-1,2-ethanediyl) derivatives [108]) and (b) Tween 80 (Polysorbate 80, also referred to as Polyoxyethylene 20 sorbitan monooleate; sorbitan mono[(Z)-9-octadecenoate], poly(oxy-1,2-ethanediyl) derivatives [108]). Taken from [109] and [110].

3.3. Determination of encapsulation efficiency

MTX encapsulation efficiency was determined by a method using UV-VIS Spectroscopy. NLCs formulations were diluted by a ratio of 1:50 in double-deionized Milli-Q water in a total volume of 2 mL and subsequently centrifuged (Heraeus™ Multifuge™ X1R Centrifuge, USA) through centrifugal filter units (Amicon® Ultra Centrifugal Filters, Ultracel – 50KDa, Darmstadt, Germany) at 3500 rpm (2260*x*g), during 30 minutes, at 20ºC (until complete separation between the nanoparticles retained in the filter unit and the aqueous phase corresponding to the supernatant). The supernatant was used to quantify the amount of non-encapsulated MTX by UV-VIS spectrophotometry (Jasco V-660 Spectrophotometer, USA) at λ_{max}=303 nm (corresponding to the maximum absorption of MTX in water and aqueous mediums [102]). A standard curve of MTX in water for absorbance values measured at 303 nm (Figure 9) was used to determine the concentration of MTX in the supernatant, with the results being correspondent to the mean ± standard deviation of three measurements.

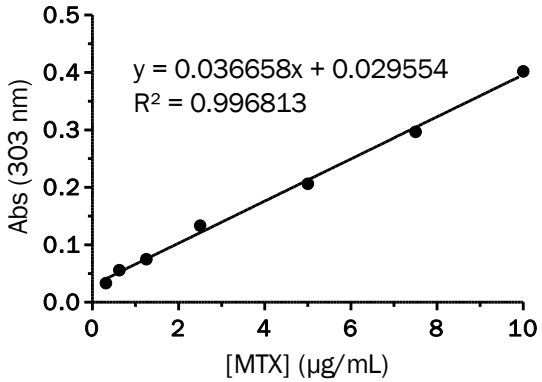

[MTX] (µg/mL)
0.3125
0.625
1.25
2.5
5
7.5
10

Figure 9. Standard curve of MTX concentration in water for absorbance values measured by UV-VIS spectrophotometry at 303 nm (n=3 measurements per data point; bars corresponding to SD values are not visible in the chart, for each point due to their small values); the supplementary table indicates the concentration values of MTX tested in order to obtain the presented standard curve.

Encapsulation efficiency was then calculated taking into account the initial amount of MTX added to the formulation by using the following equation:

$$\%\ Encapsulation\ Efficiency = \frac{Total\ amount\ of\ MTX - Unentrapped\ MTX}{Total\ amount\ of\ MTX} \times 100 \quad (1)$$

Drug loading was also calculated taking into account the total mass of excipients used in the production of the NLCs by the next equation:

$$\%\ Drug\ Loading = \frac{Total\ amount\ of\ MTX - Unentrapped\ MTX}{Total\ mass\ of\ excipients} \times 100 \quad (2)$$

3.4. Determination of mean particle size, polydispersity index (PDI) and surface charge

The mean particle size and polydispersity index (PDI) of the NLCs were determined by DLS, while the zeta potential (surface charge) was evaluated by Electrophoretic Light Scattering (ELS); both determinations were done using a ZetaPALS equipment (Brookhaven Instruments Corporation, Holtsville, NY, USA).

DLS (also referred to as Photon Correlation Spectroscopy or Quasi-Elastic Light Scattering) is one of the most powerful methods for routine measurement of particle size [99]. It is based on measuring Brownian motion (the random movement of particles due to their collision with solvent molecules around them) in order to relate it with the size of particles in a given suspension [111]. More specifically, when a monochromatic light beam (e.g. laser) is shined onto a solution containing spherical particles in Brownian motion, this causes a change in the wavelength of the incoming light, where this change is related to the size of the particles [112]. Larger particles have slower Brownian motions. The velocity of the Brownian motion is defined by a property designated as translational diffusion coefficient (D), from which the size of a particle is calculated, which is referred to as the hydrodynamic diameter [111]. Hydrodynamic diameter is that of a hypothetical sphere that possesses the same translational diffusion coefficient as the analysed particle, where a hydration layer surrounding the particle is assumed [113] (considering that this size value refers to how the particle diffuses within a fluid). This calculation is done using the Stokes-Einstein equation [111]:

$$d(H) = \frac{kT}{3\pi\eta D} \quad (3)$$

Where d(H) is the hydrodynamic diameter, D is the translational diffusion coefficient, k is Boltzmann's constant, T is the absolute temperature and η is the viscosity [111].

Light scattering can also be applied in order to measure the zeta potential of particles in a suspension, specifically by ELS.

ELS is based on the execution of electrophoresis, where the sample to be analysed is placed in a cell with electrodes, to which an electrical field is applied. The velocity of a particle in a unit electric field is thus referred to as electrophoretic mobility, being defined by the Henry equation [114]:

$$U_e = \frac{2\varepsilon z\, f(\kappa a)}{3\eta} \quad (4)$$

Where U_E corresponds to the electrophoretic mobility, z to the zeta potential, ε to the dielectric constant, η to viscosity and f(κa) to Henry's function (with κ being the Debye length and a the radius of the particle; κa measures the ratio of the particle radius to electrical double layer thickness). Considering that the determination of the zeta potential is made for an aqueous medium and with moderate electrolyte concentration, the Smoluchowski approximation can be applied, which assumes a value of 1.5 for f(κa). More specifically, systems that fit the Smoluchowski mathematical model comprise particles larger than approximately 0.2 μm dispersed in electrolytes containing more than 10^{-3} molar salt [114].

The absolute value of the zeta potential of particles in a sample gives an indication concerning their stability. Indeed, charged particles in suspension will tend to repel each other, lessening the tendency of the particles to come together, which is more pronounced for larger absolute values of zeta potential. On the contrary, particles with low absolute values of zeta potential will aggregate and flocculate much more easily. The absolute value of 30 mV is usually considered the borderline between stable and unstable colloid systems, as particles with absolute zeta potential values higher than 30 mV (i.e. < -30 mV and > 30 mV) are usually considered stable [114].

Specifically regarding the methods used in the present work, prior to measurement, NLCs formulations were diluted by a ratio of 1:400 in double-deionized Milli-Q water. Analysis was performed at 20ºC for all measurements. For size analysis, measurements were carried out at a scattering angle of 90º, where the real and imaginary refractive indexes were, correspondingly, of 1.590 and 0. For each sample, the corresponding mean ± standard deviation values were obtained from six determinations. Concerning surface charge analysis, the zeta potential Smoluchowski mathematical model was used to obtain the corresponding measurements. For each sample, the corresponding mean ± standard deviation values were obtained from ten runs, each corresponding to 10 cycles. For each final formulation, at least three batches were analysed for mean particle size, PDI and zeta potential as described.

3.5. Evaluation of NLCs storage stability

NLCs characterization parameters (namely particle size and PDI, zeta potential and encapsulation efficiency) were evaluated for the produced formulations during 2 and 4 weeks of storage at room temperature and at 4ºC. All of the determinations were performed according to the methodologies described above.

3.6. Cryo-Scanning Electron Microscopy (Cryo-SEM)

SEM constitutes one of the two types of electron microscopy (the other being TEM), which allows the acquisition of images of the surface of an object with a resolution typically between 1 nm and 10 nm [115].

Objects to be observed by SEM first need to be made conductive for current. This can be achieved by coating the surface with an extremely thin layer of gold (Au) or gold/palladium (Au/Pd) (1.5 to 3 nm). Another requirement is that the objects are capable of withstanding high vacuum and not alter it (e.g. by losing water molecules or releasing gasses). While metals, polymers and crystals usually keep their structures when observed by SEM, the same does not happen for biological material, which needs to be prefixated. Thus, Cryo-SEM can be highlighted as a particular type of SEM, in which cryo-fixation of the samples is performed, namely by the use of cold slush nitrogen [116]. The entire sample or a fracture of it can be consequently observed [117].

Specifically regarding the procedure followed for the present work, Cryo-SEM analysis was performed using a High resolution Scanning Electron Microscope with X-Ray Microanalysis and Cryo-SEM experimental facilities, comprising the equipment JEOL JSM 6301F (Tokyo, Japan), Oxford INCA Energy 350 (Abingdon, UK) and Gatan Alto 2500 (Pleasanton, CA, USA), at the Materials Centre of the University of Porto, Portugal (CEMUP). NLCs samples were firstly obtained by diluting NLCs formulations (MTX-loaded and drug-free) by a ratio of 1:400 and filtered (through a 0.45 µm filter). A minute volume of these dispersions was dropped on an adequate support and rapidly cooled by plunging into sub-cooled nitrogen (slush nitrogen) and transferred under vacuum to the cold stage of the preparation chamber. Cryofactures were then performed, with subsequent sublimation for 180 seconds at -90ºC and coating with Au/Pd by sputtering for 35 seconds. Then, the samples were transferred to the Cryo-SEM chamber and observed at a temperature of -150ºC.

3.7. Fourier Transform Infrared Spectroscopy (FTIR)

FTIR spectroscopy is a particular type of infrared spectroscopy which employs the mathematical Fourier Transform in order to compile collected raw data for the acquisition of the measured infrared spectra [118].

Regarding the methodology applied in the present work, prior to empty and MTX-loaded NLCs analysis by FTIR spectroscopy, the NLCs formulations were submitted to lyophilisation (first frozen at -80ºC and then submitted to vacuum until dry, using a lyophilisation equipment, (Bench Top Pro with Omnitronics; SP Scientific Inc., USA)). This is due to the fact that the presence of water in the samples can obscure the acquisition of the intended infrared spectra, as the corresponding bands (associated with O-H vibrations) are wide and intense. Thus, total removal of water was intended. Subsequently, FTIR transmission spectra were obtained (FT-IR Spectrophotometer, PerkinElmer; Santa Clara, California, USA) for MTX-loaded and drug-free NLCs as well as the pure drug, for a frequency range of 600 to 4000 cm^{-1}, at a resolution of 4 cm^{-1} and an applied strength of 80 units over the sample.

3.8. Separation of NLCs from non-incorporated MTX

Non-incorporated drug was separated from the NLCs prior further characterization. Several methods were tested for this purpose.

3.8.1. Separation by Gel filtration

Volumes of 200 µL, 500 µL and 1 mL of the produced NLCs formulations were added into a Sephadex® G-50 (Sigma-Aldrich, USA) gel (Figure A1, in the supplementary figures section) and eluted with running buffer composed of PBS pH 7.4 buffer (phosphate buffered saline solution with a phosphate buffer concentration of 0.01M and a sodium chloride concentration of 0.154M), allowing the separation of the non-incorporated drug from the MTX-loaded NLCs, based on the methodology used by Zhang *et al.* (2013) [119]. Aliquot collection was started when the white mass corresponding to the separated NLCs was reaching the collecting port in the separation column. Aliquots of 2 mL were obtained throughout the separation process and their contents analysed by UV-VIS spectrophotometry (Jasco V-660 Spectrophotometer, USA) with the acquisition of spectra with wavelength values ranging from 250 to 450 nm (using a speed of 1000 nm/s, UV-VIS bandwidth of 1.0 nm and data points collected in intervals of 1 nm).

3.8.2. Separation by Centrifugal Filter Units

NLCs formulations were diluted by a ratio of 1:15 and 1:30 in double-deionized Milli-Q water in a total volume of 24 mL. 3 mL of diluted NLCs were subsequently centrifuged (Heraeus™ Multifuge™ X1R Centrifuge, USA) per centrifugal filter unit (Amicon® Ultra Centrifugal Filters, Ultracel – 50K, Darmstadt, Germany) at 3500 rpm, during 30 minutes, at 20ºC (until complete separation between the nanoparticles retained in the filter unit and the aqueous phase corresponding to the supernatant, i.e. until a solid pellet without aqueous content was formed in the filter unit). The nanoparticles retained in the filter units were subsequently obtained and ressuspended in an adequate volume of PBS pH 7.4 buffer and then stored for further use. The

total mass of separated MTX contained in the total volume of supernatant was evaluated by UV-VIS spectrophotometry (Jasco V-660 Spectrophotometer, USA) at λ_{max}=303.

3.8.3. Separation by Dialysis

For each formulation, 1 to 2 mL were inserted into cellulose dialysis bags (Table 6 sums up the different dialysis membranes/tubing that were used), which were sealed on both ends with adequate clamps. Afterwards, each dialysis bag was immersed in a receptor compartment containing 80 mL of receptor medium (Table 6 indicates the different receptor mediums used to this end) and dialysed for a particular period of time (Table 6 indicates the various sampling times employed) at room temperature, with an agitation of 360 rpm provided by a magnetic stirring plate (RT 15 power IKAMAG®, Staufen, Germany). The total mass of dialysed drug was evaluated by quantifying MTX in the receptor compartment by UV-VIS spectrophotometry (Jasco V-660 Spectrophotometer, USA) at λ_{max}=303. The dialysed formulations were then stored for further use.

Table 6. Dialysis membranes/tubing (and respective Molecular Weight Cut-Off values, MWCO) and corresponding receptor mediums and sampling times utilized for the optimization of the process of separation of unincorporated MTX in the NLCs formulations (where C constitutes the definitive optimized settings used to obtain the separated NLCs formulations to be used for further study).

	Dialysis Membrane	*MWCO*	*Receptor Medium*	*Sampling times*
A	Cellu•Sep® T3 (Membrane Filtration Products Inc., Texas, USA)	12,000 - 14,000	Water	10-50min, 1.5h, 2h, 3h
			Water + 10% DMSO	10-50min, 1.5h, 2h, 3h
B	Snakeskin 10kDaMWCO dialysis tube (Thermo Scientific; Waltham, Massachusetts, USA)	10,000	Water + 20% DMSO	0.25h, 0.5h, 0.75h, 1h, 2h, 3-6h, 8h
			Water + 20% 1,2-propanodiol	0.25h, 0.5h, 0.75h, 1h, 2h, 3-6h, 8h
C	Cellu•Sep® T2 (Membrane Filtration Products Inc., Texas, USA)	6,000-8,000	PBS pH 7.4 buffer	0.25h

3.9. *In vitro* MTX release

In vitro release of MTX from the NLCs was evaluated by a dialysis bag diffusion technique [120]. Nanoparticles separated by dialysis (as explained in section 3.8.3) were used to perform the *in vitro* drug release studies, at physiological conditions, namely pH 7.4 and 37ºC. MTX-loaded NLCs suspensions in PBS pH 7.4 buffer (containing 250 µg of drug) were inserted into cellulose dialysis bags with a 6,000-8,000 molecular weight cutoff, MWCO (Cellu•Sep® T2; Membrane Filtration Products Inc., Texas, USA). After being sealed on both ends through the use of adequate clamps, the dialysis bags were immersed in a receptor compartment containing 80 mL of PBS buffer pH 7.4 and placed over a heating and magnetic stirring plate (RT 15 power IKAMAG®, Staufen, Germany) with an agitation of approximately 360 rpm and at a temperature of 37ºC (as viewed in Figure A2, in the supplementary figures section). Aliquots of 1 mL were obtained from the receptor compartment at 15, 30, 45 minutes and 1, 1,5, 2, 2,5, 3, 4, 5, 6, 7, 8 and 24 hours after the beginning of the experiment, with the addition of the corresponding volume of fresh

buffer after the acquisition of aliquots, in order to keep a constant volume of 80 mL in the receptor compartment. Sink conditions were maintained, as the maximum solubility of MTX in aqueous mediums is of <0.1 g/100 mL at 19 ºC [121], and the concentration of MTX in the receptor medium was always at least 10 times lower than this value. Drug content in the aliquots was determined spectrophotometrically (Jasco V-660 Spectrophotometer, USA), as previously depicted (using a standard curve of MTX in PBS pH 7.4 for absorbance values measured at 303 nm, Figure 10), with the results being correspondent to the mean ± standard deviation of three measurements.

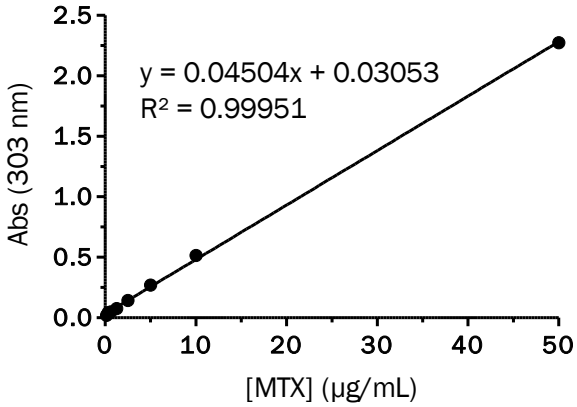

[MTX] µg/mL
50
10
5
2.5
1.25
0.625
0.3125
0.15625

Figure 10. Standard curve of MTX concentration in PBS pH 7.4 buffer for absorbance values measured by UV-VIS spectrophotometry at 303 nm (n=3 measurements per data point; bars corresponding to SD values are not visible in the chart, for each point due to their small values); the supplementary table indicates the concentration values of MTX tested in order to obtain the presented standard.

3.10. *In vitro* skin permeation

The skin permeation of MTX was evaluated using a Franz cell assembly (9 mm unjacketed Franz Diffusion Cell with 5 mL receptor volume, o-ring joint, clear glass, clamp and stirbar; PermeGear, Inc., USA) [122], where pig ear skin was used as a barrier. Firstly, the pig ear skin was excised and dissected with the use of a scalpel, allowing its separation from the ear cartilage. Subcutaneous fat tissue was removed by using scalpel, scissors and tweezers. Then, the skin was divided into square pieces of approximately the same dimensions (Figure A3a in the supplementary figures section). The receptor compartment was filled with receptor medium (PBS pH 7.4 buffer, PBS pH 7.4 buffer with 10% DMSO (dimethyl sulfoxide) and ethanol:PBS pH 7.4 buffer in a ratio of 3:7 were tested to this end) and maintained at 37ºC under constant magnetic stirring (approximately 360 rpm) using a heating and magnetic stirring plate (RT 15 power IKAMAG®, Staufen, Germany), as presented on Figure A3b, in the supplementary figures section. The skin was positioned between the donor and receptor compartments (avoiding the formation of air bubbles between the skin and the receptor compartment) and fixed in place by the use of a metallic clamp. The available diffusion area between cells was 0.64 cm^2. A donor volume inferior

to 0,5 mL containing 300 µg of MTX was placed in the donor compartment. Samples of 600 µL were taken from the sampling port at 1-hour intervals during the first 8 hours of the experiments, and at 24 and 48 hours, where the removed volume was subsequently replaced with fresh pre-warmed buffer. During the collection of samples, air bubbles that formed between the skin and the receptor compartment were always removed, in order to assure continuity between the skin barrier and this compartment. UV-VIS spectra with wavelength values ranging from 250 to 450 nm were measured for each collected sample (with a speed of 1000 nm/s, UV-VIS bandwidth of 1.0 nm and data points collected in intervals of 1 nm) and permeated drug contained in the receptor compartment samples was quantified by UV-VIS spectrophotometry (Jasco V-660 Spectrophotometer, USA) at λ_{max}=303 (using a standard curve of MTX in PBS pH 7.4 for absorbance values measured at 303 nm, Figure 10). The concentration values obtained through this process were consequently corrected in accordance to the successive dilutions suffered by the receptor medium after the collection of samples, namely by applying the next equation [123]:

$$[MTX]_{corrected} = [MTX]_{measured} + \frac{Volume\ of\ sample}{Receptor\ Volume} \times ([MTX]_1 + [MTX]_2 + \cdots + [MTX]_{measured-1} \quad (5)$$

Where $[MTX]_{corrected}$ corresponds to the corrected concentration, $[MTX]_{measured}$ corresponds to the concentration measured in the receptor medium for a given time point t, and $[MTX]_1$, $[MTX]_2$ and $[MTX]_{measured-1}$ correspond to the measured concentrations for time points number 1, 2 and t-1. This correction was necessary in order to adequately calculate the percentage of permeation of MTX through the skin over time, as well as the total flux of MTX traversing the skin for the total tested period of time.

Percentage of permeation of MTX through the skin was calculated by the next equation [123]:

$$Permeation\ (\%) = \frac{Drug\ amount\ in\ the\ receptor\ compartment}{Drug\ amount\ in\ the\ donor\ compartment} \times 100 \quad (6)$$

Flux of MTX through the skin was obtained by applying the finite flux equation [122], as depicted bellow:

$$J = \frac{Q}{A \times t} \quad (7)$$

Where Q corresponds to the quantity of MTX traversing the skin in time t, with A being the area of exposed skin in cm^2 (0.64 cm^2, as previously stated).

3.11. *In vitro* Cell Assays

3.11.1. Cell line and culture

A Human THP1 monocyte cell line was routinely grown in DMEM (DMEM GlutaMAX™-I; Gibco ®, Life Technologies™, USA) supplemented with 10% fetal bovine serum (Sigma® Life Science, USA) and 1% antibiotics (Penicillin 100 U/mL, Streptomycin 0.1 mg/mL; Sigma® Life Science, USA) in a humidified incubator with 5% CO_2 at 37ºC. Viability and cell count were monitored routinely using trypan blue dye exclusion method in a Neubauer chamber.

This human cell line is a leukemic cell line derived from cells collected from the blood of a 1-year old boy with acute monocytic leukemia (documented by Tsuchiya *et al.* (1980) [124]).

3.11.2. MTT reduction assay

The MTT (3-[4,5-dimethylthiazol-2-yl]-2,5-diphenyl tetrazolium bromide) reduction assay has the purpose of quantifying cytotoxicity by measuring viable cells, after exposure to a particular agent (drugs, nanoparticles, and others) in a certain range of concentration values, without the need for cell counting. MTT is a tetrazolium salt that can be reduced to formazan crystals (which can be solubilized in solvents such as DMSO) through mitochondrial activity of viable cells. Testing the cytotoxic action of a range of multiple concentration values of a drug or a nanoparticle formulation (empty or incorporating a drug) can be done through this assay in order to evaluate the concentration needed of the tested agent to achieve 50% cell growth inhibition, when compared to the untreated controls, corresponding to the 50% inhibitory concentration (IC_{50}) [125].

The cytotoxicity of both MTX-loaded and drug-free particles was evaluated for one NLCs formulation replicate from which unincorporated MTX was removed by the optimized dialysis process (as depicted on section 3.8.3). Cytotoxicity was tested using a human THP1 monocyte cell line as proof of concept, considering the intended anti-inflammatory action envisioned for the MTX-loaded NLCs formulations and the role of monocytes in mediating inflammation. Human THP1 monocytes (10^5 cells/well) were incubated in a 96-well plate for 1 hour (until cell adherence) and then treated with different concentrations of NLCs (diluted in culture medium), with subsequent incubation during 24h at 37ºC. Afterwards, the medium containing the NLCs was removed and 100 µL of MTT (0.5 mg/mL per well, diluted in culture medium) were added to each well. After an incubation of 3 hours, the resulting supernatant was removed and 100 µL of DMSO were added to each well in order to solubilize the formazan crystals. Absorbance was subsequently measured in a microplate reader (Synergy™ HT Multi-mode Microplate Reader; BioTek Instruments Inc, Winooski, VT, USA) at λ=590/630 nm. One independent experiment was run for each final NLCs formulation, with 5 replicates for each tested concentration. Both MTX-containing and drug-free formulations were accessed. The percentage of viability was compared

to control wells by the ratio of corrected absorbance measured for the tested conditions and the untreated cells.

3.12. Statistical Analysis

Results are reported as mean ± standard deviation for n replicates. The Student's t-test (two-tailed) was used to evaluate the statistical significance of differences in mean values of experimental groups. Differences were considered significant at $P < 0.05$.

Data were analysed and compiled with Microsoft® Excel (Microsoft® Office Professional Plus 2010, USA) and all statistical analyses were performed with the software GraphPad Prism Version 5.03 for Windows (GraphPad Software, La Jolla, CA, USA).

4.Results and Discussion

4.1. Optimization of the characteristics of NLCs formulations (particle size, PDI, surface charge and encapsulation efficiency)

With the intent of obtaining NLCs formulations with adequate characteristics for a potential dermal application in the context of the treatment of psoriasis (with MTX as the therapeutic agent), several optimization steps were taken, concerning the type and proportions of excipients, as well as conditions used in their production. A total of five stages of optimization were executed, in which the produced NLCs formulations were characterized in terms of particle size, PI, zeta potential and percent encapsulation efficiency. NLCs with a size ranging from 100 to 300 nm (with low PDI, namely < 0.2), with absolute zeta potential values higher than 30 mV and high encapsulation efficiency values (at least higher than 50% of the total drug used) were intended. These stages involved the studying of the influence of the type and ratio of solid and liquid lipid, as well as type and ratio of surfactant, the percentage of MTX used and parameters concerning NLCs production (namely the times associated with high-shear homogenization and sonication steps). Statistical evaluation was not performed for these results as only one replicate of each formulation was obtained.

Regarding particle size, it should be noted that, although intact nanoparticles with sizes above 100 nm are not considered to permeate the stratum corneum (due to their dimensions and rigidity), uptake of the incorporated MTX is to be expected, not only considering the hydrating/occlusive properties of NLCs (detailed on further sections) but also because of the high lipid content present in the stratum corneum, allowing for lipid exchange between this skin layer and the NLCs. In addition, permeation of particles with sizes in the aforementioned range would not be particularly hurdled for drug delivery in the follicles (transappendageal pathway, as already documented), in which lipid nanoparticles such as the ones produced could be trapped (thus allowing a continued drug release and targeting of cells present in these structures), due to the presence of sebum produced by the sebaceous glands in the follicles [99]. Thus, the acquisition of NLCs with sizes in the said range was intended, as there could also be concerns regarding the quality (in terms of PDI, surface charge and encapsulation efficiency) and stability of NLCs with sizes lower than 100 nm.

4.1.1. Optimization Process, Stage 1 – Influence of Solid Lipid and % MTX

Concerning the first stage of production of the NLCs formulations, several solid lipids were tested together with the same liquid lipid (Miglyol 812) and surfactant (polysorbate 60),

maintaining the same proportions of every excipient; two different percentages of MTX were tested for these formulations (0.5% and 1% w/w of the total mass of excipients).

The characterization of the NLCs formulations A-G.1 and A-G.2 (with A-G corresponding to the several solid lipids tested, and 1 and 2 corresponding to 0.5% and 1% w/w of the total mass of excipients of MTX) is presented in Table 7.

Table 7. Characterization in terms of mean size distribution, PDI, zeta potential, percent encapsulation efficiency and percent drug loading for the NLCs formulations designated as A-G with MTX corresponding to 1. 0,5% and 2. 1% of the total mass of excipients.

% MTX	*NLCs formulation*	*Size (nm)*	*PDI*	*Zeta Potential (mV)*	*% Encapsulation Efficiency*	*% Drug Loading*
0.5%	A.1. Witepsol H32	571.42 ± 64.71	0.293 ± 0.060	-35.55 ± 3.16	33.142 ± 0.013	0.17 ± 0.00
	B.1. Lipocire CM	465.87 ± 59.42	0.252 ± 0.052	-29.97 ± 3.59	43.810 ± 0.021	0.22 ± 0.00
	C.1. Witepsol E85	557.02 ± 94.68	0.245 ± 0.059	-32.25 ± 2.16		
	D.1. Witepsol S51	317.32 ± 19.13	0.215 ± 0.022	-31.97 ± 2.14	30.111 ± 0.005	0.15 ± 0.00
	E.1. Cetyl Palmitate	475.20 ± 55.88	0.173 ± 0.090	-34.23 ± 1.06	29.054 ± 0.022	0.15 ± 0.00
	F.1. Imwitor 308	95.25 ± 1.45	0.132 ± 0.018	-20.96 ± 3.36		
	G.1. Precirol ATO 5	334.32 ± 13.80	0.186 ± 0.037	-31.92 ± 2.06	16.230 ± 0.002	0.08 ± 0.00
1%	A.2. Witepsol H32	535.32 ± 44.99	0.303 ± 0.017	-37.70 ± 2.68	73.554 ± 0.008	0.74 ± 0.00
	B.2. Lipocire CM	426.28 ± 27.88	0.265 ± 0.037	-34.85 ± 0.96	75.274 ± 0.017	0.75 ± 0.00
	C.2. Witepsol E85	454.98 ± 45.81	0.256 ± 0.062	-30.09 ± 2.42		
	D.2. Witepsol S51	324.42 ± 15.09	0.193 ± 0.037	-32.80 ± 1.20	72.811 ± 0.018	0.73 ± 0.00
	E.2. Cetyl Palmitate	344.45 ± 24.83	0.118 ± 0.094	-40.39 ± 4.21	69.618 ± 0.012	0.70 ± 0.00
	F.2. Imwitor 308	94.50 ± 3.08	0.157 ± 0.027	-26.26 ± 2.15		
	G.2. Precirol ATO 5	389.35 ± 23.08	0.211 ± 0.041	-35.04 ± 1.61	76.613 ± 0.011	0.77 ± 0.00

Each result represents the mean ± standard deviation for n=6 measurements for size, PDI and Zeta Potential measurements, and n=3 for the percent encapsulation efficiency determinations, per NLCs formulation (one replicate per formulation).

Concerning size, all the formulations presented dimensions superior to 300 nm with the exception of the formulations F.1. and F.2. (with Imwitor 308 as the solid lipid) where the size was inferior to 100 nm. As previously stated, for the purpose of the present work, intermediate dimensions were intended for the obtained NLCs, specifically ranging from 100 to 300 nm; thus, these results showed the need for further optimization. Nonetheless, the PDI values were inferior to 0.25 for the formulations with the smallest sizes, namely D-G.1 and D-G.2, which suggests that the particle size distributions are still fairly narrow and monomodal, without aggregation [123]. It should be noted that this type of width distribution is to be expected in lipid nanoparticles obtained by the method described in this work (involving high-shear homogenization and sonication), with complete monomodal distribution of particle sizes being very difficult to achieve [126].

In regard to the zeta potential results, all the NLCs were shown to be negatively charged. Absolute zeta potential values were approximately equal or superior to 30 mV (ranging from circa -30 mV to -40 mV), with the exception of the formulations F.1. and F.2., which had zeta potential values ranging from approximately -20 mV to -25 mV. The zeta potential values obtained for the above-mentioned NLCs formulations indicate that they will most likely possess good physical stability.

The mass percentage of MTX did not significantly alter the values of size, PDI and zeta potential for the NLCs formulations, as no specific trend of increase or decrease was verified to exist between the two sets of data, upon comparison. However, the results show that a higher percentage of MTX (1%) led to the acquisition of higher values of encapsulation efficiency for all the evaluated formulations. Please note that C.1. and C.2. were not evaluated in terms of encapsulation efficiency due to their unfavourable size values, and F.1. and F.2. due to their unfavourable size and zeta potential values. This was attributed to the fact that the error associated with the weighting of 3 mg of MTX (for the production of NLCs formulations with 0.5% of MTX) could be potentially considerably larger than the error associated with the weighting of 6 mg (for the production of NLCs formulations with 1% of MTX), thus introducing this difference in the presented results. To counteract this effect, the next steps of NLCs production optimization were executed using doubled values of excipient and drug mass, as well as water volume. Nevertheless, considering the results obtained for 1% of MTX, encapsulation efficiencies were found to be superior to 50% for all of the tested formulations, which ranged from approximately 69% to 77% (with drug loading ranging from 0.35 to 0.39% w/w). This shows the potential of NLCs to not only encapsulate more lipophilic compounds, but also compounds characterized by lower lipophilicity; indeed, while still considerable insoluble in water and aqueous mediums, MTX is characterized by not very elevated lipophilicity, considering its low partition coefficient (log P Octanol/Water) of -1.85 [127].

4.1.2. Optimization Process, Stage 2 – Influence of Solid and Liquid Lipids, and % MTX

Considering the topical application intended for the developed NLCs, the next step in the optimization process focused on the comparison between NLCs formulations obtained using Miglyol 812 and oleic acid as liquid lipids.

For this purpose, NLCs formulations were produced for every tested solid lipid. New formulations incorporating Witepsol H32 and Cetyl Palmitate as solid lipids (chosen, for the current stage of optimization, in view of their correspondent size, zeta potential and encapsulation efficiency results) were produced with Mygliol 812 (A.1. and E.1., respectively) and oleic acid (A.1.2. and E..1.2., respectively) for comparison purposes; NLCs formulations B-G.1.2. used oleic acid as the liquid lipid. Solid to liquid lipid ratios were maintained. All the NLCs

formulations incorporated the same surfactant (polysorbate 60). One percentage of MTX was evaluated for all the referred formulations (0.5% w/w).

The characterization of the NLCs formulations A.1.-G.1.2. is summarized in Table 8.

Table 8. Characterization in terms of mean size distribution, PDI, zeta potential, percent encapsulation efficiency and percent drug loading for the NLCs formulations designated as A.1.-G.1.2.

% MTX	NLCs formulation	Solid Lipid		Liquid Lipid	Size (nm)	PDI	Zeta Potential (mV)	% Encapsulation Efficiency	% Drug Loading
0,5%	A.1.	Witepsol H32	+	Mygliol-812	515.80 ± 80.82	0.259 ± 0.037	-24.96 ± 2.65	46.705 ± 0.003	0.23 ± 0.00
	A.1.2.			Oleic Acid	312.25 ± 13.84	0.173 ± 0.025	-35.39 ± 1.58	65.437 ± 0.014	0.33 ± 0.00
	E.1.	Cetyl Palmitate	+	Mygliol-812	467.33 ± 76.25	0.248 ± 0.057	-21.41 ± 2.07	40.929 ± 0.033	0.20 ± 0.00
	E.1.2.			Oleic Acid	348.17 ± 10.77	0.242 ± 0.029	-31.50 ± 2.97	66.380 ± 0.011	0.33 ± 0.00
	B.1.2.	Lipocire CM	+	Oleic Acid	317.75 ± 15.89	0.182 ± 0.038	-55.11 ± 2.18	69.782 ± 0.007	0.35 ± 0.00
	C.1.2.	Witepsol E85	+	Oleic Acid	338.72 ± 20.31	0.229 ± 0.044	-35.53 ± 2.56	67.818 ± 0.014	0.34 ± 0.00
	D.1.2.	Witepsol S51	+	Oleic Acid	293.43 ± 13.51	0.175 ± 0.031	-41.13 ± 2.33	67.678 ± 0.021	0.34 ± 0.00
	F.1.2.	Imwitor 308	+	Oleic Acid	369.32 ± 18.75	0.221 ± 0.036	-45.74 ± 3.22	64.678 ± 0.035	0.32 ± 0.00
	G.1.2.	Precirol ATO 5	+	Oleic Acid					

Each result represents the mean ± standard deviation for n=6 measurements for size and PDI, n=10 for Zeta Potential, and n=3 for the percent encapsulation efficiency determinations, per NLCs formulation (one replicate per formulation).

Concerning size measurements, a comparison between the NLCs formulations containing Miglyol 812 and oleic acid as liquid lipids indicates a difference, as NLCs formulations containing oleic acid possess size values considerably lower than their Miglyol 812-containing counterparts. This can be observed by comparing the results for the formulations A.1. and A.1.2. (with Witepsol H32 as the solid lipid) and E.1. and E.1.2. (with Cetyl Palmitate as the solid lipid), as well as by comparing the results obtained for the formulations B.1.2.-D.1.2. with their correspondent formulations containing Mygliol 812 (B.1.-D.1.), as presented in Table 7. Still, there was one exception to the observed trend, as the NLCs formulation G.1.2., with Imwitor 308 as the solid lipid, showed a particle size much larger (369.32 ± 18.75 nm) than the value observed for its equivalent formulation containing Miglyol 812 (95.25 ± 1.45 nm). Nonetheless, the inclusion of oleic acid as the liquid lipid in the formulations A.1.2., E.1.2. and B.1.2.-D.1.2. allowed the acquisition of size values approximately equal or inferior to 300 nm, as intended for the present work. The potential action of oleic acid as an emulsifying agent (as opposed to Miglyol 812) may be the cause to the observed decrease in particle size since the addition of more emulsifiers not only aids emulsification but grants a more rigid structure to the NLCs resulting in smaller particle size [99]. No general effect associated with the inclusion of oleic acid as the liquid lipid was observed in terms in PDI values.

The inclusion of oleic acid in the NLCs formulations revealed to have influence over the zeta potential values. Indeed, comparing the NLCs formulations A.1. and E.1. with A.1.2. and

E.1.2., an increase in the absolute values of zeta potential can be observed for A.1.2. and E.1.2., with the acquisition of zeta potential values with an absolute value superior to 30 mV. The same comparison can be performed for the NLCs formulations B.1.2.-F.1.2., which all had absolute zeta potential values superior to the ones observed for their Miglyol 812-containing counterparts (as presented on Table 7), and all of them superior to 30 mV. This suggests that NLCs formulations containing oleic acid will have a better physical stability than their counterparts containing Miglyol 812 as the liquid lipid. Nonetheless, the zeta potential value obtained for the NLCs formulation B.1.2. (-55.11 ± 2.18) is highlighted in this context, as it was shown to be the largest absolute value amongst all the analysed formulations. This increased value could lead to unexpected behaviours (e.g. in terms of physical stability) concerning this NLCs formulation, so the corresponding solid lipid (Lipocire CM) was eliminated from subsequent stages of optimization.

Concerning encapsulation efficiency, the inclusion of oleic acid also led to different results than the ones observed for the inclusion of Miglyol 812 as the liquid lipid. Comparison between the NLCs formulations A.1. and E.1. with A.1.2. and E.1.2. revealed an increase in the encapsulation efficiency values in the presence of oleic acid (A.1.2. and E.1.2.). More specifically, an increase of approximately 20% and 25% for A.1.2. and E.1.2. in comparison to the observed for A.1.1. and E.1. was observed, correspondingly (resulting in encapsulation efficiency values of approximately 66% in both cases). The same could be observed when comparing the encapsulation efficiency obtained for the NLCs formulations B.1.2.-F.1.2. with their correspondent equivalent formulations containing Miglyol 812 (namely B.1.-F.1., as shown on Table 7).

The NLCs formulation G.1.2. (containing Precirol ATO 5 as the solid lipid and oleic acid as the liquid lipid) could not be characterized, as it acquired a gelatinous consistency overnight, after its production (see Figure A4 in the supplementary figures section). This suggests that, for this particular formulation, the inclusion of oleic acid (as opposed to the inclusion of Miglyol 812) as the liquid lipid, together with the solid lipid Precirol ATO 5, led to the acquisition of a very unstable NLCs formulation, resulting in its unexpected quick aggregation. This could also be explained by the possibility that the produced NLCs had a density different from the dispersant, namely water, thus undergoing sedimentation and forming a close packed bed [114].

4.1.3. Optimization Process, Stage 3 – Influence of % Oleic Acid and % MTX

Taking into account the results presented so far, the next step in the optimization process had the purpose of assessing the effect of the percentage of oleic acid in the total mass of excipients. The percentage of MTX in the tested NLCs formulations was evaluated again given the fact that using oleic acid as the liquid lipid in these formulations showed them to have an increased visible stability. Indeed, while the NLCs formulations containing Miglyol 812 showed a macroscopically visible yellow deposit of MTX, their counterparts containing oleic acid had a more

homogenous yellow aspect. This led to the hypothesis that the inclusion of oleic acid in the NLCs formulations could provide larger encapsulation efficiency, so this possibility was tested.

To this end, two solid lipids were chosen, namely Witepsol E85 and Witepsol S51, as their correspondent NLCs formulations showed the best compromise between particle size, zeta potential and encapsulation efficiency results. For each solid lipid, NLCs formulations incorporating two different percentages of oleic acid (12.5% and 25% of the total mass of excipients) and two different percentages of MTX (0.5% and 1% w/w) were obtained (C.1.2.-C.1.2.3. with Witepsol SE85, and D.1.2.-D.1.2.3 with Witepsol S51 as the solid lipids, correspondingly), while maintaining the mass of surfactant. Another additional NLCs formulation with Cetyl Palmitate as the solid lipid was obtained, with 12.5% of oleic acid and 0.5% w/w of MTX (E.1.2.1.), for comparison purposes; this solid lipid was chosen since its correspondent NLCs formulations showed the third best compromise between particle size, zeta potential and encapsulation efficiency results, after the NLCs formulations obtained with Witepsol E85 and Witepsol S51.

Table 9 shows the results obtained for the characterization of the NLCs formulations C.1.2.-E.1.3.

Table 9. Characterization in terms of mean size distribution, PDI, zeta potential, percent encapsulation efficiency and percent drug loading for the NLCs formulations designated as C.1.2-E.1.3.

	NLCs formulation			*Size (nm)*	*PDI*	*Zeta Potential (mV)*	*% Encapsulation Efficiency*	*% Drug Loading*
	Solid Lipid	*Oleic Acid*	*% MTX*					
C.1.2.1.	Witepsol E85	25%	1%	385.25 ± 20.08	0.285 ± 0.011	-29.02 ± 2.69	66.295 ± 0.022	0.33 ± 0.00
C.1.2.			0.5%	355.78 ± 12.59	0.270 ± 0.015	-33.76 ± 1.69	65.768 ± 0.063	0.33 ± 0.00
C.1.2.2.		12,5%	1%					
C.1.2.3.			0.5%					
D.1.2.1.	Witepsol S51	25%	1%	292.10 ± 6.06	0.182 ± 0.044	-39.58 ± 0.78	59.600 ± 0.026	0.30 ± 0.00
D.1.2.			0.5%	279.10 ± 8.74	0.206 ± 0.020	-40.59 ± 2.58	66.885 ± 0.050	0.33 ± 0.00
D.1.2.2.		12,5%	1%	283.22 ± 13.94	0.187 ± 0.021	-35.18 ± 1.90	59.687 ± 0.006	0.30 ± 0.00
D.1.2.3.			0.5%	269.70 ± 13.21	0.161 ± 0.024	-35.38 ± 3.63	62.763 ± 0.030	0.31 ± 0.00
E.1.2.1.	Cetyl Palmitate	12,5%	0.5%	360.70 ± 20.40	0.220 ± 0.031	-35.94 ± 1.69	55.274 ± 0.023	0.28 ± 0.00

Each result represents the mean ± standard deviation for n=6 measurements for size and PDI, n=10 for Zeta Potential, and n=3 for the percent encapsulation efficiency determinations, per NLCs formulation (one replicate per formulation).

Concerning the results obtained for the NLCs formulations with Witepsol E85 as the solid lipid (C.1.2.-C.1.2.3.), it was not possible to characterize C.1.2.2. and C.1.2.3. (containing 12.5% of oleic acid) as they acquired a gelatinous consistency overnight after their production. Formulations C.1.2.1. and C.1.2. (containing 25% of oleic acid), while remaining liquid, had a slight increase in viscosity. This was not observed for any of the NLCs formulations D.1.2.-D.1.2.3. This suggests that the produced NLCs formulations using Witepsol E85 as the solid lipid have a decreased physical stability, which becomes more pronounced with a larger percentage of solid

lipid. Nevertheless, characterization results could be obtained for C.1.2.1. and C.1.2. In view of these results, the NLCs formulation E.1.2.1. was produced so that the influence of the percentages of MTX and oleic acid could be evaluated for yet another solid lipid, in the composition of NLCs.

Concerning particle size results, the percentage of MTX appears to influence this parameter, as a decrease in MTX percentage (from 1% to 0.5% w/w) led to a small decrease in particle size. This could be verified for both the NLCs formulations containing Witepsol E85 and Witepsol S51 as their correspondent solid lipid (when comparing formulations containing the same percentage of oleic acid). This could suggest that part of the MTX contained in the produced NLCs is adsorbed to their surface (so larger amounts of MTX lead to a larger particle size, by further increasing the thickness of the adsorbed MTX) [123]. Oleic acid percentage also had an effect on particle size, as it was observed, for the formulations containing Witepsol S51 that a decrease in this parameter from 25% to 12.5% resulted in a small decrease in particle size (when comparing formulations containing the same percentage of MTX). However, this could not be observed for E.1.2.1. (with Cetyl Palmitate as the solid lipid, and 12.5% of oleic acid). Comparing E.1.2.1. with its correspondent formulation containing 25% of oleic acid (formulation E.1.2., Table 8) showed a slight increase in particle size when the percentage of oleic acid varies from 25% to 12.5%. In regard to PDI values, these were shown to be consistently larger for the formulations containing Witepsol E85 as the solid lipid (C.1.2.1. and C.1.2., with PDI > 0.27), in contrast to the smaller values obtained for the formulations with Witepsol S51 as the solid lipid (D.1.2.-D.1.2.3., with PDI < 0.22). These results further support the possibility that the formulations C.1.2.-C.1.2.3. are characterized by a decreased physical stability, as shown by the existence of wider size distributions, which subsequently indicates the presence of aggregates. On the other hand, NLCs formulations with Witepsol S51 as the solid lipid show lower PDI values (PDI < 0.22), indicating narrow and tendentiously more monomodal particle size distributions. No observable differences were found for the PDI values as a result of the variation of the percentage of oleic acid or MTX.

Regarding the results obtained for zeta potential, the percentage of MTX was shown to have a slight influence, as a decrease in the percentage of MTX appeared to lead to a small increase in the absolute zeta potential values, namely for the formulations containing Witepsol E85 as the solid lipid. A reduction in the percentage of oleic acid from 25% to 12.5%, in the formulations D.1.2.-D.1.2.3. appeared to induce a concomitant increase in the absolute zeta potential values (when comparing formulations containing the same the same percentage of MTX). No particular variation of zeta potential due to the reduction in the percentage of oleic acid was observed for E.1.2.1., compared to formulation E.1.2. (Table 8).

As far as encapsulation results are concerned, the amount of MTX did not have any effect in this parameter (when comparing formulations containing the same solid lipid and the same percentage of oleic acid). On the other hand, the percentage of oleic acid showed influence over

this characteristic (with the exception of the formulations containing Witepsol E85 as the solid lipid), as observed for the formulations D.1.2.-D.1.2.3. Indeed, a decrease in oleic acid percentage led to a slight decrease in the encapsulation efficiency values. In this case, the same could be observed for the formulation E.1.2.1., in comparison with formulation E.1.2. (Table 8), where a decrease in 15% of this value could be observed for a decrease in the percentage of oleic acid from 25% to 12.5%. In addition, deposition of MTX could be macroscopically observed for all the NLCs formulations containing 12.5% of oleic acid, for all the tested solid lipids. Nevertheless, these results corroborate that the inclusion of oleic acid as the liquid lipid, in detriment to Miglyol 812, had a beneficial effect in the encapsulation efficiency of MTX. This was shown by the increase in the encapsulation efficiency values when the percentage of oleic acid was increased. It should be highlighted that testing NLCs formulations containing a higher percentage of liquid lipid (namely oleic acid) was considered, in order to increase encapsulation efficiency, but not performed. This was due to the fact that higher percentage values of oleic acid in the composition of the NLCs could lead to the acquisition of NLCs formulations characterized by unpredictable behaviour, also considering the range of solid to liquid lipid ratios recommended by the existing literature for the production of NLCs (99.9:0.1 to 70:30) [95].

4.1.4. Optimization Process, Stage 4 – Influence of NLCs production procedure parameters

In view of the results enunciated until this point, the following step in the optimization process had the purpose of evaluating the effect on particle size, PDI, zeta potential and encapsulation efficiency of specific procedure parameters in the production of NLCs. These parameters consisted in the duration of the high-shear homogenization and the sonication of the NLCs formulations.

For this purpose, Witepsol S51 and Cetyl Palmitate were used as solid lipids to produce NLCs formulations containing 25% of oleic acid and 0.5% (w/w) of MTX. Witepsol E85 was not used for this evaluation considering the previously presented results (having been eliminated from the optimization process).

Concerning the optimization of the duration of the high-shear homogenization procedure, 2 and 5 minutes were tested (maintaining 15 minutes for the sonication procedure) for the production of NLCs formulations with the composition stated above (with Witepsol S51 as the solid lipid for D.1.2. and D.1.2.4., and Cetyl Palmitate for E.1.2. and E.1.2.4.). Table 10 lists the results obtained for the characterization of these NLCs formulations.

No difference could be observed as a result of the variation of the time interval associated with high-shear homogenization in terms of particle size, PDI, zeta potential and encapsulation efficiency, when comparing formulations containing the same solid lipid.

Table 10. Characterization in terms of mean size distribution, PDI, zeta potential, percent encapsulation efficiency and percent drug loading for the NLCs formulations designated as D.1.2-E.1.2.4.

	NLCs formulations							
	Solid Lipid	*High-shear homogenization time (min)*	*Sonication time (min)*	*Size (nm)*	*PDI*	*Zeta Potential (mV)*	*% Encapsulation Efficiency*	*% Drug Loading*
D.1.2.	Witepsol S51	2	15	289.47 ± 14.15	0.178 ± 0.026	-40.26 ± 1.88	60.928 ± 0.087	0.30 ± 0.00
D.1.2.4.		5	15	282.07 ± 14.45	0.189 ± 0.021	-42.00 ± 1.77	61.576 ± 0.052	0.31 ± 0.00
E.1.2.	Cetyl Palmitate	2	15	330.30 ± 9.53	0.188 ± 0.017	-41.46 ± 1.47	48.623 ± 0.024	0.24 ± 0.00
E.1.2.4.		5	15	319.78 ± 3.60	0.200 ± 0.012	-39.39 ± 2.10	48.084 ± 0.035	0.24 ± 0.00

Each result represents the mean ± standard deviation for n=6 measurements for size and PDI, n=10 for Zeta Potential, and n=3 for the percent encapsulation efficiency determinations, per NLCs formulation (one replicate per formulation).

Regarding the optimization of the duration of the sonication procedure, 10, 15 and 20 minutes were tested (maintaining 2 minutes for the high-shear homogenization procedure) for the production of NLCs formulations with the already referred composition (with Witepsol S51 as the solid lipid for D.1.2., D.1.2.5. and D.1.2.6., and Cetyl Palmitate for E.1.2.. E.1.2.5. and E.1.2.6.). The results obtained for their corresponding characterization are presented on Table 11.

Variation of the duration of the sonication procedure did not result in any visible change of particle size, PDI, zeta potential and encapsulation efficiency values, when comparing formulations containing the same solid lipid.

Table 11. Characterization in terms of mean size distribution, PDI, zeta potential, percent encapsulation efficiency and percent drug loading for the NLCs formulations designated as D.1.2-E.1.2.6.

	NLCs formulations							
	Solid Lipid	*High-shear homogenization time (min)*	*Sonication time (min)*	*Size (nm)*	*PDI*	*Zeta Potential (mV)*	*% Encapsulation Efficiency*	*% Drug Loading*
D.1.2.5.	Witepsol S51	2	10	284.30 ± 8.63	0.177 ± 0.016	-35.94 ± 1.05	61.494 ± 0.051	0.31 ± 0.00
D.1.2.			15	289.47 ± 14.15	0.178 ± 0.026	-40.26 ± 1.88	60.928 ± 0.087	0.30 ± 0.00
D.1.2.6.			20	289.33 ± 9.83	0.170 ± 0.043	-37.30 ± 2.67	61.867 ± 0.019	0.31 ± 0.00
E.1.2.5.	Cetyl Palmitate	2	10	314.05 ± 14.02	0.196 ± 0.015	-39.98 ± 2.38	40.846 ± 0.022	0.20 ± 0.00
E.1.2.			15	330.30 ± 9.53	0.188 ± 0.017	-41.46 ± 1.47	48.623 ± 0.024	0.24 ± 0.00
E.1.2.6.			20	334.02 ± 7.64	0.212 ± 0.023	-39.49 ± 2.38	33.720 ± 0.038	0.17 ± 0.00

Each result represents the mean ± standard deviation for n=6 measurements for size and PDI, n=10 for Zeta Potential, and n=3 for the percent encapsulation efficiency determinations, per NLCs formulation (one replicate per formulation).

Overall, these results showed that variation of the high-shear homogenization and sonication times in the procedure used for the production of NLCs formulations had no appreciable effect on their characterization parameters. While these two parameters were chosen for optimization purposes, others could also have been tested, such as the velocity used in the high-shear homogenization step as well as the frequency amplitude used in the sonication step (with pertinence to the execution of future works concerning this study). Temperature could

hypothetically by optimized (as it could affect MTX and its incorporation in the NLCs), however, as the minimum temperature needed to solubilize the used excipient mixture was already utilized, it would be difficult to further decrease it in the context of the hot homogenization method here described (other methods for NLC production would need to be tested to this end).

4.1.5. Optimization Process, Stage 5 – Influence of the type and % of Surfactant

The final step of this optimization process had the goal of assessing the influence of the type and amount of surfactant present in the excipients used to produce the NLCs formulations. Given the fact that it provided the best compromise between particle size, PDI, zeta potential and encapsulation efficiency, Witepsol S51 was chosen as the solid lipid for the NLCs formulations produced in this optimization stage. Indeed, for a duration of 2 minutes for high-shear homogenization and 15 minutes of sonication, this formulation showed a particle size of 289.47 ± 14.15 nm, PDI of 0.178 ± 0.026, zeta potential of -40.26 ± 1.88 mV and encapsulation efficiency of 60.928% ± 0.087%.

Two types of surfactant were tested, namely polysorbate 60 and polysorbate 80, as well as three different values of surfactant mass, specifically 100 mg, 200 mg and 300 mg (corresponding to the NLCs formulations D.1.2.7., D.1.2-ALT and D.1.2.8. for polysorbate 60, and D.1.2.9.-D.1.2.11. for polysorbate 80; Figure A5 in the supplementary figures section), while maintaining the total mass of excipients and the proportion between solid and liquid lipids. Also, a different (albeit similar) process for the production of NLCs (based on the hot homogenization methodology used by Abdelbary *et al.* (2011) [120]) was used to obtain the NLCs formulation D.1.2.-ALT (considering its composition was already tested for the production methodology presented in this work, namely as the formulation D.1.2., Table 10). This was done in order to verify if any beneficial change in particle size, zeta potential and encapsulation efficiency could be obtained. The difference between this procedure and the methodology described in section 3.2. is that the surfactant and drug were dissolved in water warmed up to the temperature used for lipid fusion, with subsequent addition of this mixture to the melted lipid phase (with the following methodology being the same as described in section 3.2.).

Table 12 lists the characterization results obtained for the NLCs formulations D.1.2-ALT and D.1.2.7.-D.1.2.11.

Regarding particle size evaluation, differences could be observed as an influence of the type and amount of surfactant present in each formulation. For the formulations containing polysorbate 60 as the surfactant (D.1.2.7., D.1.2. and D.1.2.8.), an increase in the mass of surfactant appeared to lead to decrease in particle size. The same could also be partially observed for the formulations containing polysorbate 80 (D.1.2.9.-D.1.2.11.); indeed, an increase in the mass of surfactant from 100 mg to 200 mg led to a decrease of particle size from 402.05 ± 46.25 nm to 301.02 ± 12.04 nm; further increasing the mass of polysorbate 80 to 300 mg only

showed a small decrease in particle size (namely to 294.82 ± 7.83 nm). Both results were expected, as the existing literature shows that the addition of more emulsifiers (such as the used surfactants) facilitates the emulsification process in the production of NLCs, allowing for a more rigid structure and thus leading to a reduction in size [99]. Concerning PDI values, no particular trend in terms of increased or decreased values could be observed, which all remained under 0.22, thus indicating the presence of fairly monomodal particle size distributions. Comparing formulation D.1.2-ALT with D.1.2., a small increase in particle size was observed for D.1.2.-ALT in comparison to D.1.2.-ALT, although not very significant.

Table 12. Characterization in terms of mean size distribution, PDI, zeta potential, percent encapsulation efficiency and percent drug loading for the NLCs formulations designated as D.1.2.-ALT (produced by a methodology based on the one described by Abdelbary et al. [120]) and D.1.2.7.-D.1.2.11.

NLCs formulations			*Size (nm)*	*PDI*	*Zeta Potential (mV)*	*% Encapsulation Efficiency*	*% Drug loading*
	Surfactant	*Mass (mg)*					
D.1.2.7.		100	462.75 ± 40.50	0.224 ± 0.044	-37.84 ± 1.21	55.516 ± 0.012	0.28 ± 0.00
D.1.2-ALT	Tween 60	200	305.52 ± 15.65	0.189 ± 0.042	-36.01 ± 1.81	58.463 ± 0.063	0.29 ± 0.00
D.1.2.8.		300	232.72 ± 8.89	0.107 ± 0.028	-31.87 ± 1.95	52.923 ± 0.019	0.26 ± 0.00
D.1.2.9.		100	402.05 ± 46.25	0.141 ± 0.070	-34.56 ± 1.60	57.148 ± 0.027	0.29 ± 0.00
D.1.2.10.	Tween 80	200	301.02 ± 12.04	0.135 ± 0.039	-31.22 ± 1.69	60.171 ± 0.005	0.30 ± 0.00
D.1.2.11.		300	294.82 ± 7.83	0.115 ± 0.088	-29.61 ± 1.51	62.333 ± 0.003	0.31 ± 0.00

Each result represents the mean ± standard deviation for n=6 measurements for size and PI, n=10 for Zeta Potential, and n=3 for the percent encapsulation efficiency determinations, per NLCs formulation (one replicate per formulation).

In regard to zeta potential values, the type and amount of surfactant appeared to be of influence. For both types of surfactant, an increase in the mass led to a small decrease in absolute zeta potential values. Comparing the two types of surfactant, formulations containing polysorbate 60 (D.1.2.7., D.1.2. and D.1.2.8.) showed increased absolute zeta potential values in comparison to their polysorbate 80 counterparts (D.1.2.9.-D.1.2.11.), when comparing formulations with the same mass of surfactant. Comparing formulation D.1.2-ALT with D.1.2., a small reduction in the absolute zeta potential value was observed for D.1.2-ALT, in comparison to D.1.2., even though it was not very significant either (analogously to the observed for particle size).

Assessment of the encapsulation efficiency showed no particular difference between the NLCs containing two types of surfactant. For the formulations D.1.2.7., D.1.2. and D.1.2.8., the amount of surfactant did not show a clear influence in terms of increase or decrease of the obtained results; however, for the formulations D.1.2.9.-D.1.2.11. an increase in the amount of surfactant led to a slight increase in the encapsulation efficiency values. A small and detrimental decrease in encapsulation efficiency was observed for D.1.2-ALT when compared to D.1.2., so the alternative method of production did not result in any improvement of this aspect.

Generally, while the amount and type of surfactant were shown to have a slight influence over particle size, zeta potential and encapsulation efficiency, these changes were not significant in view of the optimization process. Also, comparing the NLCs formulations D.1.2. and D.1.2-ALT,

it was found that the modification of the production methodology as described by the literature did not result in any visible improvement of the tested properties of the NLCs.

4.1.6. Overall view on the results of the optimization process

Considering the overall results presented in this section and the totality of the optimization process, two NLCs formulations were considered to hold the best compromise between particle size, PDI, zeta potential and encapsulation efficiency: D.1.2. and D.1.2.10. (which will be further referred to in the document as NLC-P60 and NLC-P80). These formulations employ Witepsol S51 as the solid lipid, oleic acid as the liquid lipid (25% of the total mass of excipients) and 0.5% w/w of MTX, differing only in the type of surfactant in their composition, respectively polysorbate 60 and polysorbate 80 (200 mg). Both formulations exhibited mean particle sizes encompassed in the interval of 100 to 300 nm; the fact that both types of formulation possessed low PDI values and absolute zeta potential levels superior to 30 mV strongly suggested that they would be characterized by good physical stability during storage without the formation of aggregates (the obtained negative values for zeta potential, in detriment to positive values, could also contribute to this good stability [99]); the elevated values of encapsulation efficiency suggested that the therapeutic effect of MTX would be maintained and exercised as intended. The following sections will focus on the study of these NLCs formulations as defined by the objectives proposed for the present thesis work.

Further optimization of the NLCs formulations could have been performed using other types of solid and liquid lipids and surfactants, as well as by further varying proportions of all of the used excipients (in the ranges recommended by the literature) and changing the aforementioned production parameters. It could also be relevant to test other alternative methods of NLC production (e.g. cold homogenization and microemulsion, enumerated by the existing literature on the subject as being the other two major types of methodology employed for the production of NLCs other than hot homogenization [99]). This is pertinent as future work concerning this study.

4.2. Optimized NLCs formulations

4.2.1. Characterization (particle size, PDI, surface charge, encapsulation efficiency and morphology)

As indicated in the previous section, the final optimized formulations that constitute the basis for the rest of the work presented in this document are NLC-P60 and NLC-P80. These formulations employ Witepsol S51 as the solid lipid, oleic acid as the liquid lipid (25% of the total mass of excipients) and 0.5% w/w of MTX, and differ only in the type of surfactant in their composition, respectively polysorbate 60 and polysorbate 80 (200 mg). These formulations were

characterized in terms of particle size and PDI, surface charge and encapsulation efficiency, as listed on Table 13. A graphical representation of these results is also provided in Figure 11 (particle size and PDI) and Figure 12 (zeta potential).

Table 13. Characterization in terms of mean size distribution, PDI, zeta potential, percent encapsulation efficiency and percent drug loading for the NLCs formulations resulting from the optimization process, designated as NLC-P60 (MTX-loaded and drug-free) and NLC-P80 (MTX-loaded and drug-free).

Formulation		*Size (nm)*	*PDI*	*Zeta Potential (mV)*	*% Encapsulation Efficiency*	*% Drug Loading*	n
MTX	NLC-P60	288.77 ± 2.52	0.176 ± 0.018	-39.24 ± 2.61	62.214 ± 1.917	0.31 ± 0.01	4
	NLC-P80	290.94 ± 8.17	0.122 ± 0.023	-37.23 ± 2.89	63.475 ± 4.152	0.32 ± 0.02	4
Drug-free	NLC-P60	298.13 ± 2.99	0.194 ± 0.012	-40.03 ± 1.45			3
	NLC-P80	270.49 ± 7.00	0.139 ± 0.019	-36.48 ± 3.38			3

Each result represents the mean ± standard deviation for n independent replicates (for each replicate, n=6 measurements were obtained for size and PDI, n=10 for Zeta Potential, and n=3 for the percent encapsulation efficiency).

Mean particle size observed for the MTX-loaded formulations NLC-P60 and NLC-P80 was of 288.77 ± 2.52 nm and 290.94 ± 8.17 nm, respectively, while their drug-free equivalents had mean particle size values of 298.13 ± 2.99 and 270.49 ± 7.00 nm, respectively. The Student's t test showed mean particle size to be different between MTX-loaded and drug-free NLC-P60 (P=0.0063) and NLC-P80 (P=0.0179) (with higher size values for MTX-loaded NLCs). This could potentially indicate that part of the MTX contained in the produced NLCs is adsorbed to their surface, thus resulting in an increase in particle size. The mean particle size between drug-free NLC-P60 and NLC-P80 was shown to be different (P=0.0033), but for MTX-loaded NLC-P60 and NLC-P80 (P > 0.05) no statistically significant difference was observed. PDI was similar between MTX-loaded and drug-free formulations, being lower for the formulations NLC-P80 when compared to NLC-P60, thus suggesting a potential higher stability and less amount of aggregates in the formulation NLC-P80.

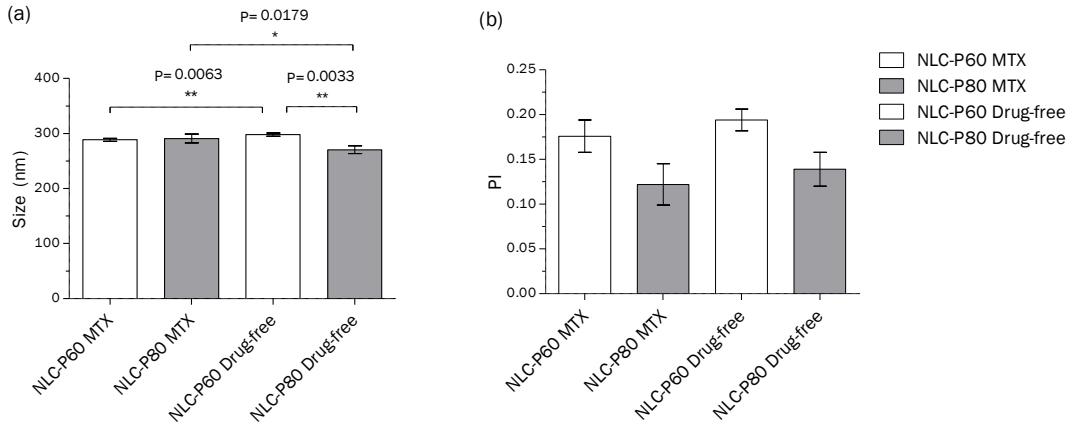

Figure 11. Graphical summary of the characterization in terms of (a) mean size distribution (nm) and (b) PDI for the NLCs formulations NLC-P60 (MTX-loaded and drug-free) and NLC-P80 (MTX-loaded and drug-free). Each result represents the mean ± standard deviation for n=4 independent replicates for MTX-loaded NLC-P60 and NLC-P80, and n=3 for Drug-free NLC-P60 and NLC-P80. The Student's t-test (unpaired, two-tailed, P < 0.05) showed mean particle size to be statistically different between MTX-loaded and drug-free NLC-P60 (P=0.0063) and NLC-P80 (P=0.0179), as well as between drug-free NLC-P60 and NLC-P80 (P=0.0033).

Zeta potential values measured for the MTX-loaded formulations NLC-P60 and NLC-P80 were of -39.24 ± 2.61 and -37.23 ± 2.89 mV, while their corresponding drug-free equivalents had zeta potential values of -40.03 ± 1.45 and -36.48 ± 3.38 mV, correspondingly. No statistical differences were observed between all the values ($P > 0.05$).

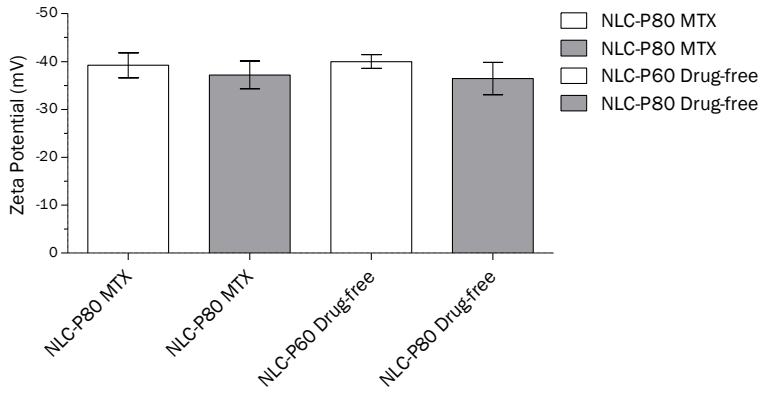

Figure 12. Graphical summary of the characterization in terms of zeta potential for the NLCs formulations NLC-P60 (MTX-loaded and drug-free) and NLC-P80 (MTX-loaded and drug-free). Each result represents the mean ± standard deviation for n=4 independent replicates for MTX-loaded NLC-P60 and NLC-P80, and n=3 for Drug-free NLC-P60 and NLC-P80. The Student's t-test (unpaired, two-tailed, $P > 0.05$) showed no statistical difference between the zeta potential values obtained for all the depicted NLCs formulations.

Concerning encapsulation efficiency, the values obtained for NLC-P60 and NLC-P80 were of 62.214 ± 1.917% and 63.475 ± 4.152%, correspondingly and no statistical differences were observed ($P > 0.05$).

4.2.1.1. Morphology

NLCs morphology in terms of particle shape and size was evaluated by Cryo-SEM for the NLCs formulations NLC-P60 and NLC-P80 (MTX-loaded and drug-free) (Figure 13).

The images show that the NLCs were almost spherical in shape and with smooth surfaces, regardless of their composition. During Cryo-SEM analysis, visualized diameters ranged from approximately 200 to 450 nm; most of the particles presented on Figure 13 show a size range from approximately 230 nm to 280 nm, with no observable difference being noted between NLC-P60 and NLC-P80 (MTX-loaded and drug-free). This range is lower than the values measured by DLS due to the fact that DLS measures the hydrodynamic diameter of particles surrounded by hydration layers in the aqueous medium; to execute Cryo-SEM, all water at the surface of the sample was removed by sublimation, leaving only the particles exposed, which explains this difference in measured size. In addition, it should be noted that results obtained by DLS measurement constitute an average of the sizes of all the particles present in a formulation, thus justifying the total range of diameters visualized during Cryo-SEM analysis. The observed range for particle size was not very surprising since, as previously stated, the hot homogenization process used for NLC production does not allow the acquisition of fully monomodal size distributions [126], and while PDI values measured by DLS were not higher than 0.2 for these formulations, they still indicate the existence of polydispersion.

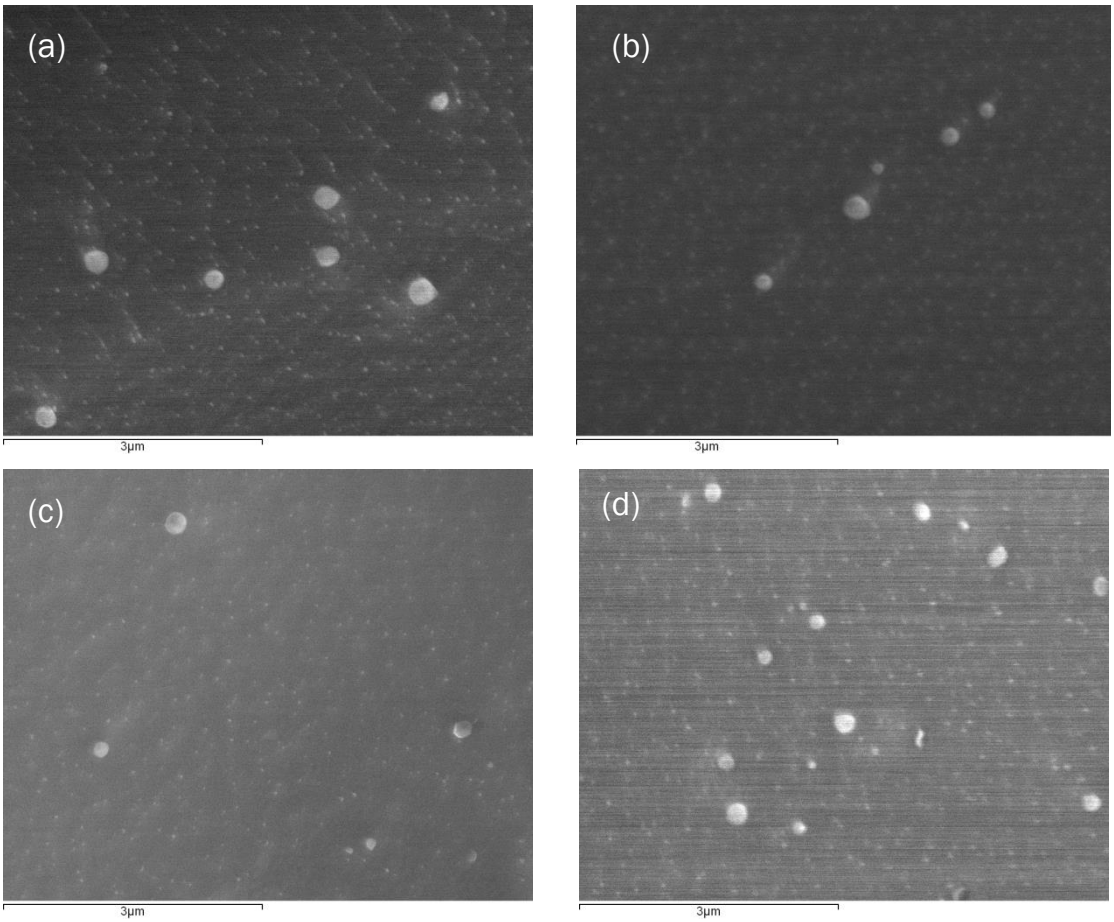

Figure 13. Cryo-Scanning Electron Microscopy (Cryo-SEM) images of NLC (a) MTX-loaded NLC-P60; (b) MTX-loaded NLC-P80; (c) drug-free NLC-P60 and (d) drug-free NLC-P80. The scale indicated below the pictures is 3 µm. Amplification: x20,000. The images are representative of the particles that were most observed in terms of number.

Considering that image resolution of Cryo-SEM is not as good as the one than can be provided by TEM analysis [115], a future work of pertinence in this context would be to observe these NLCs with this technique, in order to further ascertain their morphology.

4.2.1.2. Fourier Transform Infrared (FTIR) Spectroscopy

In order to prove that it was possible to encapsulate MTX in the produced NLCs, infrared spectra of drug-free and MTX-loaded NLCs formulations were obtained, as well as of free MTX, for comparison purposes. The infrared spectra obtained by FTIR analysis are presented on Figure 14.

Comparing the spectra obtained for drug-free and MTX-loaded NLCs with the spectrum of free MTX, it is possible to identify the presence of a peak characteristic of MTX in the spectra of both MTX-loaded NLCs, in contrast to its the absence for the drug-free NLCs, namely at the frequency of 1648 cm^{-1} [128]. The same peak can be observed in the spectrum obtained for free MTX at approximately the same frequency, namely 1640 cm^{-1}, thus corroborating the presence of encapsulated MTX in the MTX-loaded NLCs formulations. This peak is associated with the vibration of the functional groups –COOH present in the structure of MTX [128]. The fact there's a

considerable difference in the intensity of the aforementioned peaks between free MTX and MTX present in the NLCs formulations is due to the fact that the mass of lyophilised NLCs formulations that were tested contained much lower values of MTX mass than those utilized to obtain the spectrum for free MTX.

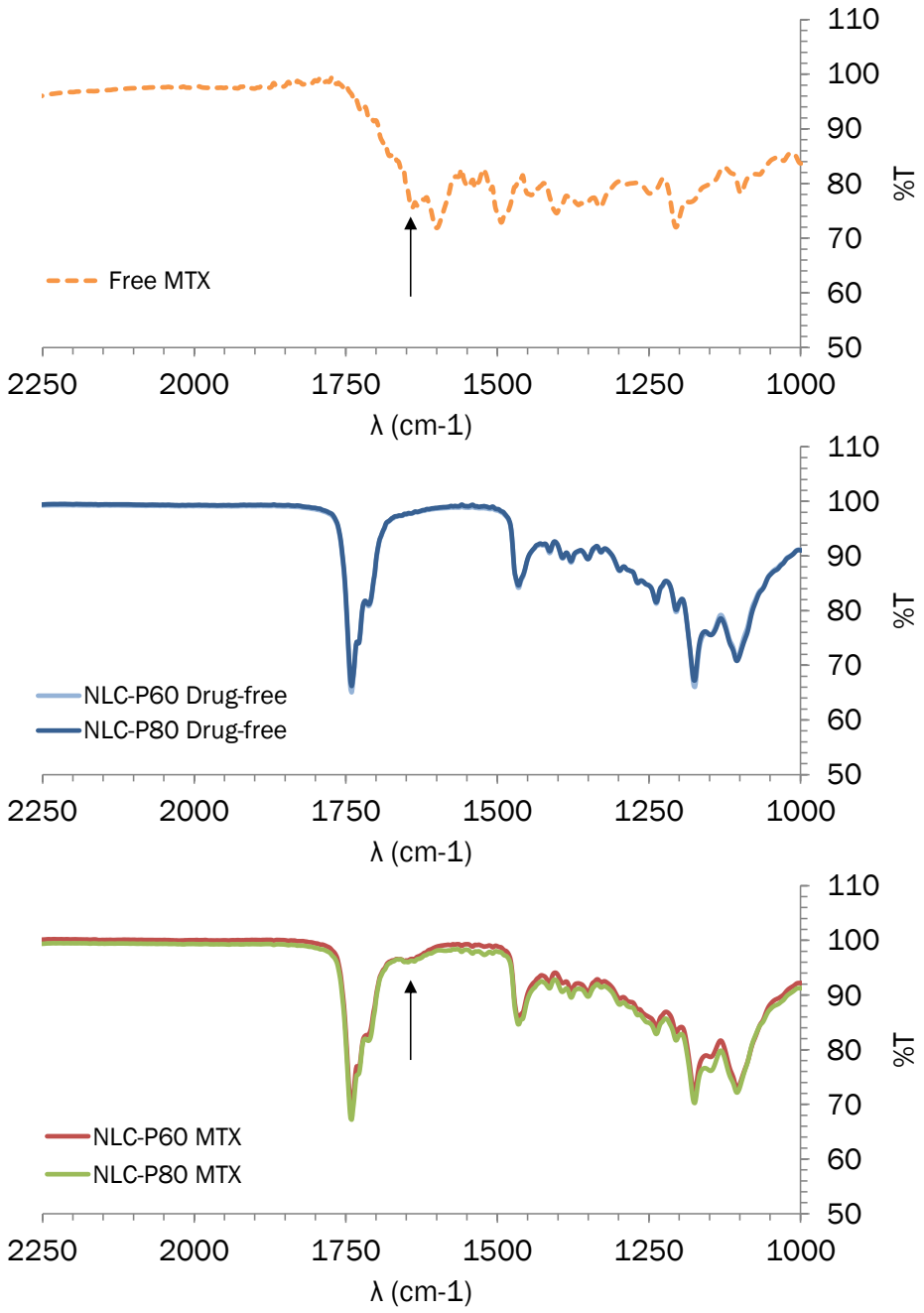

Figure 14. Infrared spectra obtained for FTIR analysis of NLCs formulations NLC-P60 and NLC-P80 (MTX-loaded and drug-free) and free MTX (for comparison purposes). The arrows indicate peaks characteristic of the presence of MTX (1648 cm^{-1} for NLC-P60 and NLC-P80 MTX-loaded and 1640 cm^{-1} for free MTX).

4.2.2. Physical stability of optimized NLCs formulations

NLCs formulations NLC-P60 and NLC-P80 (MTX-loaded and drug-free) were characterized in terms of particle size, PDI, zeta potential and encapsulation efficiency over time (2 and 4 weeks) in order to evaluate their stability during storage at room temperature and 4ºC, two environments of interest regarding the storage of pharmaceutical formulations.

4.2.2.1. Physical stability for storage at room temperature

Concerning storage at room temperature, the results obtained for NLCs formulation characterization over 2 and 4 weeks are presented on Table 14, as well as graphically summarized on Figure 15 for mean particle size and PDI, and Figure 16 for zeta potential.

Table 14. Characterization in terms of mean size distribution, PDI, zeta potential, percent encapsulation efficiency and percent drug loading for the NLCs formulations resulting from the optimization process, designated as NLC-P60 (MTX-loaded and drug-free) and NLC-P80 (MTX-loaded and drug-free) stored at room temperature 2 and 4 weeks after production.

Week	*Formulation*		*Size (nm)*	*PDI*	*Zeta Potential (mV)*	*n*	*% Encapsulation Efficiency*	*% Drug Loading*	*n*
2	MTX	NLC-P60	291.24 ± 7.34	0.175 ± 0.016	-38.32 ± 0.46	3	66.837 ± 0.963	0.33 ± 0.00	4
		NLC-P80	284.73 ± 11.36	0.106 ± 0.038	-34.80 ± 2.24	3	69.620 ± 2.463	0.35 ± 0.01	4
	Drug-free	NLC-P60	296.88 ± 6.81	0.182 ± 0.031	-38.83 ± 2.61	3			
		NLC-P80	267.86 ± 4.82	0.186 ± 0.064	-35.08 ± 0.14	3			
4	MTX	NLC-P60	280.38 ± 11.07	0.146 ± 0.019	-37.71 ± 2.13	1	69.849 ± 1.892	0.35 ± 0.01	4
		NLC-P80	293.90 ± 8.37	0.147 ± 0.019	-36.11 ± 2.06	1	71.620 ± 0.978	0.36 ± 0.00	4

Each result represents the mean ± standard deviation for n independent replicates (for each replicate, n=6 measurements were obtained for size and PDI, n=10 for Zeta Potential, and n=3 for the percent encapsulation efficiency).

Mean particle size, PDI and zeta potential values remained approximately the same for 4 weeks of storage (after production), for both NLCs formulations NLC-P60 and NLC-P80 (MTX-loaded and drug-free). The obtained results indicate a good physical stability without the formation of aggregates of the evaluated NLCs formulations during storage at room temperature, which was already suggested by their characterization after production (by their correspondent PDI and zeta potential values). Regarding the encapsulation efficiency, an apparent increasing trend was observed for the values measured throughout the weeks, although the increase in the depicted values is not elevated and stabilizes after week 4 (with the values of encapsulation efficiency being 68.225 ± 12.323% and 70.606 ± 7.632% for NLC-P60 and NLC-P80, correspondingly, at week 6). This behaviour constitutes the opposite of the expected, namely a decrease in the encapsulation efficiency overtime due to the gradual leaking of therapeutic agent from the NLCs during storage.

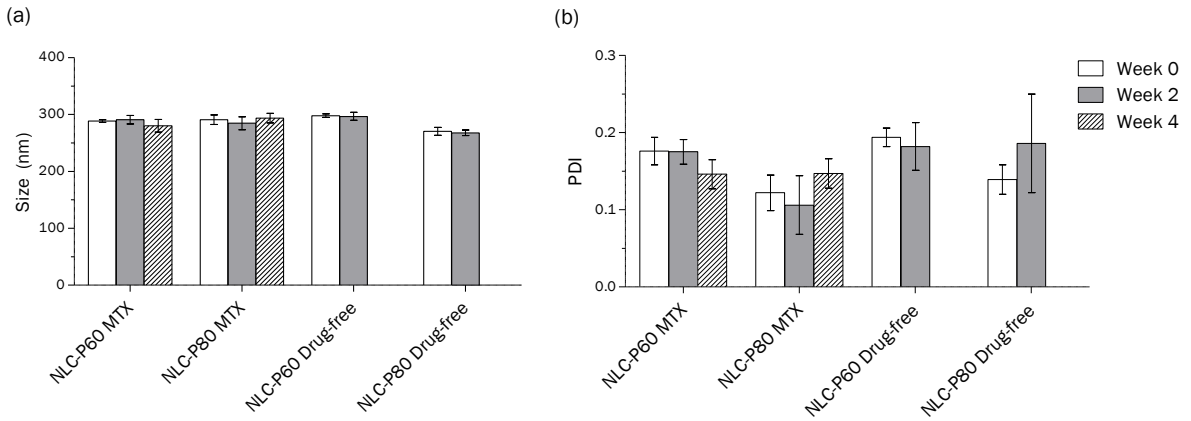

Figure 15. Graphical summary of the characterization in terms of (a) mean size distribution (nm) and (b) PDI for the NLCs formulations resulting from the optimization process, designated as NLC-P60 (MTX-loaded and drug-free) and NLC-P80 (MTX-loaded and drug-free) stored at room temperature for 2 and 4 weeks after production. Each result represents the mean ± standard deviation for n independent replicates (as indicated in Table 14).

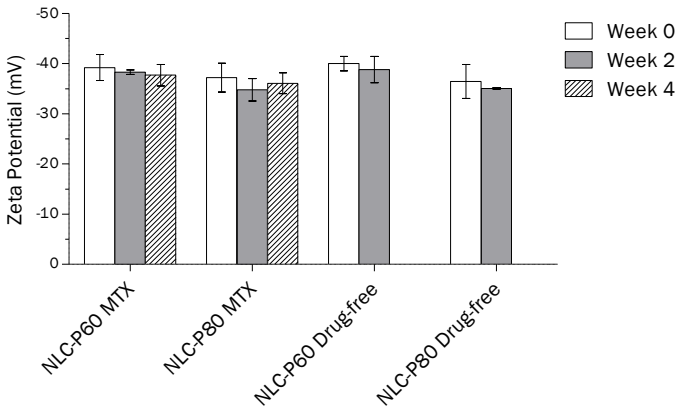

Figure 16. Graphical summary of the characterization in terms of zeta potential for the NLCs formulations resulting from the optimization process, designated as NLC-P60 (MTX-loaded and drug-free) and NLC-P80 (MTX-loaded and drug-free) stored at room temperature for 2 and 4 weeks after production. Each result represents the mean ± standard deviation for n independent replicates (as indicated in Table 14).

4.2.2.2. Physical stability for storage at 4ºC

Regarding storage at 4ºC, the results obtained for NLCs formulation characterization over 2 and 4 weeks are presented on Table 15, as well as graphically summarized on Figure 17 for mean particle size and PDI, and Figure 18 for zeta potential.

During the indicated period of time of storage at a temperature of 4ºC, a significant difference between the stability of the NLCs formulations NLC-P60 and NLC-P80 (both MTX-loaded and drug-free) could be observed. Indeed, by week 2 after production, the NLCs formulations NLC-P60 (MTX-loaded and drug-free) had acquired a gelatinous consistence, thus limiting their characterization. The NLCs formulations NLC-P80 (MTX-loaded and drug-free) both remained with a liquid consistency throughout the weeks. These results suggest that, for storage conditions characterized by lower temperatures, the NLCs formulations with polysorbate 60 as

the surfactant possess lower physical stability, when compared to their polysorbate 80 counterparts. A possible explanation could take into account the fact that polysorbate 60, at temperatures lower than 25ºC, assumes a gelatinous consistency [108] (as opposed to polysorbate 80, which remains liquid [108]), thus inducing the acquisition of the gelatinous consistency observed for the NLCs formulation NLC-P60 during storage at 4ºC. It can also be underlined that the lower PDI values observed for formulation NLC-P80 (0.122 ± 0.023 for MTX-loaded NLCs and 0.139 ± 0.019 for drug-free NLCs) at week 0 after production (in comparison to NLC-P60, with 0.176 ± 0.018 for MTX-loaded NLCs and 0.194 ± 0.012 for drug-free NLCs) already indicated this potential difference in stability and aggregation.

Table 15. Characterization in terms of mean size distribution, PDI, zeta potential, percent encapsulation efficiency and percent drug loading for the NLCs formulation resulting from the optimization process designated as NLC-P80 (MTX-loaded and drug-free) stored at 4ºC for 2 and 4 weeks after production.

Week	*Formulation*		Size (nm)	PDI	Zeta Potential (mV)	n	% Encapsulation Efficiency	*% Drug Loading*	n
2	MTX	NLC-P80	302.43 ± 6.52	0.165 ± 0.049	-35.75 ± 2.78	3	65.352 ± 0.523	0.33 ± 0.00	3
	Drug-free	NLC-P80	278.10 ± 7.77	0.165 ± 0.003	-38.29 ± 1.45	3			
4	MTX	NLC-P80					68.954 ± 0.482	0.34 ± 0.00	3

Each result represents the mean ± standard deviation for n independent replicates (for each replicate, n=6 measurements were obtained for size and PDI, n=10 for Zeta Potential, and n=3 for the percent encapsulation efficiency).

Concerning the results obtained for the NLCs formulations NLC-P80 (MTX-loaded and drug-free), over the course of two weeks, no statistical differences were observed between the values for particle size and PDI ($P > 0.05$). The same behaviour was observed for zeta potential values, which remained approximately the same. Regarding encapsulation efficiency, the same unexpected behaviour associated with an increase of this parameter over time could also be observed, although later in time, namely at week 4 (in detriment to week 2, as observed for the formulation NLC-P80 stored at room temperature). At week 6, the encapsulation efficiency possessed a value similar to the one measured for the same formulation after production (namely 63.809 ± 0.023%).

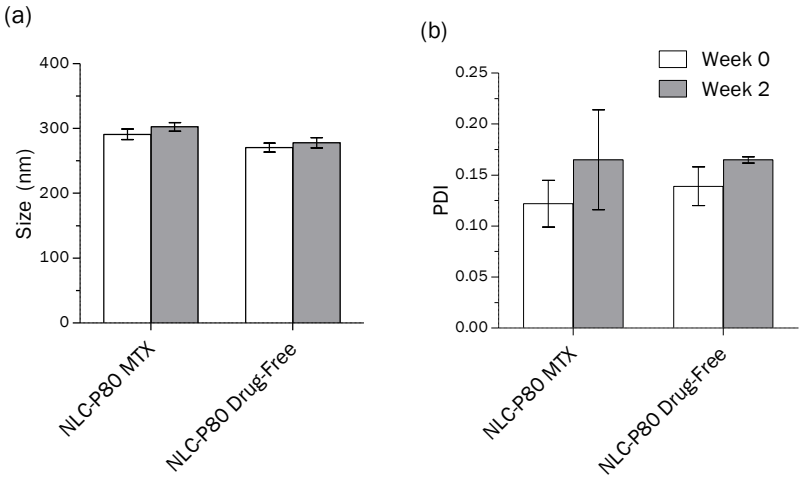

Figure 17. Graphical summary of the characterization in terms of (a) mean size distribution (nm) and (b) PDI for one of the NLCs formulations resulting from the optimization process, designated as NLC-P80 (MTX-loaded and drug-free) stored at 4ºC for 2 weeks after production. Each result represents the mean ± standard deviation for n independent replicates (as indicated in Table 15).

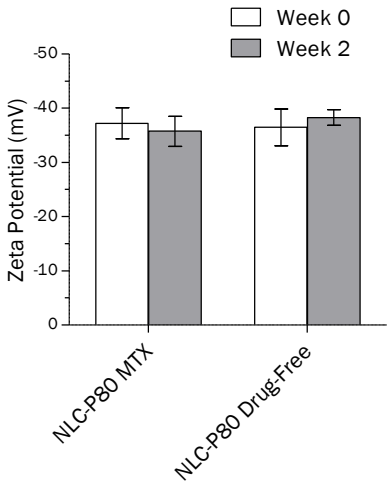

Figure 18. Graphical summary of the characterization in terms of zeta potential for one of the NLCs formulations resulting from the optimization process, designated as NLC-P80 (MTX-loaded and drug-free) stored at 4ºC for 2 weeks after production. Each result represents the mean ± standard deviation for n independent replicates (as indicated in Table 15).

A pertinent future work in the context of the evaluation of the physical stability of the NLCs would be to perform their characterization in terms of particle size, PDI and zeta potential after lyophilisation, with their consequent resuspension in an aqueous medium (considering the fact that lyophilisation could be used as a process to prolong even further the storage time of NLCs).

4.3. Separation of NLCs from unincorporated MTX

In order to further study the optimized NLCs formulations NLC-P60 and NLC-P80, it was necessary to separate the MTX-loaded NLCs from the unincorporated drug present in the corresponding formulations, as it could influence or obscure the acquired data to unknown extents (considering that unseparated formulations comprise of a dose of unincorporated drug

and a dose of encapsulated drug) [129]. For that purpose, three types of methodology were employed, with different outcomes, namely separation by gel filtration, centrifugal units and dialysis, which are commonly applied to this end [99]. The results obtained for each type of tested separation are presented in the following sections.

4.3.1. Separation by Gel filtration

Gel filtration is a technique of interest for separating nanoparticles from unincorporated drug, being inexpensive and allowing quick separation of nanoparticles, and also due to the fact that the capacity of the gel columns used to this end is sufficient for preparative work [129].

The two optimized NLCs formulations were separated by this process (one replicate per formulation), where volumes of 200 µL, 500 µL and 1 mL of original formulation were separated for NLC-P60, and a volume of 200 µL was separated for NLC-P80 (for comparison purposes).

For all the performed separations, after the application of the NLCs formulation, it was possible to quickly visualize the separation between the NLCs and the unincorporated drug (which became more apparent for larger volumes of NLCs formulation). The separated NLCs (appearing as a white mass inside the Sephadex column) eluted first, as their larger molecular weight induced a quicker descending movement (aided by gravity). On the other hand, unincorporated drug could be visualized as a yellow mass spreading over the column as it eluted (considering that free MTX drug constitutes a yellow powder), which was more easily visualized for larger volumes of separated formulation (as they possessed, proportionally, larger masses of unincorporated drug). Unincorporated drug eluted more slowly, due to its smaller molecular weight, which led to the accumulation of drug in the microscopic crevices inside the column's matrix, thus slowing down the descending movement of these molecules.

The volume of separated formulation was shown to affect the time needed for complete elution of the unincorporated drug phase. The separation of NLCs from the unincorporated drug occurred relatively rapidly (as already described), with subsequent elution of the NLCs (which took an average of 10-15 minutes after the beginning of the separation for 200 µL and 500 µL of formulation, and approximately 40-60 minutes for 1 mL). On the other hand, considering the separations performed for the NLCs formulation NLC-P60, complete removal of unincorporated MTX from the Sephadex column was achieved in approximately 2h (after the beginning of the separation) for a volume of 200 µL, 2.5h for a volume of 500 µL, and almost 4h for 1 mL. This is to be expected considering that, as already stated, a larger volume of formulation will proportionally possess a larger mass of unincorporated drug that needs to be eluted.

Figure 19 presents the spectra obtained for aliquots containing unincorporated drug (refer to Figure A6 for the spectra obtained for the aliquots containing the separated NLCs, in the supplementary figures section).

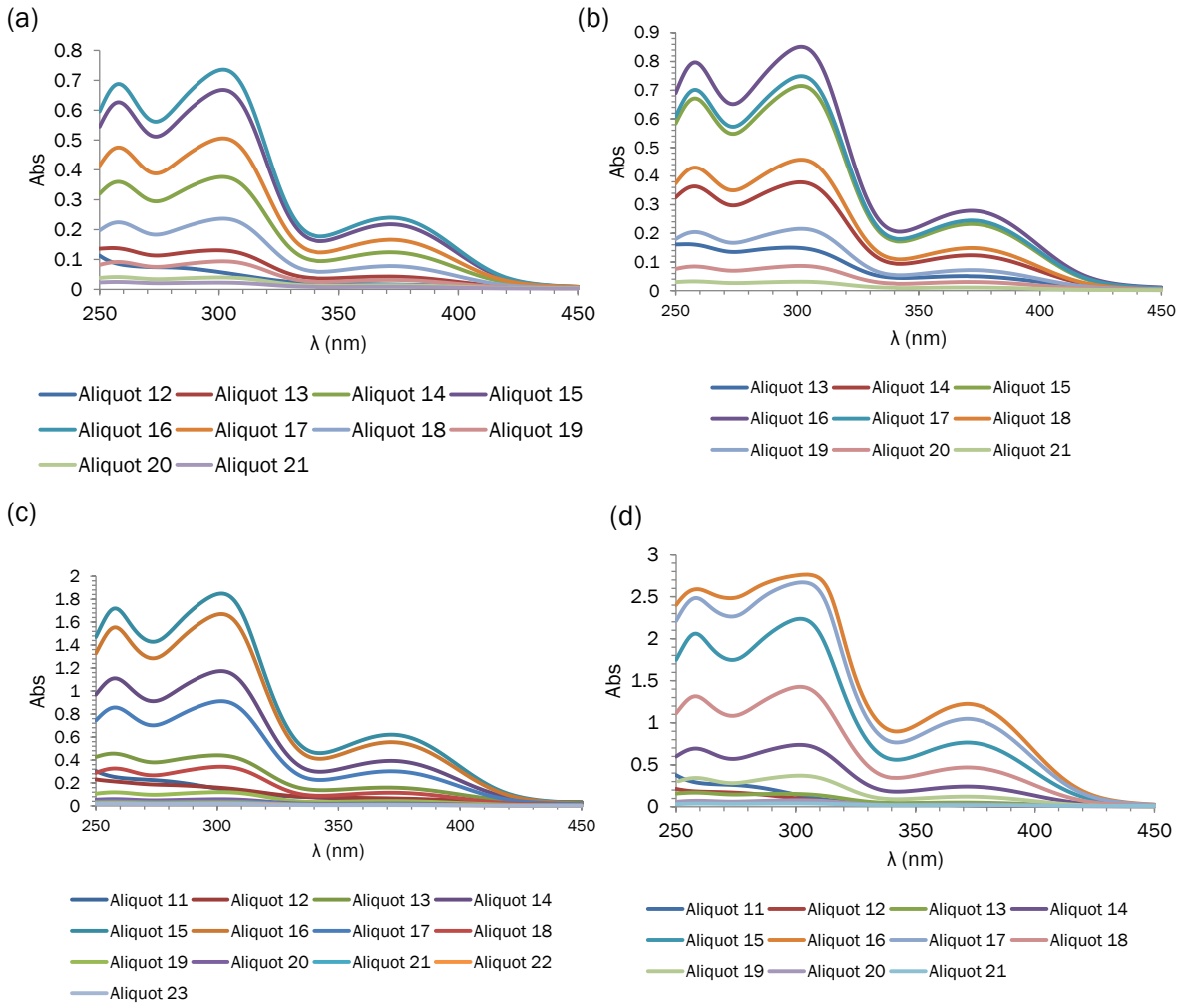

Figure 19. UV-VIS spectra measured for (a) Aliquots 12-21 obtained for the separation of 200 µL of the NLCs formulation NLC-P60, (b) Aliquots 13-21 obtained for the separation of 200 µL of the NLCs formulation NLC-P80, (c) Aliquots 11-23 obtained for the separation of 500 µL of the NLCs formulation NLC-P60, (d) Aliquots 11-21 obtained for the separation of 1 mL of the NLCs formulation NLC-P60 from unincorporated drug (2 mL per aliquot) in a Sephadex G-50 column with a moving phase composed of PBS pH 7.4 buffer. Data points are correspondent to one absorbance measurement for each sample.

Regarding the UV-VIS spectra obtained for the separation of 200 µL of the NLCs formulation NLC-P60, two aliquots of 2 mL each (aliquots 2, 3) contained separated NLCs (with a non-significant amount of separated NLCs present in aliquots 4 and none in 5). Unincorporated MTX was collected from aliquot 13 to 21, reaching the highest value of absorbance for aliquot 16 (as observable by the values of absorbance for the maximum absorbance of MTX, λ_{max}=303 nm). The UV-VIS spectra obtained for aliquot 12 did not present the characteristic peak of absorbance at 303 nm, thus not being considered for MTX quantification. UV-VIS spectra obtained for the separation of 200 µL of the NLCs formulation NLC-P80 show that this separation was analogous to the one performed for NLC-P60, as two aliquots of 2 mL each (aliquots 2, 3) containing separated NLCs were also obtained and the unincorporated MTX was collected from aliquot 13 to 21, reaching the highest value of absorbance for aliquot 16. For the separation of 500 µL of the

NLCs formulation NLC-P60, three aliquots of 2 mL each (aliquots 2-4) contained separated NLCs (with a non-significant amount of separated NLCs present in aliquot 5), thus indicating that the separation of larger volumes of formulation leads to the acquisition of a larger volume of separated NLCs resuspended in PBS pH 7.4 buffer. Unincorporated MTX was collected from aliquot 11 to 23, reaching the highest value of absorbance for aliquot 15. At last, for the separation of 1 mL of the NLCs formulation NLC-P60, three aliquots of 2 mL each (aliquots 2-4) contained separated NLCs (with a non-significant amount of separated NLCs present in aliquot 5). The fact that the same volume of separated NLCs could be obtained for the separation of 1 mL of formulation, in comparison to the observed for the separation of 500 µL, indicates that a higher concentration of separated NLCs (and thereby encapsulated drug) could be obtained for the separation of 1 mL of formulation, in comparison to 500 µL. Unincorporated MTX was collected from aliquot 11 to 21, reaching the highest value of absorbance for aliquot 16.

Overall, the separation profile observed for the various performed separations was the same in terms of number of aliquots containing unincorporated drug and the evolution obtained for the corresponding UV-VIS spectra, differing only in the speed of the separation, as already described (with a slower separation for larger volumes of NLCs formulation). Volume of formulation increased, to a certain point, the volume of separated NLCs. Besides allowing the separation of NLCs from unincorporated MTX, this process also enabled their resuspension in PBS pH 7.4 buffer, as intended for further studying (particularly for cell assays, where a physiologically adequate environment must be provided).

The expected concentration of encapsulated MTX in the separated NLCs was calculated (considering the total obtained volume of separated NLCs and their corresponding encapsulation efficiency values). Unincorporated drug separated in the performed separations was also quantified in order to verify the amount of MTX left in the NLCs formulations. These results are summed up on Table 16. Taking into account the dilution suffered by the NLCs during the separation process, the expected concentration values of encapsulated MTX obtained were low (24.07 µg/mL, 40.12 µg/mL and 80.24 µg/mL for the separation of 200 µL, 500 µL and 1 mL of NLC-P60, correspondingly; 24.33 µg/mL for the separation of 200 µL of NLC-P80). Also, quantification of unincorporated MTX that was separated through this process revealed values larger than those expected for all the formulations, leading to very low percentages of remaining MTX in the separated NLCs. This is unexpected, as the percentage of remaining MTX for each formulation should have been equivalent to their corresponding values of encapsulation efficiency. Furthermore, gel filtration is a separation process well-suited to separate molecules sensitive to harsh environmental conditions, it is not expected to alter parameters such as particle size, zeta potential and encapsulation efficiency [130], so it is not likely that it caused the premature release of MTX during the course of the separation process, also considering that the separation of the NLCs and subsequent elution was very quick in all of the performed separations

(taking 10-15 minutes after the beginning of the separation for 200 µL and 500 µL of formulation, and approximately 40-60 minutes for 1 mL). Nonetheless, the results strongly suggest that NLCs disruption did happen, with unintended loss of MTX.

Table 16. Summarized results obtained for the separation of NLCs from unincorporated drug contained in the NLCs formulations NLC-P60 (200 µL, 500 µL and 1 mL) and NLC-P80 (200 µL) through the use of a Sephadex G-50 column with a moving phase composed of PBS pH 7.4 buffer.

NLCs formulation	*Separated Volume (µL)*	*Total MTX (mg)*	*% Encapsulation Efficiency**	*Number of Aliquots containing separated NLCs (2 mL/ aliquot)*	*Expected [MTX] in the total volume of separated NLCs (µg/mL)*	*Removed MTX (mg)*	*% Remaining MTX*
NLC-P60	200	0.136	70.610 ± 0.038	2	24.07	0.109	20.07
	500	0.341		3	40.12	0.260	23.76
	1000	0.682		3	80.24	0.484	29.00
NLC-P80	200	0.136	71.374 ± 0.010	2	24.33	0.145	-6.03

*Specifically correspondent to the replicate used for each formulation for the depicted experiments.
The results correspond to one replicate of each tested formulation.

Overall, it was found that the process of gel filtration for the separation of unincorporated MTX from the NLCs formulations was not viable, since even though it allowed for separation between the NLCs and free drug, it led to the excessive dilution of the separated NLCs, for all separations.

4.3.2. Separation by Centrifugal Filter Units

The methodology for separation of unincorporated drug by using centrifugal filter units was adapted from the methodology already used to measure the encapsulation efficiency of the produced NLCs formulations. As formulations need to be diluted prior to their centrifugation, multiple simultaneous centrifugations were performed for each formulation; this allowed the collection and resuspension of multiple identical pellets (in PBS pH 7.4 buffer), with the acquisition of more concentrated separated NLCs suspensions than those obtained for the separation by gel filtration. Table 17 lists the results obtained for performed separations (in terms of NLCs formulation and dilution prior to centrifugation).

Analysing the obtained results, it was possible to verify that, for all the separations, it was not possible to separate the entire unincorporated drug present in the formulations. Additionally, it was found that the dilution prior to the centrifugation greatly influenced the amount of MTX removed by this process. Indeed, 53.44 ± 0.49 µg of MTX could be removed from the NLCs formulation NLC-P60 when it was diluted 1:30, while only approximately half of this value (23.25 ± 10.75 µg) could be removed for a dilution of 1:15. This could be explained by the fact that a lower dilution of the formulation prior to centrifugation could have induced the clogging of the filter unit upon centrifugation, thus disabling the movement of unincorporated MTX through the filter (which remained retained in the filter unit, together with the pellet corresponding to the

NLCs) [129]. Formulation NLC-P80, diluted 1:30 prior to centrifugation, had similar results to the ones presented by NLC-P60

Table 17. Summarized results obtained for the separation of NLCs from unincorporated drug contained in the NLCs formulations NLC-P60 (diluted 1:15 and 1:30 prior to separation, with n=2 replicates and n=1 replicates, respectively) and NLC-P80 (diluted 1:15 prior to separation, with n=1 replicate) by the application of centrifugal filter units and collection followed by resuspension of the pellets (containing NLCs separated from free MTX) in PBS pH 7.4 buffer.

NLCs formulations	*Dilution used to separate*	*Total Separated Volume of NLCs (mL)*	*Total MTX prior to separation (µg)*	*Unincorporated MTX prior to separation (µg)*	*Removed MTX (µg)*	*Total MTX remaining (µg)*	*Incorporated MTX (µg)*	*Unincorporated MTX remaining (µg)*	*n*
NLC-P60	1:15	1.6	1090.91	612.32	23.25 ± 10.75	1067.66	478.59 ± 6.72	301.92 ± 17.19	2
NLC-P80	1:15	1.6	1090.91	604.27	22.95 ± 0.37	1067.96	486.64 ± 0.05	289.33	1
NLC-P60	1:30	0.8	545.45	-406.04	53.44 ± 0.49	492.02	951.49 ± 0.23	111.42	1

Overall, this separation process apparently allowed the acquisition of separated NLCs formulations with a higher concentration than the one obtained for gel filtration, thus indicating a larger concentration of encapsulated MTX; however, as a much lower amount of unincorporated drug was separated, these separations were considered to be unsuccessful.

4.3.3. Separation by Dialysis

The methodology of dialysis can be used to separate unincorporated drug contained in nanoparticle formulations [99]. Thus, several optimization steps were taken in order to use this methodology as a viable solution for the separation of unincorporated MTX present in the NLCs formulations.

The first attempt at separation by dialysis employed the settings described as A on Table 6, namely a dialysis membrane with a MWCO of 12,000-14,000, receptor mediums composed of water and water with 10% of DMSO, and sampling times of 10-50 min, 1.5h, 2h and 3h. The NLCs formulation D.1.2.4 was used, as it is similar to NLC-P60 (differing only in the time that it was subjected to high-shear homogenization, namely 5 minutes) as a proof of concept. A volume of 2 mL of formulation was used for each dialysis. Water with 10% DMSO was used considering the increased solubility of MTX in DMSO (100 mM [131]), a polar aprotic solvent that can dissolve polar and nonpolar compounds (as opposed to the low solubility of MTX in water, namely <0.1 g/100 mL at 19ºC [121]), in order to aid the dialysis process. The results obtained for this optimization step are shown on Table 18.

Table 18. Summarized results obtained for the separation of NLCs from unincorporated drug contained in the NLCs formulation D.1.2.4 using a dialysis membrane with a MWCO of 12,000-14,000 and receptor mediums composed of water and water with 10% of DMSO.

NLCs formulation	*Receptor Medium*	*Time (h)*	*Dialysed volume (mL)*	*Total MTX prior to separation (µg)*	*MTX removed (µg)*	*% MTX Removed*	*n*
D.1.2.4	Water	2	2	1409.09	10.76 ± 0.31	0.76% ± 0.02%	1
		3			18.44 ± 0.75	1.31% ± 0.05%	
	Water + 10% DMSO	1.5	2	1409.09	11.10 ± 1.32	0.79% ± 0.09%	
		2			17.34 ± 0.51	1.23% ± 0.04%	
		3			36.55 ± 0.11	2.59% ± 0.01%	

Data points correspond to one replicate (n=3 measurements for MTX removed).

While samples of the external receptor medium were collected overtime, as already explained, Table 18 only shows the results obtained for the quantification of MTX 2 and 1.5 hours after the beginning of the dialysis (for water and water with 10% of DMSO as receptor mediums, correspondingly). This is due to the fact that no detectable MTX was found in the receptor mediums prior to these time points. The fact that the process of dialysis was faster for the receptor medium containing 10% of DMSO corroborates the proposition that its inclusion would promote the dialysis process by further solubilizing the removed MTX. Nonetheless, considering that approximately 40% of the total MTX in the tested formulation was comprised of unincorporated drug (D.1.2.4 had an encapsulation efficiency of approximately 60%, as indicated on Table 10), the amount of separated MTX over the course of 3 hours was very small. Indeed, not more than 1.31% ± 0.05% and 2.59% ± 0.01% of the total MTX contained in the tested formulation could be removed, with the receptor mediums composed of water and water with 10% of DMSO, correspondingly.

Consequently, the next step in the optimization process employed the settings described as B in Table 6, namely dialysis tubing with a MWCO of 10,000, receptor mediums composed of water with 20% of DMSO and water with 20% of 1,2-propandiol [132], and sampling times of 0.25h, 0.5h, 0.75h, 1h, 2h, 3-6h and 8h. One replicate of the NLCs formulation NLC-P60 was used (2 mL of formulation for each dialysis). The results obtained for this optimization stage are listed on Table 19.

Table 19. Summarized results obtained for the separation of NLCs from unincorporated drug contained in the NLCs formulation NLC-P60 using a dialysis membrane with a MWCO of 10,000 and receptor mediums composed of water with 20% of DMSO and water with 20% of 1,2-propandiol.

NLCs formulation	*Receptor Medium*	*Time (h)*	*Initial dialysed volume (mL)*	*Final dialysed volume (mL)*	*Total MTX prior to separation (µg)*	*MTX removed (µg)*	*% MTX removed*	*Free MTX in the dialyzed volume (µg)*	*n*
NLC-P60	Water + 20% DMSO	0.25	2	1.25	1363.64	36.28	2.66		1
		0.5				66.93	4.91		
		0.75				86.75	6.36		
		1.5				97.01	7.11		
		2				132.93	9.75		
		3				157.44	11.55		
		4				217.59	15.96		
		5				258.94	18.99		
		6				293.21	21.50		
		8				329.73	24.18	513.02 ± 0.05	
	Water + 20% 1,2-propandiol	0.75	2	1.25	1363.64	10.78	0.79		
		1.5				12.35	0.91		
		2				31.77	2.33		
		3				49.79	3.65		
		4				99.10	7.27		
		5				134.42	9.86		
		6				171.03	12.54		
		8				208.44	15.29	628.90 ± 0.56	

Data points correspond to one replicate (with n=1 measurement for MTX removed).

Analysing the obtained results, it is possible to observe that an increase in the percentage of DMSO led to an increase in the speed and quantity of MTX removed from the tested formulations, comparing the dialysis performed with receptor mediums containing water with 10% and 20% of DMSO. The same type of behaviour could also be observed for the dialysis in the receptor medium containing water and 20% of 1,2-propandiol, although this dialysis was slower and, for the same period of time (8h), removed less MTX (208.44 ± 15.29 µg) than its DMSO-containing counterpart (329.73 ± 24.18 µg). In this optimization step, the measurement of the encapsulation efficiency was performed with the dialysed formulation (as documented in section 3.3), in order to quantify the amount of unincorporated drug present. A large amount of unincorporated MTX was quantified for both dialysed formulations, namely 513.02 ± 0.05 µg and 628.90 ± 0.56 µg, corresponding to the two performed dialysis. A possible explanation to this premature release of MTX over the course of the dialysis is that both DMSO and 1,2-propandiol could have entered the dialysis bag (considering the diffusion principle underlying the process of dialysis), thus interfering with the NLCs and inducing the unintended release of encapsulated drug. Since it was possible to remove a large percentage of MTX (approximately 24% and 15% for

the dialysis with the receptor mediums containing 20% DMSO and 20% 1,2-propandiol, correspondingly), it was expected to obtain reduced values of unincorporated drug in the dialysed formulations (considering that the tested replicate for the formulation NLC-P60 had an encapsulation efficiency value of approximately 70%). However, this was not verified. Also, it should be underlined that, upon further analysis of the dialysis tubing used for this process, it was revealed that its use adulterated the quantification of MTX. This could have been due to components used in the manufacturing of this dialysis tubing, which that could have been released during the dialysis process and interfered in the UV-VIS spectrophotometric quantification of MTX. Thus, the quantification of removed MTX overtime for the present results must have been inflated, as a consequence of the use of this dialysis tubing.

The next step in the optimization process was based on the methodology used by Misra *et al.* (2010) [132], specifically in terms of the receptor medium utilized, namely PBS pH 7.4 buffer. Besides favouring a quicker removal of unincorporated MTX present in the formulations, it allowed the acquisition of NLCs formulations that are suspended in PBS pH 7.4 due to the principle of diffusion (and as intended for further studying). The other settings utilized in this last step of optimization are those described as C in Table 6, namely a dialysis membrane with a MWCO of 6,000-8,000 and a sampling time of 15 minutes. Both NLCs formulations (NLC-P60 and NLC-P80) were used in this step (1 mL of formulation for each dialysis). Table 20 summarizes the results obtained for the step of optimization of the dialysis process of separation.

Table 20. Summarized results obtained for the separation of NLCs from unincorporated drug contained in the NLCs formulations NLC-P60 and NLC-P80 using a dialysis membrane with a MWCO of 6,000-8,000 and a receptor medium composed of PBS pH 7.4 buffer.

	NLCs formulation	*Receptor Medium*	*Time (min)*	*Initial dialysed volume (mL)*	*Final dialysed volume (mL)*	*Total MTX prior to separation (µg)*	*MTX removed (µg)*	*% MTX removed*	*n*
A	NLC-P60	PBS pH 7.4	15	1	1	681.82	84.97	12.46%	1
	NLC-P80		15	1	1	681.82	87.84	12.88%	1
B	NLC-P60		15	1	1	681.82	128.64 ± 33.54	18.87% ± 4.92%	2
	NLC-P80		15	1	1	681.82	112.59 ± 0.79	16.51% ± 0.12%	2

Data points correspond to (A) one replicate (with n=1 measurements of MTX removed) and (B) two replicates (with n=3 measurements of MTX removed).

Concerning the results presented on Table 20, these were obtained for one replicate of each of the NLCs formulations (NLC-P60 and NLC-P80, A) and for the repetition of the dialysis process with two replicates for each NLCs formulation (NLC-P60 and NLC-P80, B). Regarding the separations identified as (A), a 15 minute long dialysis was able to remove approximately 13% of MTX from both formulations, thus reducing the amount of unincorporated drug in these formulations (considering that these replicates had encapsulation efficiency levels of approximately 70%). For the separations identified as (B), the results were similar to the ones

already discussed above: the 15 minute long dialysis process was able to remove 18.87 ± 4.92% and 16.51 ± 0.12% of the total MTX present in the formulations NLC-P60 and NLC-P80, respectively.

Analysing the results obtained for this optimization sequence, a 15 minute-long dialysis of 1 mL of NLCs formulation in a receptor medium containing PBS pH 7.4 buffer was revealed to be the best alternative to separate unincorporated drug present in these formulations. Consequently, this process was chosen to obtain NLCs formulations separated from unincorporated drug to be further studied (as described in the next sections).

4.4. *In vitro* MTX release

To evaluate the release of MTX from the optimized NLCs formulations, *in vitro* release assays were performed using a dialysis cellulose membrane diffusion technique. All the presented *in vitro* release assays were performed for the simulated physiological conditions of the plasma, employing a receptor medium composed of PBS pH 7.4 buffer at a temperature of 37ºC, thus evaluating the MTX release profile from the NLCs after topical application.

4.4.1. In vitro *release assay for the evaluation of the influence of dialysis membranes in MTX quantification*

Figure 20 shows an *in vitro* release assay executed for one replicate of the NLCs formulation NLC-P80, prior to separation of the unincorporated drug. This assay was performed for two types of dialysis membranes, namely dialysis tubing with a MWCO of 10,000 (Figure 20A) and a dialysis membrane with a MWCO of 6,000-8,000 (Figure 20B; these values of MWCO were chosen in regard to the molecular weight of MTX, namely 454.4 Da [127], thus allowing its movement out of the dialysis bag, while preventing the release of the NLCs). These assays were performed in order to verify whether the type of dialysis membrane used could affect the results, considering the results obtained for the separation of unincorporated drug from the NLCs formulations by dialysis listed on Table 19 (section 4.3.3). To this end, samples were collected only for the first 5 hours of the release assays. Indeed, for the same volume of the NLCs formulation NLC-P80 (corresponding to 250 µg of incorporated MTX), two different drug release profiles could be obtained, depending on the dialysis membrane. While both profiles had the same shape, the profile obtained for the dialysis tubing (A) showed % MTX release values that were much larger than 100% of MTX release (reaching values as high as approximately 150%). In contrast, the pattern obtained for the dialysis membrane (B) showed the expected release behaviour already observed for the previous preliminary assays performed with the NLCs formulation NLC-P80. This could have been due to molecular elements used in the manufacturing of the aforementioned dialysis tubing, which could have been released during the dialysis process

and interfered in the UV-VIS spectrophotometric quantification of MTX. Thus, these results indicated the dialysis membrane with a MWCO of 6,000-8,000 as being the most adequate one to perform further assays (both *in vitro* release assays as well as separation of unincorporated drug by dialysis, as described earlier).

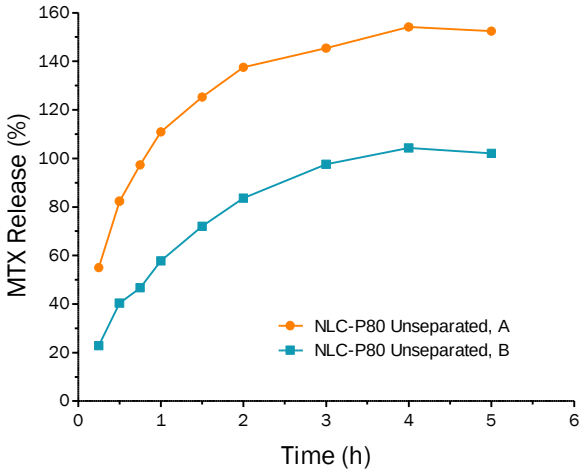

Figure 20. *In vitro* release of MTX from NLCs formulation NLC-P80 (unseparated from unincorporated drug) in (A) dialysis tubing with a MWCO of 10,000 and (B) a dialysis membrane with a MWCO of 6,000-8,000, to a receptor medium containing PBS pH 7.4 buffer (80 mL) at 37ºC. Data points correspond to one replicate (n=3 measurements for MTX release).

4.4.2. In vitro *release assays for NLCs formulations*

Figure 21 shows *in vitro* release assays obtained for three replicates of the NLCs formulations NLC-P60 and NLC-P80 separated from unincorporated drug by the optimized dialysis process (as depicted on section 4.3.3, Table 20). It is possible to observe a similar biphasic drug release profile for both types of formulation, characterized by a first phase (burst release) where approximately 70-80% of the MTX contained in the formulation was released (in the first 3-4 hours), followed by a phase of sustained release over the remaining period of time until 24h. This quick release profile suggests that, upon topical application, the MTX would diffuse from the NLCs, and diffusion through the skin layers would be aided by the presence of the NLCs, due to their hydrating/moisturizing and occlusive properties (specifically through the hydration of the stratum corneum, reducing corneocyte packing and widening gaps between these cells [99]).

The quick release of MTX observed in the first phase further supports the hypothesis that not all MTX is incorporated in the core of the produced NLCs, but also adsorbed to their surface [99, 129] or present in their outer shell [99]. Thus, this leads to a quick release of MTX in the first phase (corresponding to the MTX adsorbed to the NLCs and incorporated in their outer shells) and a more prolonged release in the second phase (associated with the drug incorporated in the core of the NLCs). Other possible explanations for this fast release of MTX include the fact that a portion of MTX could also be solubilized on surfactant micelles present in the formulation [120]. Furthermore, this type of release pattern is consistent with the work of Abdelbary *et al.* (2011)

[120], which documents the encapsulation of MTX (as a model drug for the treatment of multiple diseases) in NLCs, in which similar biphasic drug release profiles were obtained for the same period of 24 hours. These authors propose, based on previous studies, that biphasic drug release profiles, such as the ones here presented, indicate that the difference in melting points between the solid and liquid lipids lead to the crystallization of the solid lipid first, causing the formation of a solid core in the NLCs, from which the drug is slowly release (as verified in the second phase of these release profiles). The outer shell of the NLCs, comprised mostly of liquid lipid and surfactants, leads to the formation of a drug-enriched interface layer, which is subsequently associated with the fast release of MTX observed in the first phase of the biphasic drug release profile (together with the drug contained in surfactant micelles potentially formed during the process of NLC production) [120].

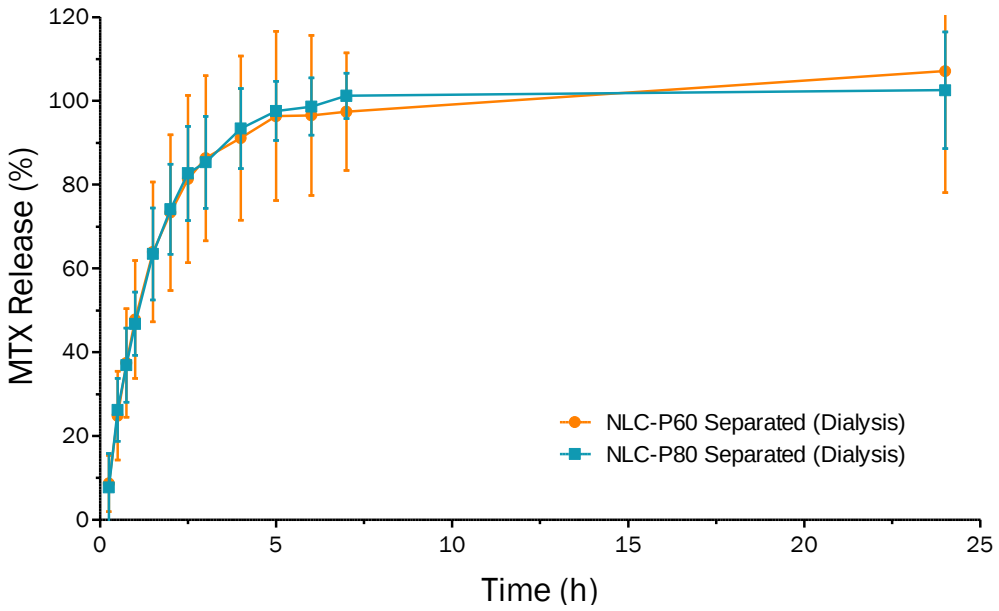

Figure 21. *In vitro* release of MTX from NLCs formulations NLC-P60 and NLC-P80 in dialysis membranes with a MWCO of 6,000-8,000 to a receptor medium containing PBS pH 7.4 buffer (80 mL) at 37°C. Data points correspond to the mean ± standard deviation for n=3 replicates (n=3 measurements of MTX release per replicate).

While a sustained drug release profile characterized by a steadier and slower release would potentially be more favourable (as characteristic of ideal drug-release systems [89, 95]), this rapid release biphasic profile may prove to be useful, considering the dermal application intended for these NLCs formulations. Indeed, upon topical application of therapeutic formulations on the skin, it could be argued that these formulations would not stay on the skin for periods of time longer than 24h; indeed, daily actions such as changing clothes and bathing, as well as physiologic reactions like sweating, would restrict the permanence of the applied topical formulations on the skin (thus potentially restricting the actual therapeutic dose administered to the patients suffering from psoriasis). Hence, the rapid but subsequent gradual release profile of

MTX from these NLCs could prove to be useful to psoriasis patients, allowing for a quick and still gradual administration of MTX on the skin for a smaller period of time, with a full therapeutic dose (without the unintended loss of therapeutic substance due to the already enumerated reasons). Nevertheless, further optimization of the NLCs formulations in view of their drug release patterns (in addition to their characterization in terms of particle size, surface charge and encapsulation efficiency) would be of interest in order to further modulate MTX release by these drug-delivering systems (with pertinence as future work in the context of this study).

4.5. *In vitro* skin permeation

Permeation studies are important for evaluating the capacity of a formulation and the therapeutic compounds it incorporates to move through a barrier, specifically the skin, as this is crucial to the achievement of the therapeutic effect mediated by the released substance. Thus, in accordance to the dermal application intended for the produced NLCs formulations, the permeation profile of MTX was evaluated *in vitro* through the use of Franz Cell Diffusion Assemblies. As a model barrier, pig ear skin was chosen, as pig soft tissue is very similar to its human counterpart when it comes to morphology and function [122]. Care was taken in keeping consistency between the used skin fragments, in order to allow for comparison between different assays, within the same sets of results.

4.5.1. Preliminary results using PBS pH 7.4 as the receptor medium, for MTX-loaded and drug-free NLCs, and free MTX

A preliminary set of results was obtained utilizing PBS pH 7.4 buffer as the receptor medium and three different compositions in the donor chamber, with one replicate per assay, as presented on Figure A7, in the supplementary figures section. More specifically, MTX-loaded and drug-free NLCs formulations (NLC-P60) were tested for permeation (prior to separation of unincorporated drug, with 300 µg of total MTX in the MTX-loaded formulation and an equivalent mass of excipients used for the drug-free NLCs formulation) as well as free MTX (300 µg in PBS pH 7.4 buffer). UV-VIS spectra were measured for the samples collected over time (1-6h/1-8h, 24h and 48h after the beginning of the assay), in order to observe their evolution overtime.

Analysing the UV-VIS spectra obtained for the abovementioned preliminary assays, it was not possible to observe a trend for the majority of the spectra obtained for the samples collected over time for the three assays. Moreover, these results suggest that elements associated with the skin fragments are released overtime into the receptor medium and could strongly affect the adequate detection and quantification of the permeated drug, constituting a strong source of interference.

4.5.2. Optimization of the type of receptor medium by testing the permeation of free MTX

The second set of results was obtained with the purpose of optimizing the receptor medium utilized in the permeation assays by adding solubilizers, so that a better definition of the absorbance peak at 303 nm correspondent to the presence of MTX could be achieved (thereby allowing its adequate quantification). Receptor mediums comprised of PBS pH 7.4 buffer, PBS pH 7.4 buffer with 10% DMSO and ethanol:PBS pH 7.4 buffer in a ratio of 3:7 were tested to this end, with one replicate per assay, as visualized on Figure 22.

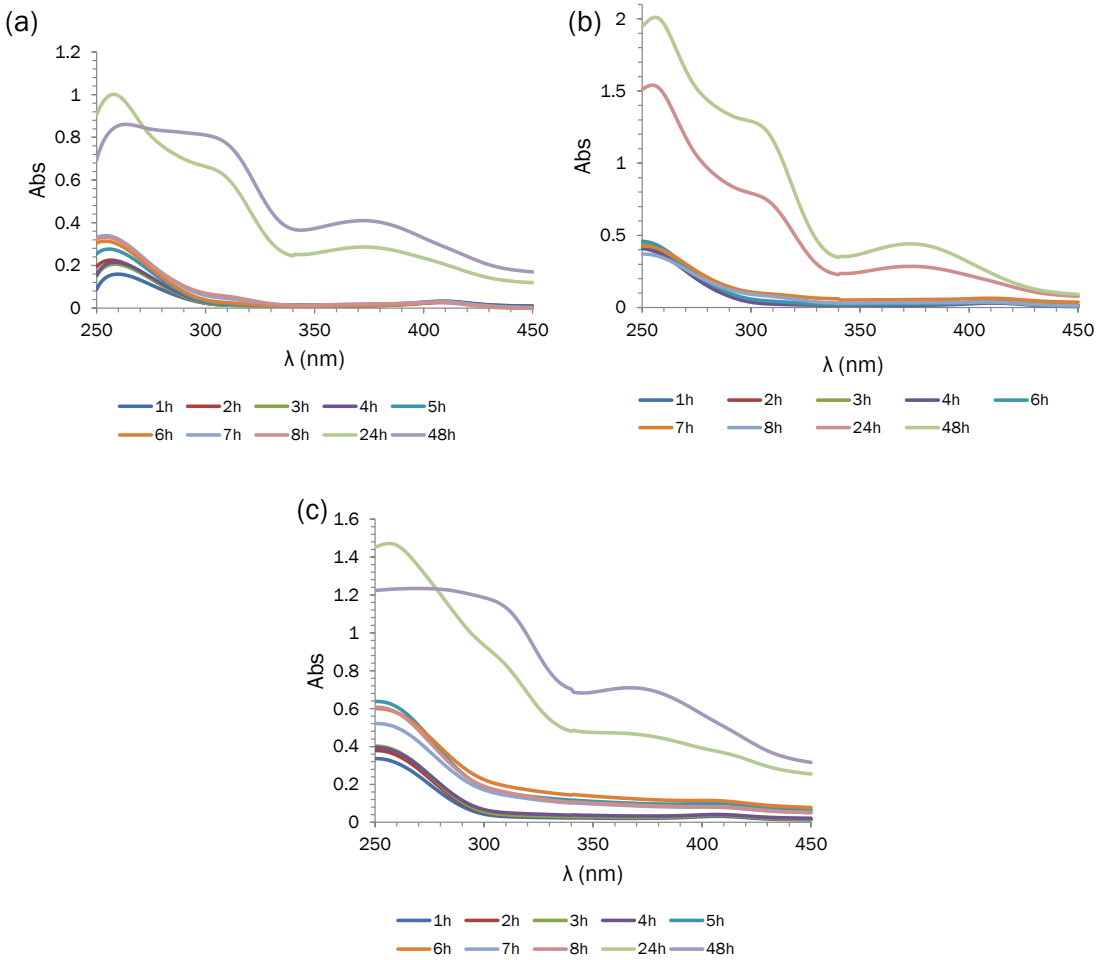

Figure 22. UV-VIS spectra obtained for samples collected overtime for *in vitro* skin permeation assays performed at 37ºC with donor volume corresponding to 300 µg of free MTX in PBS pH 7.4 (1 mg/mL), where the receptor medium consisted of (a) PBS pH 7.4 buffer with 10% DMSO (total volume of 5 mL), (b) Ethanol:PBS pH 7.4 buffer (3:7, total volume of 5 mL) and (c) PBS pH 7.4 buffer (5 mL). Data points are correspondent to the mean of n=3 absorbance measurements for each sample, with one replicate per assay.

Analysing the obtained results, it was possible to observe a much clearer trend in values of absorbance in the UV-VIS spectra, in comparison to the above-referenced preliminary set of results. Indeed, for all the three assays, it was possible to observe spectra with approximately the same aspect for the period ranging 1-8h (with a gradual increase of the absorbance values until

the period of 8h for the receptor mediums composed of PBS pH 7.4 with 10% of DMSO, and PBS pH 7.4 buffer). For the receptor mediums containing DMSO and ethanol (Figure 22a and Figure 22b) it was also possible to observe the peak in absorbance at 303 nm corresponding to the presence of MTX, although with very low absorbance values, for the period of time of 1-8h. For 24h-48h, it was possible to observe a large increase in absorbance values for all the assays. For the receptor mediums containing PBS pH 7.4 with 10% of DMSO and PBS pH 7.4 (Figure 22a and Figure 22c), the corresponding spectra for 24h-48h had the same aspect, although the range of absorbance levels was larger for PBS pH 7.4 than for its DMSO-containing counterpart; in addition, the definition of the peak corresponding to MTX at 303 nm was more defined for the receptor medium containing DMSO, at 24h, with a loss in definition of the peak for both assays at 48h. On the other hand, for the receptor medium containing ethanol:PBS pH 7.4 buffer in a ratio of 3:7 (Figure 22b) it was possible to observe distinct and increasing peaks of absorbance at 303 nm for both the samples collected at 24h and 48h.

DMSO was incorporated in the receptor medium for the same reason already explained in section 4.3.3. – the increased solubility of MTX in this compound should aid in its permeation and subsequent quantification, allowing for the acquisition of a more defined peak of absorbance for the wavelength of 303 nm; the incorporation of ethanol in the receptor medium was also tested for the same reason, based on the methodology employed by Lin *et al.* (2010) [102], where the authors used the same receptor medium configuration to perform *in vitro* permeation assays of MTX (and calcipotriol). The donor volume utilized for the three assays contained 300 µg of MTX in PBS pH 7.4, in order to characterise the general permeation profile of MTX through the skin barrier.

Assessing these results from a general perspective, it is possible to state that the most adequate receptor medium for the identification and quantification of MTX permeated through the skin barrier proved to be ethanol:PBS pH 7.4 buffer in a ratio of 3:7, although absorbance values obtained at 303 nm for this receptor medium were similar to the ones obtained for PBS pH 7.4. In addition, it was also shown that the freshness of the acquired pig ear skin (assured by a provider of trust) is of major importance for the quality of the results, as the current set of results did not show major interference from the components released from the skin barrier, as opposed to the previously presented set of results (where the pig ear skin was obtained from another provider).

From this set of results, it was possible to quantify the amount of MTX permeated over time through the skin and consequently obtain the percent permeation of this compound over time, as represented in Figure 23, for the three different receptor mediums utilized (presented for comparison purposes). It should be noted that this quantification was performed using a calibration curve of MTX in PBS pH 7.4 for all the assays; however, calibration curves for MTX in ethanol:PBS pH 7.4 (3:7) and in PBS pH 7.4 with 10% DMSO should have been obtained for the

purpose of quantification (which was not possible due to time restraints). Nonetheless, major differences in quantification arising from this point are not expected.

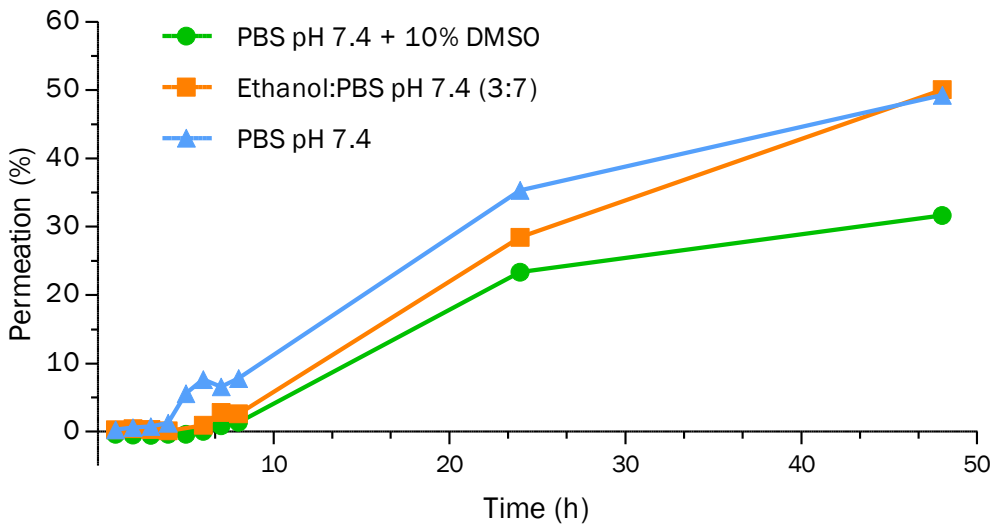

Figure 23. Permeation of free MTX (300 µg in PBS pH 7.4, 1 mg/mL MTX) through pig ear skin over a total period of 48 hours to different receptor mediums (PBS pH 7.4 buffer containing 10% of DMSO, Ethanol:PBS pH 7.4 buffer in a ratio of 3:7 and PBS pH 7.4 buffer, in a total volume of 5 mL). Data points are correspondent to the mean of n=3 measurements for each sample, with one replicate per assay.

The observed permeation profiles have an expected behaviour, namely comprising a lag phase, where the compound is permeating through the skin barrier to reach the receptor compartment (corresponding to the first 6-8h) and a steady state phase where the compound is permeating through the skin at a constant rate (indicated by the results obtained for 24h and 48h). It should be noted that, in this case, as only free MTX was tested, the only rate-limiting step associated with this process (characterized by the aforementioned lag phase) is permeation of the drug itself through the skin. In the presence of MTX-loaded NLCs, the release of MTX from the NLCs could also prove to be a rate-limiting step in the permeation process (although this is not suggested by the previously presented *in vitro* drug release assays, where a quick release of MTX was observed). Nonetheless, a different strategy concerning sampling times would be needed in order to obtain a better definition of the presented permeation profiles, so that the range of the lag and steady state phase of MTX movement through the skin barrier could be more accurately defined. The obtained curves show that, for a time period of 48h, not more than 50% of the drug present in the donor chamber permeated through the skin barrier into the receptor compartment. This could be due to the fact that, as formerly referred, MTX has a low partition coefficient (log P Octanol/Water), namely of -1.85, and the current literature states that, ideally, a topically administrated drug should not only have poor aqueous solubility (as is the case of MTX) but also high lipophilicity, characterized by a partition coefficient higher than 6.0 [90], which does not happen in this case. Moreover, the stratum corneum greatly reduces the passage of molecules with a size larger than 500 Da [90], which could have constituted a partial hurdle to the passage

of MTX through the skin barrier (since its molecular weight is close to 500 Da, namely 454.4 Da [127]). Even so, it should be noted that the skin model utilized for this assays is healthy, thus not possessing the characteristics of diseased skin present in psoriatic plaques. Indeed, drug delivery to an integral skin barrier is very challenging [91]. However, when this barrier function is compromised by a pathology such as psoriasis (in terms of inflammation and keratinocyte hyperproliferation), enhanced diffusion of therapeutic agents (and correspondent drug-delivery carriers) should be observed [94]. Indeed, this has been observed by Lin *et al.* (2010) for the permeation of MTX released from NLCs, which was increased in hyperproliferative skin, in comparison to normal skin [102]. The same should be observed for the disruption of the skin barrier by using penetration enhancers [91], such as alcoholic solutions. Nevertheless, an increase in the permeation of MTX is expected, when released by the produced NLCs, due to the hydrating and occlusive properties of these particles, which should greatly aid in the delivery and subsequent diffusion of MTX through the skin layers, further aided by the lipid exchange between the stratum corneum and the NLCs. The potential diffusion of these particles through the skin into the follicles (transappendageal pathway of permeation) could also help in this direction, with subsequent accumulation of the NLCs in these structures (due to the high lipid content present in them, corresponding to the sebum produced by the sebaceous glands), resulting in prolonged action [99]. In addition, as already stated, the produced NLCs incorporate oleic acid in their composition, which can act as a penetration enhancer [99] (although inclusion of other penetration enhancers could still be relevant in aiding this diffusion).

Further analysing the obtained results, it was possible to observe that, at 48h, a percent permeation of only 30% was obtained with PBS pH 7.4 with 10% DMSO as the receptor medium, in contrast to the observed for the other receptor mediums, for which a 50% of MTX permeation was observed. Nevertheless, the most correct release profile can be considered to be the one with the receptor medium composed of ethanol:PBS pH 7,4 buffer (3:7), as it was shown earlier that this receptor medium allowed the acquisition of more defined absorbance peaks at 303 nm (as well as the overall spectra) for the quantification of MTX, thus providing more reliable absorbance values to proceed to MTX quantification and subsequent calculations.

Besides percent permeation of MTX overtime, flux (J, calculated by equation 7), which is the amount of compound moving through the barrier overtime (in this case, for the total period of time tested, namely 48h), was also obtained for the present assays, as listed on Table 21.

Analogously to the observed for the permeation profiles, for a testing period of 48h, the flux of MTX through the skin was diminished for the receptor medium containing PBS pH 7.4 with 10% DMSO, in comparison to the observed for the other tested receptor mediums. Nevertheless, for the reasons explained above, it could be argued that the most correct value of flux is the one obtained for the receptor medium containing ethanol:PBS pH 7.4 (3:7), which was of 4.891 ± 0.019 $\mu g/cm^2/h$.

Table 21. Flux of free MTX (300 µg in PBS pH 7.4, 1 mg/mL MTX) through pig ear skin over 48 hours to different receptor mediums (PBS pH 7.4 buffer containing 10% of DMSO, Ethanol:PBS pH 7.4 buffer in a ratio of 3:7 and PBS pH 7.4 buffer, in a total volume of 5 mL). Each value corresponds to the mean of n=3 measurements for the same assay, with one replicate per assay.

Free MTX in the donor compartment (µg)	*Receptor Medium*	*Flux (µg/cm²/h)*
300	PBS pH 7.4 + 10% DMSO	3.092 ± 0.010
	Ethanol:PBS pH 7.4 (3:7)	4.891 ± 0.005
	PBS pH 7.4	4.809 ± 0.019

Further continuation of the *in vitro* permeation studies in the context of this work would involve the testing of the MTX-loaded and drug-free NLCs formulations (with the simultaneous testing of at least three replicates per formulation, considering the biological variability of skin) using a receptor medium containing ethanol:PBS pH 7.4 (3:7), in order to adequately quantify the permeated MTX. As previously noted, special care must be given to the freshness and source of the used biological material, as it can strongly affect the obtained results. Still, a pertinent solution to bypass the difficulty associated with MTX quantification arising from the interference of the skin components would be the use of High-Performance Liquid Chromatography (HPLC) to quantify the permeated drug in the collected samples [123].

It should be noted that, for these sets of results, samples were collected for a total period of 48h (where the contents inserted in the donor compartments remained, throughout the whole course of the experiments); however, considering the topical application intended for the produced NLCs formulations, a maximum period of testing of 24h should suffice, as it is not expected that the NLCs formulations applied on the skin of psoriasis patients would remain on its surface for long periods of time (due to daily activities such as bathing and changing clothes, and physiological reactions such as sweating, as already discussed for the results obtained for the *in vitro* release assays).

Future works in this context could involve the inclusion of the produced NLCs in pertinent pharmaceutical formulations, in view of the intended topical application, with their subsequent evaluation by *in vitro* skin permeation assays. The inclusion of the produced NLCs in hydrogels would be of interest. Hydrogels are three-dimentional polymeric networks characterized by hydrophilic behaviour and consequent capability of absorbing great amounts of water. They resemble natural living tissue more than other types of synthetic biomaterials and their high water content increases their biocompatibility. The soft texture of swollen hydrogels provides a better felling to the skin, in comparison to ointments and patches, thus increasing patient compliance. Other important advantages of the incorporation of the produced NLCs in hydrogels would be the possibility for further modulation of the drug release profile, thus making it possible for the acquisition of a longer drug release and at a more constant rate [133]. One example of an hydrogel used to this end would be a Carbopol 934P gel, like the one described by Agrawal *et al.*

(2010) for the incorporation of acitretin for dermal treatment of psoriasis [100]. The inclusion of permeation enhancers, as discussed, could also be done using this pharmaceutical formulation. Pertinent penetration enhancers (in addition to the oleic acid present in the NLCs) could be cholic-acid derivatives, volatile oils, terpenes and terpenoids; menthol could also be of interest, as described by Nagle *et al.* (2011) [134], not only because of its function as a penetration enhancer, but also because of other properties such as cosolubilization, analgesia and anti-itch activity, with pertinence in the context of psoriasis [134].

It would also be pertinent to perform the already enunciated assays using different models of skin barrier, such as hyperproliferative skin, in order to simulate a condition of psoriasis [102], or also human cadaver skin and human skin equivalents (3D engineered tissues) [122].

4.6. MTT reduction assay

With the goal of studying the cytotoxicity of the optimized NLCs formulations NLC-P60 and NLC-P80 (MTX-loaded and drug-free), the MTT reduction assay was employed. The results obtained for the performed MTT reduction assays are presented on Figure 24.

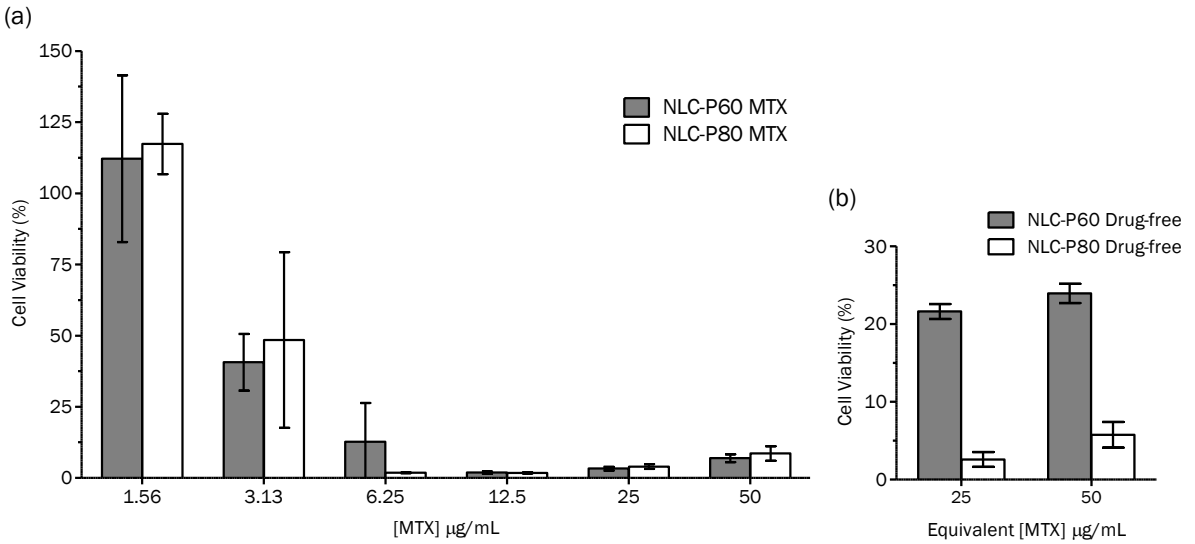

Figure 24. Cytotoxicity of (a) MTX-loaded NLCs (NLC-P60 and NLC-P80, separated from unincorporated drug) for a range of MTX encapsulated concentrations from 1.56 to 50 μg/mL and (b) drug-free NLCs (NLC-P60 and NLC-P80) for NLC mass concentrations equivalent to the NLC mass concentrations attained for 25 and 50 μg/mL of encapsulated MTX (equivalent mass of excipients, see Table 22), in a human THP1 monocyte cell line. Each result represents the mean ± standard deviation for n=5 replicates of one assay.

Both MTX-loaded NLCs formulations NLC-P60 and NLC-P80 exhibited approximately the same behaviour in terms of cytotoxicity. For an encapsulated MTX concentration of 1.56 μg/mL, the evaluated cell viability was of approximately 100% for both formulations, lowering to approximately 40% for a MTX concentration of 3.13 μg/mL and being decreased to almost 0% for

MTX concentration values larger than 6.25 μg/mL. Thus, in order to verify and further study the cytotoxicity of the MTX-loaded formulations, this assay would need to be repeated, considering only the interval of encapsulated MTX concentrations ranging from 1.56 μg/mL to 6.25 μg/mL (with the study of more concentration values in-between this range). This would allow the corresponding IC_{50} values to be obtained (i.e. encapsulated MTX concentration values for each of the NLCs formulations that lead to a 50% inhibition in cell viability).

Regarding the drug-free NLCs formulations NLC-P60 and NLC-P80, a volume of formulation equivalent in terms of excipient mass to the volume of MTX-loaded formulations was tested. More specifically, drug-free NLCs formulation volumes equivalent to the MTX encapsulated concentrations of 50 μg/mL and 25 μg/mL (the two largest encapsulated MTX values assessed) were tested. The corresponding excipient concentrations are listed on Table 22.

Table 22. Excipient concentration values equivalent to 25 μg/mL and 50 μg/mL of encapsulated MTX in MTX-loaded NLCs formulations and, consequently, in drug-free NLCs formulations.

		[Excipient] mg/mL	
	Equivalent [MTX] μg/mL	*NLC-P60 Drug-free*	*NLC-P80 Drug-free*
Eq. C1	50	8.60	8.26
Eq. C2	25	4.30	4.13

The assessment of cytotoxicity for the drug-free NLCs showed that, for the largest excipient concentration values, NLCs without MTX proved to have a strong cytotoxic effect, although their corresponding excipients include biodegradable and well-tolerated solid and liquid lipids (namely GRAS lipids) used in pharmaceutical and cosmetic industries [98, 99]. Only approximately 22-24% and 3-6% of cell viability remained (for both excipient concentrations) for the NLCs formulations NLC-P60 and NLC-P80, correspondingly. Nevertheless, it could also be observed, for both excipient concentrations, that NLC-P60 was less cytotoxic than NLC-P80. This assay would need to be complemented with the testing of lower values of excipient concentration, in order to verify to which point the cytotoxicity of these NLCs can be attributed to the action of the encapsulated MTX or the NLCs themselves. In any case, for the largest evaluated concentrations of excipient (and thereby, their MTX-loaded counterparts), the observed cytotoxicity was most likely due to the NLCs and not to the action of MTX. This was more evident for the formulation NLC-P80, considering that cell viability for NLC-P60, while small, was still larger for the absence of MTX than in its presence (thus further indicating the less cytotoxic action of these NLCs). As the only difference between these two types of NLCs formulations constitutes the surfactant used, namely polysorbate 60 and polysorbate 80 for NLC-P60 and NLC-P80, correspondingly, this suggests that the difference in cytotoxicity arises from this parameter. Generally regarding polysorbate toxicity, it should be taken into account that these surfactants

are also generally regarded as nontoxic and nonirritant materials (being incorporated in cosmetics, food products, and oral, parenteral, and topical pharmaceutical formulations); nonetheless, occasional events of hypersensitivity following their topical and intramuscular use have been reported [135].

Overall, further optimization concerning the tested values of concentration (encapsulated MTX and excipient concentration values) would be needed, being pertinent for future works concerning the evaluation of the cytotoxicity of these NLCs formulations. Pertinent future works could also include the execution of the same assays using other cells of pertinence in the context of psoriasis. Using differentiated cells, specifically THP1 macrophages differentiated from the employed cell line (using phorbol 12-myristate 13-acetate, PMA [136]), would be of interest. This is due to the important role of macrophages in mediating inflammatory processes in psoriasis (through binding and specific activation and co-stimulation of T cells [2], also secreting cytokines associated with psoriasis pathogenesis [5, 7]), while monocytes mostly circulate in the blood stream, even though they also participate in the early events leading to inflammation in psoriasis [2]. Cytotoxicity testing on dendritic cells would also be of importance, as these cells a play an important role as APCs [2] and in cytokine production in the context of inflammatory processes in psoriasis [5, 7] (analogously to macrophages), thus constituting a pertinent target for the treatment of this disease. In view of the key role of the subset of Th17 cells (a subset of $CD4^+$ T cells) in psoriasis pathogenesis [5, 17], a cell line model emulating the characteristics of these cells (e.g. through the use of adequate stimulus for the differentiation of $CD4^+$ T cell lines) would be pertinent to use for cytotoxicity testing of the NLCs formulations. Likewise, regarding the characteristic epidermal keratinocyte rapid proliferation and aberrant differentiation causing the formation of a thickened epidermis in psoriasis [18], it would also be of interest to test cytotoxicity on the HaCaT cell line, which constitutes a human cell line of immortalized keratinocytes (as analogously performed by Ridolfi *et al.* (2012), in order to test the cytotoxicity of tretinoin-loaded SLNs for topical delivery [137]).

At last, considering that the drug-free NLCs may possess strong cytotoxicity, as suggested by these preliminary results, this would point to the need for further optimization of these NLCs formulations regarding the excipients used for their production, in order to reduce their cytotoxicity and thus ensure therapeutic action associated with MTX, in their drug-loaded counterparts.

4.7. Other Future Works of pertinence in the context of this work

Throughout this document, future works of pertinence in the context of the study of the produced NLCs were enumerated. Nonetheless, other experiments of pertinence could further enrich this study, and are accordingly enumerated in this section.

Differential Scanning Calorimetry (DSC) would be a pertinent experimental addition [138], as it would provide information about the melting and recrystallization behaviour of the lipids contained in the NLCs, as various lipid modifications have various melting points and enthalpies. The degree of crystallinity of the NLCs is calculated by the ratio of their corresponding enthalpy and bulk lipid enthalpy, having the total weight taken as a basis. DSC profiles are especially useful to find out if drug dissolution occurs preferentially in the solid or liquid lipids comprising the NLCs [99]. The polymorphism status of the nanoparticles could also be evaluated by wide angle X-ray diffraction, which would also provide information of interest to confirm the results obtained by DSC [99].

Another interesting addition to the present work would be the surface functionalization of the produced NLCs with molecular components of interest. These could include monoclonal antibodies targeting surface markers of interest in pertinent target cells (associated with the pathogenesis of psoriasis, such as macrophages, dendritic cells, T cells, and others), as well as monoclonal antibodies used as biologic therapies in the context of psoriasis. The addition of the latter would not only grant a targeted action to the NLCs (by their penetration on the skin through the transappendageal pathway, into the follicles, from which they could further migrate and exert their action) but also allow for the acquisition of a combined therapy for psoriasis. Indeed, MTX-loaded NLCs functionalized with monoclonal antibodies used as biologic therapies (such as Adalimumab and Ustekinumab, and others) would be expected to have a synergic effect in terms of therapeutic efficacy; they would encompass the advantages of non-biologic and biologic therapy for psoriasis, while reducing side effects associated with the systemic use of these therapeutic agents, as well as sow the benefits of combined therapy.

5. Concluding Remarks

Psoriasis is one of the major chronic inflammatory diseases that plague modern society, being associated with genetic predisposition and high morbidity factors that substantially affect the lives of people afflicted with this disease. While it still remains incurable, efficacious psoriasis management and treatment can be achieved by an extensive number of therapeutic agents (both topically and systemically administrated) and methodologies (including phototherapy). Even so, the other side of the coin must also be considered, as multiple and wide-ranging adverse consequences can arise from every treatment strategy in existence, with more or less prominence depending on the therapy itself. An important example in this context is that of MTX - while constituting the gold standard for treatment of severe psoriasis by systemic administration, its use is associated with an extensive list of side effects to the patient. Thus, as a way of bypassing these troubling limitations, the role of nanomedicine can be emphasized, as one of the most promising divisions of nanotechnology. This field of knowledge is now starting to revolutionize therapy in psoriasis (and in plenty of other dermatologic diseases as well). Its adequate application, by the employment of suitable drug-carrying nanosystems, holds the potential of targeted, more efficient and less adverse administration of pertinent therapeutic substances for the treatment of psoriasis. Furthermore, these drug-delivering vehicles encompass valuable economic interest, as there is the possibility of upscaling their production to an industrial range.

Indeed, the work here presented was supported on the premise of nanotechnology and its potential for the treatment of psoriasis. Through this work, it was possible to produce drug-delivery systems, namely NLCs incorporating MTX, which possess characteristics that would render them a promising alternative for the topical treatment of mild to moderate psoriasis, in comparison to the sole use of the therapeutic agent in question.

Optimization of NLC features led to the design of two NLCs formulations with similar composition (differing only in the type of surfactant used), oriented towards the intended topical application, namely through the inclusion of oleic acid as the liquid lipid, which also functions as a penetration enhancer. These particles had acceptable dimensions (< 300 nm) accompanied by elevated absolute zeta potential levels (> 30 mV), low values of PI (< 0.2) and reasonably high values of encapsulation efficiency (> 60%), with almost spherical shape and smooth surface in terms of morphology. The elevated absolute zeta potential values and low PDI values suggested high physical stability of the formulations, which was confirmed for storage at room temperature for at least 4 weeks. Furthermore, MTX encapsulation was confirmed by the acquisition of infrared spectra indicating the presence of this drug in MTX-loaded NLCs.

By testing different methods for the separation of unincorporated drug from the NLCs formulations, it was possible to develop a dialysis method to this end, thus making possible the

execution of further studies regarding the obtained particles without the potential adulteration of results caused by the presence of unincorporated drug.

In vitro evaluation of drug release from the produced NLCs in a simulated physiological environment revealed a biphasic drug release profile characterized by a quick initial phase of drug release (burst release) followed by a phase with prolonged release. While the acquisition of slower and more prolonged drug release patterns is of most interest in the application of nanoparticulate drug-delivery systems, it can be concluded that this drug release profile is nonetheless pertinent with regard to the intended topical application. Its rapid but still gradual release of MTX would avoid the loss of therapeutic agent (due to daily actions like changing clothes and physiological reactions such as sweating) and allow its enhanced administration through the skin (in regard to the hydrating/occlusive properties of NLCs), followed by a more gradual and prolonged release of this drug (further reinforcing over time the effect of the main drug dose administrated to the patient).

Evaluation of the *in vitro* permeation of MTX showed its capability to go through the skin barrier. Subsequent testing involving the produced NLCs could not be performed; however, it is expected that these drug-carrying nanosystems would enhance the permeation of this drug, due to their multiple beneficial properties in the context of topical application, as well as through their incorporation in a pharmaceutical formulation (a hydrogel) and addition of penetration enhancers.

Preliminary cytotoxicity testing showed the cytotoxic potential of the produced NLCs formulations in cells associated with the mediation of inflammatory processes (namely monocytes), thus indicating their pertinence for use in psoriasis treatment. Nevertheless, it was also found that the drug-free NLCs may be characterized by high cytotoxicity, thus showing the need for further cytotoxicity testing of these particles and potential optimization of the excipients comprised in them.

Overall, both of the developed drug-delivery nanosystems can be considered to be suitable carriers for the purpose of topical administration of psoriasis with MTX, thus enhancing the treatment with this drug by increasing MTX efficacy whilst preventing toxicity associated with it. Patient compliance should be increased, as topical applications are much more comfortable and friendlier to patients. Potential improvements could still be performed to perfect the therapeutic potential of these drug-carrying nanosystems, which are suitable as future works in this context. Such improvements comprise inclusion in pharmaceutical formulations to modulate drug release and increase patient compliance, as well as potential functionalization of the NLCs with monoclonal antibodies used as biologic therapies in the context of psoriasis, which would allow a targeted action of these nanoparticles (in view of the cytokine networks underlying the pathogenesis of psoriasis), as well as the acquisition of a combined therapy holding the advantages of both non-biologic and biologic therapies used in the context of psoriasis.

The future in the treatment of psoriasis lies in the intersection of nanomedicine with knowledge about its pathogenesis, as well as the current and emerging treatments for this chronic inflammatory genetically predisposed disease. This multidisciplinary approach can only benefit the evolving treatment landscape for this complex multifactorial disease, as was shown with the present work. Accordingly, more research needs to be done in this context, so that psoriasis treatment can be heightened through the application of nanomedicine and thus and benefit patients suffering from this yet incurable disease.

6. References

1. Raho G, Koleva DM, Garattini L, Naldi L: The Burden of Moderate to Severe Psoriasis. *Pharmacoeconomics* 2012, 30:1005–1013.

2. Daly JAO: Psoriasis , a Systemic Disease Beyond the Skin , as Evidenced by Psoriatic Arthritis and Many Comorbities – Clinical Remission with a Leishmania Amastigotes Vaccine , a Serendipity Finding. 2011, 18:1–57.

3. Chandran V, Raychaudhuri SP: Geoepidemiology and environmental factors of psoriasis and psoriatic arthritis. *J Autoimmun* 2010, 34:J314–21.

4. Chandran V: The genetics of psoriasis and psoriatic arthritis. *Clin Rev Allergy Immunol* 2013, 44:149–56.

5. Chong HT, Kopecki Z, Cowin AJ: Lifting the Silver Flakes: The Pathogenesis and Management of Chronic Plaque Psoriasis. *Biomed Res Int* 2013, 2013:168321.

6. Clarke P: Psoriasis. *Aust Fam Physician* 2011, 40:468–73.

7. Monteleone G, Pallone F, MacDonald TT, Chimenti S, Costanzo A: Psoriasis: from pathogenesis to novel therapeutic approaches. *Clin Sci* 2011, 120:1–11.

8. Oram Y, Akkaya AD: Treatment of nail psoriasis: common concepts and new trends. *Dermatol Res Pract* 2013, 2013:180496.

9. Parisi R, Symmons DPM, Griffiths CEM, Ashcroft DM: Global epidemiology of psoriasis: a systematic review of incidence and prevalence. *J Invest Dermatol* 2013, 133:377–85.

10. Wohlrab J, Fiedler G, Gerdes S, Nast A, Philipp S, Radtke M a, Thaçi D, Koenig W, Pfeiffer AFH, Härter M, Schön MP: Recommendations for detection of individual risk for comorbidities in patients with psoriasis. *Arch Dermatol Res* 2013, 305:91–8.

11. Pietrzak A, Bartosińska J, Chodorowska G, Szepietowski JC, Paluszkiewicz P, Schwartz R a: Cardiovascular aspects of psoriasis: an updated review. *Int J Dermatol* 2013, 52:153–62.

12. Kupetsky E a, Mathers AR, Ferris LK: Anti-cytokine therapy in the treatment of psoriasis. *Cytokine* 2013, 61:704–12.

13. Mitra A, Fallen RS, Lima HC: Cytokine-based therapy in psoriasis. *Clin Rev Allergy Immunol* 2013, 44:173–82.

14. Prieto-Pérez R, Cabaleiro T, Daudén E, Ochoa D, Roman M, Abad-Santos F: Genetics of Psoriasis and Pharmacogenetics of Biological Drugs. *Autoimmune Dis* 2013, 2013:613086.

15. Raychaudhuri SP: Role of IL-17 in psoriasis and psoriatic arthritis. *Clin Rev Allergy Immunol* 2013, 44:183–93.

16. Smith RL, Warren RB, Griffiths CE, Worthington J: Genetic susceptibility to psoriasis: an emerging picture. *Genome Med* 2009, 1:72.

17. Ariza M-E, Williams M V, Wong HK: Targeting IL-17 in psoriasis: from cutaneous immunobiology to clinical application. *Clin Immunol* 2013, 146:131–9.

18. Martin DA, Towne JE, Kricorian G, Klekotka P, Gudjonsson JE, Krueger JG, Russel CB: The Emerging Role of Interleukin-17 in the Pathogenesis of Psoriasis: Preclinical and Clinical Findings. *J Invest Dermatol* 2013, 133:17–26.

19. Sigurdardottir SL, Thorleifsdottir RH, Valdimarsson H, Johnston a: The role of the palatine tonsils in the pathogenesis and treatment of psoriasis. *Br J Dermatol* 2013, 168:237–42.

20. Girolomoni G, Mrowietz U, Paul C: Psoriasis: rationale for targeting interleukin-17. *Br J Dermatol* 2012, 167:717–24.

21. Lowes MA, Russell CB, Martin DA, Towne JE, Krueger JG: The IL-23/T17 pathogenic axis in psoriasis is amplified by keratinocyte responses. *Trends Immunol* 2013, 34:174–81.

22. Brotas AM, Cunha JMT, Lago EHJ, Machado CCN, Carneiro SCDS: Tumor necrosis factor-alpha and the cytokine network in psoriasis. *An Bras Dermatol* 2012, 87:673–81; quiz 682–3.

23. Goldminz AM, Au SC, Kim N, Gottlieb AB, Lizzul PF: NF-κB: an essential transcription factor in psoriasis. *J Dermatol Sci* 2013, 69:89–94.

24. Laws PM, Young HS: Current and emerging systemic treatment strategies for psoriasis. *Drugs* 2012, 72:1867–80.

25. Murphy G, Reich K: In touch with psoriasis: topical treatments and current guidelines. *J Eur Acad Dermatol Venereol* 2011, 25 Suppl 4:3–8.

26. Mitra A, Wu Y: Topical delivery for the treatment of psoriasis. *Expert Opin Drug Deliv* 2010, 7:977–92.

27. Samarasekera EJ, Sawyer L, Wonderling D, Tucker R, Smith CH: Topical therapies for the treatment of plaque psoriasis: systematic review and network meta-analyses. *Br J Dermatol* 2013, 168:954–67.

28. Bhatia A, Singh B, Amarji B, Negi P, Shukla A, Katare OP: Novel stain-free lecithinized coal tar formulation for psoriasis. *Int J Dermatol* 2011, 50:1246–8.

29. Zeichner JA: Use of Topical Coal Tar Foam for the Treatment of Psoriasis in Difficult-to-treat Areas. *J Clin Aesthet Dermatol* 2010, 3:37–40.

30. Rahman M, Alam K, Ahmad MZ, Gupta G, Afzal M, Akhter S, Kazmi I, Jyoti, Ahmad FJ, Anwar F: Classical to current approach for treatment of psoriasis: a review. *Endocr Metab Immune Disord Drug Targets* 2012, 12:287–302.

31. Castela E, Archier E, Devaux S, Gallini A, Aractingi S, Cribier B, Jullien D, Aubin F, Bachelez H, Joly P, Le Maître M, Misery L, Richard M, Paul C, Ortonne JP: Topical corticosteroids in plaque psoriasis: a systematic review of risk of adrenal axis suppression and skin atrophy. *J Eur Acad Dermatol Venereol* 2012, 26 Suppl 3(February):47–51.

32. Devaux S, Castela a, Archier E, Gallini a, Joly P, Misery L, Aractingi S, Aubin F, Bachelez H, Cribier B, Jullien D, Le Maître M, Richard M, Ortonne J-P, Paul C: Topical vitamin D analogues alone or in association with topical steroids for psoriasis: a systematic review. *J Eur Acad Dermatol Venereol* 2012, 26 Suppl 3:52–60.

33. Horn EJ, Domm S, Katz HI, Lebwohl M, Mrowietz U, Kragballe K: Topical corticosteroids in psoriasis: strategies for improving safety. *J Eur Acad Dermatol Venereol* 2010, 24:119–24.

34. Kamangar F, Koo J, Heller M, Lee E, Bhutani T: Oral vitamin D, still a viable treatment option for psoriasis. *J Dermatolog Treat* 2013, 24:261–7.

35. Gorman S, Judge MA, Hart PH: Immune-modifying properties of topical vitamin D: Focus on dendritic cells and T cells. *J Steroid Biochem Mol Biol* 2010, 121:247–9.

36. Gustafson CJ, Watkins C, Hix E, Feldman SR: Combination therapy in psoriasis: an evidence-based review. *Am J Clin Dermatol* 2013, 14:9–25.

37. Paul C, Gallini a, Archier E, Castela E, Devaux S, Aractingi S, Aubin F, Bachelez H, Cribier B, Joly P, Jullien D, Le Maître M, Misery L, Richard M, Ortonne J-P: Evidence-based recommendations on topical treatment and phototherapy of psoriasis: systematic review and expert opinion of a panel of dermatologists. *J Eur Acad Dermatol Venereol* 2012, 26 Suppl 3(February):1–10.

38. Hendriks AGM, Keijsers RRMC, de Jong EMGJ, Seyger MMB, van de Kerkhof PCM: Efficacy and safety of combinations of first-line topical treatments in chronic plaque psoriasis: a systematic literature review. *J Eur Acad Dermatol Venereol* 2013, 27:931–51.

39. Richard EG, Hönigsmann H: Phototherapy, psoriasis, and the age of biologics. *Photodermatol Photoimmunol Photomed* 2014, 30:3–7.

40. Wong T, Hsu L, Liao W: Phototherapy in psoriasis: a review of mechanisms of action. *J Cutan Med Surg* 2013, 17:6–12.

41. Maza a, Montaudié H, Sbidian E, Gallini a, Aractingi S, Aubin F, Bachelez H, Cribier B, Joly P, Jullien D, Le Maître M, Misery L, Richard M, Ortonne J-P, Paul C: Oral cyclosporin in psoriasis: a systematic review on treatment modalities, risk of kidney toxicity and evidence for use in non-plaque psoriasis. *J Eur Acad Dermatol Venereol* 2011, 25 Suppl 2:19–27.

42. Amor KT, Ryan C, Menter A: The use of cyclosporine in dermatology: part I. *J Am Acad Dermatol* 2010, 63:925–46; quiz 947–8.

43. Colombo MD, Cassano N, Bellia G, Vena GA: Cyclosporine regimens in plaque psoriasis: an overview with special emphasis on dose, duration, and old and new treatment approaches. *ScientificWorldJournal* 2013, 2013:805705.

44. Ryan C, Amor KT, Menter A: The use of cyclosporine in dermatology: part II. *J Am Acad Dermatol* 2010, 63:949–72; quiz 973–4.

45. Carretero G, Ribera M, Belinchón I, Carrascosa JM, Puig L, Ferrandiz C, Dehesa L, Vidal D, Peral F, Jorquera E, Gonzalez-Quesada a, Muñoz C, Notario J, Vanaclocha F, Moreno JC: Guidelines for the use of acitretin in psoriasis. *Actas Dermosifiliogr* 2013, 104:598–616.

46. Sbidian E, Maza a, Montaudié H, Gallini a, Aractingi S, Aubin F, Cribier B, Joly P, Jullien D, Le Maître M, Misery L, Richard M, Paul C, Ortonne J-P, Bachelez H: Efficacy and safety of oral retinoids in different psoriasis subtypes: a systematic literature review. *J Eur Acad Dermatol Venereol* 2011, 25 Suppl 2:28–33.

47. Kim IH, West CE, Kwatra SG, Feldman SR, O'Neill JL: Comparative efficacy of biologics in psoriasis: a review. *Am J Clin Dermatol* 2012, 13:365–74.

48. Shen S, O'Brien T, Yap LM, Prince HM, McCormack CJ: The use of methotrexate in dermatology: a review. *Australas J Dermatol* 2012, 53:1–18.

49. Snyder R: Some aspects of the development of methotrexate therapy. *Clin Exp Pharmacol Physiol Suppl* 1979, 5:1–4.

50. Gubner R: Introduction of antifolics in psoriasis. A twenty-five year retrospect of antineoplastic agents in nonmalignant disease. *Cutis* 1979, 23:425–428.

51. Dogra S, Mahajan R: Systemic methotrexate therapy for psoriasis: past, present and future. *Clin Exp Dermatol* 2013, 38:573–88.

52. Montaudié H, Sbidian E, Paul C, Maza A, Gallini A, Aractingi S, Aubin F, Bachelez H, Cribier B, Joly P, Jullien D, Le Maître M, Misery L, Richard M, Ortonne J: Methotrexate in psoriasis: a systematic review of treatment modalities, incidence, risk factors and monitoring of liver toxicity. *J Eur Acad Dermatol Venereol* 2011, 25 Suppl 2(January):12–8.

53. Micha R, Imamura F, Wyler von Ballmoos M, Solomon DH, Hernán M a, Ridker PM, Mozaffarian D: Systematic review and meta-analysis of methotrexate use and risk of cardiovascular disease. *Am J Cardiol* 2011, 108:1362–70.

54. Meephansan J, Ruchusatsawat K, Sindhupak W, Thorner P, Wongpiyabovorn J: Effect of methotrexate on serum levels of IL-22 in patients with psoriasis. *Eur J Dermatol* 2011, 21:501–504.

55. Gudjonsson JE, Johnston A, Ellis CN: Novel systemic drugs under investigation for the treatment of psoriasis. *J Am Acad Dermatol* 2012, 67:139–47.

56. Palfreeman AC, McNamee KE, McCann FE: New developments in the management of psoriasis and psoriatic arthritis: a focus on apremilast. *Drug Des Devel Ther* 2013, 7:201–10.

57. Shutty B, West C, Pellerin M, Feldman S: Apremilast as a treatment for psoriasis. *Expert Opin Pharmacother* 2012, 13:1761–70.

58. Zerbini CAF, Lomonte ABV: Tofacitinib for the treatment of rheumatoid arthritis. *Expert Rev Clin Immunol* 2012, 8:319–31.

59. Kawalec P, Mikrut A, Wiśniewska N, Pilc A: The effectiveness of tofacitinib, a novel Janus kinase inhibitor, in the treatment of rheumatoid arthritis: a systematic review and meta-analysis. *Clin Rheumatol* 2013, 32:1415–24.

60. Koo J: Etanercept in the treatment of plaque psoriasis. *Clin Cosmet Investig Dermatol* 2009:77–84.

61. Burmester GR, Panaccione R, Gordon KB, McIlraith MJ, Lacerda APM: Adalimumab: long-term safety in 23 458 patients from global clinical trials in rheumatoid arthritis, juvenile idiopathic arthritis, ankylosing spondylitis, psoriatic arthritis, psoriasis and Crohn's disease. *Ann Rheum Dis* 2013, 72:517–24.

62. Saraceno R, Saggini A, Pietroleonardo L, Chimenti S: Infliximab in the treatment of plaque type psoriasis. *Clin Cosmet Investig Dermatol* 2009, 2:27–37.

63. Reich K, Nestle FO, Papp K, Ortonne J-P, Evans R, Guzzo C, Li S, Dooley LT, Griffiths CEM: Infliximab induction and maintenance therapy for moderate-to-severe psoriasis: a phase III, multicentre, double-blind trial. *Lancet* 2005, 366:1367–74.

64. Mrowietz U, Kragballe K, Reich K, Griffiths CEM, Gu Y, Wang Y, Rozzo SJ, Laboratories A, Road AP, Park A: An assessment of adalimumab efficacy in three Phase III clinical trials using the European Consensus Programme criteria for psoriasis treatment goals. *Br J Dermatol* 2013, 168:374–380.

65. Fallahi-Sichani M, Flynn JL, Linderman J, Kirschner DE: Differential risk of tuberculosis reactivation among anti-TNF therapies is due to drug binding kinetics and permeability. *J Immunol* 2013, 188:3169–3178.

66. Papp KA, Tyring S, Lahfa M, Prinz J, Griffiths CEM, Nakanishi AM, Zitnik R, van de Kerkhof PCM, Melvin L: A global phase III randomized controlled trial of etanercept in psoriasis: safety, efficacy, and effect of dose reduction. *Br J Dermatol* 2005, 152:1304–12.

67. Michelon MA, Gottlieb AB: Role of golimumab, a TNF-alpha inhibitor, in the treatment of the psoriatic arthritis. *Clin Cosmet Investig Dermatol* 2010, 3:79–84.

68. Jenneck C, Novak N: The safety and efficacy of alefacept in the treatment of chronic plaque psoriasis. *Ther Clin Risk Manag* 2007, 3:411–20.

69. Krueger GG: Clinical response to alefacept: results of a phase 3 study of intravenous administration of alefacept in patients with chronic plaque psoriasis. *J Eur Acad Dermatol Venereol* 2003, 17 Suppl 2:17–24.

70. Gandhi M, Alwawi E, Gordon KB: Anti-p40 antibodies ustekinumab and briakinumab: blockade of interleukin-12 and interleukin-23 in the treatment of psoriasis. *Semin Cutan Med Surg* 2010, 29:48–52.

71. Quatresooz P, Hermanns-Lê T, Piérard GE, Humbert P, Delvenne P, Piérard-Franchimont C: Ustekinumab in psoriasis immunopathology with emphasis on the Th17-IL23 axis: a primer. *J Biomed Biotechnol* 2012, 2012.

72. Gottlieb A, Narang K: Ustekinumab in the treatment of psoriatic arthritis: latest findings and clinical potential. *Ther Adv Musculoskelet Dis* 2013, 5:277–85.

73. Papp KA, Langley RG, Lebwohl M, Krueger GG, Szapary P, Yeilding N, Guzzo C, Hsu M-C, Wang Y, Li S, Dooley LT, Reich K: Efficacy and safety of ustekinumab, a human interleukin-12/23 monoclonal antibody, in patients with psoriasis: 52-week results from a randomised, double-blind, placebo-controlled trial (PHOENIX 2). *Lancet* 2008, 371:1675–84.

74. Papp KA, Langley RG, Lebwohl M, Krueger GG, Szapary P, Yeilding N, Guzzo C, Hsu M-C, Wang Y, Li S, Dooley LT, Reich K: Efficacy and safety of ustekinumab, a human interleukin-12/23 monoclonal antibody, in patients with psoriasis: 52-week results from a randomised, double-blind, placebo-controlled trial (PHOENIX 2). *Lancet* 2008, 371:1675–84.

75. Wada Y, Cardinale I, Khatcherian A, Chu J, Kantor AB, Gottlieb AB, Tatsuta N, Jacobson E, Barsoum J, Krueger JG: Apilimod inhibits the production of IL-12 and IL-23 and reduces dendritic cell infiltration in psoriasis. *PLoS One* 2012, 7:e35069.

76. Johnson-Huang LM, Lowes MA, Krueger JG: Putting together the psoriasis puzzle: an update on developing targeted therapies. *Dis Model Mech* 2012, 5:423–33.

77. Langley RG, Papp K, Gottlieb AB, Krueger GG, Gordon KB, Williams D, Valdes J, Setze C, Strober B: Safety results from a pooled analysis of randomized, controlled phase II and III clinical trials and interim data from an open-label extension trial of the interleukin-12/23 monoclonal antibody, briakinumab, in moderate to severe psoriasis. *J Eur Acad Dermatol Venereol* 2013, 27:1252–61.

78. Ren V, Dao H: Potential role of ixekizumab in the treatment of moderate-to-severe plaque psoriasis. *Clin Cosmet Investig Dermatol* 2013, 6:75–80.

79. Rich P, Sigurgeirsson B, Thaci D, Ortonne J-P, Paul C, Schopf RE, Morita a, Roseau K, Harfst E, Guettner a, Machacek M, Papavassilis C: Secukinumab induction and maintenance therapy in moderate-to-severe plaque psoriasis: a randomized, double-blind, placebo-controlled, phase II regimen-finding study. *Br J Dermatol* 2013, 168:402–11.

80. Leonardi C, Matheson R, Zachariae C, Cameron G, Li L, Edson-Heredia E, Braun D, Banerjee S: Anti-interleukin-17 monoclonal antibody ixekizumab in chronic plaque psoriasis. *N Engl J Med* 2012, 366:1190–9.

81. Papp KA, Langley RG, Sigurgeirsson B, Abe M, Baker DR, Konno P, Haemmerle S, Thurston HJ, Papavassilis C, Richards HB: Efficacy and safety of secukinumab in the treatment of moderate-to-severe plaque psoriasis: a randomized, double-blind, placebo-controlled phase II dose-ranging study. *Br J Dermatol* 2013, 168:412–21.

82. Papp KA, Leonardi C, Menter A, Ortonne J-P, Krueger JG, Kricorian G, Aras G, Li J, Russell CB, Thompson EHZ, Baumgartner S: Brodalumab, an Anti-Interleukin-17–Receptor Antibody for Psoriasis. *N Engl J Med* 2012, 366:1181–1189.

83. Domm S, Mrowietz U: Combination therapy in the treatment of psoriasis. *J Dtsch Dermatol Ges* 2011, 9:94–8.

84. Bailey EE, Ference EH, Alikhan A, Hession MT, Armstrong AW: Combination treatments for psoriasis: A systematic review and meta-analysis. *Arch Dermatol* 2012, 148:511–522.

85. Gupta S, Bansal R, Gupta S, Jindal N, Jindal A: Nanocarriers and nanoparticles for skin care and dermatological treatments. *Indian Dermatol Online J* 2013, 4:267–272.

86. Saraceno R, Chiricozzi A, Gabellini M, Chimenti S: Emerging applications of nanomedicine in dermatology. *Ski Res Technol* 2013, 19:e13–9.

87. Abramovits W, Granowski P, Arrazola P: Applications of nanomedicine in dermatology: use of nanoparticles in various therapies and imaging. *J Cosmet Dermatol* 2010, 9:154–9.

88. DeLouise LA: Applications of nanotechnology in dermatology. *J Invest Dermatol* 2012, 132(3 Pt 2):964–75.

89. Papakostas D, Rancan F, Sterry W, Blume-Peytavi U, Vogt A: Nanoparticles in dermatology. *Arch Dermatol Res* 2011, 303:533–50.

90. Gupta M, Agrawal U, Vyas SP: Nanocarrier-based topical drug delivery for the treatment of skin diseases. *Expert Opin Drug Deliv* 2012, 9:783–804.

91. Desai P, Patlolla RR, Singh M: Interaction of nanoparticles and cell-penetrating peptides with skin for transdermal drug delivery. *Mol Membr Biol* 2010, 27:247–259.

92. Zhang Z, Tsai P-C, Ramezanli T, Michniak-Kohn BB: Polymeric nanoparticles-based topical delivery systems for the treatment of dermatological diseases. *Wiley Interdiscip Rev Nanomed Nanobiotechnol* 2013, 5:205–18.

93. Basavaraj KH: Nanotechnology in medicine and relevance to dermatology: present concepts. *Indian J Dermatol* 2012, 57:169–74.

94. Prow TW, Grice JE, Lin LL, Faye R, Butler M, Becker W, Wurm EMT, Yoong C, Robertson T a, Soyer HP, Roberts MS: Nanoparticles and microparticles for skin drug delivery. *Adv Drug Deliv Rev* 2011, 63:470–91.

95. Pardeike J, Hommoss A, Müller RH: Lipid nanoparticles (SLN, NLC) in cosmetic and pharmaceutical dermal products. *Int J Pharm* 2009, 366:170–84.

96. Kumar S, Randhawa JK: High melting lipid based approach for drug delivery: solid lipid nanoparticles. *Mater Sci Eng C Mater Biol Appl* 2013, 33:1842–52.

97. Almeida AJ, Souto E: Solid lipid nanoparticles as a drug delivery system for peptides and proteins. *Adv Drug Deliv Rev* 2007, 59:478–90.

98. Iqbal MA, Md S, Sahni JK, Baboota S, Dang S, Ali J: Nanostructured lipid carriers system: recent advances in drug delivery. *J Drug Target* 2012, 20:813–30.

99. Fang C-L, Al-Suwayeh SS, Fang J-Y: Nanostructured lipid carriers (NLCs) for drug delivery and targeting. *Recent Pat Nanotechnol* 2013, 7:41–55.

100. Agrawal Y, Petkar KC, Sawant KK: Development, evaluation and clinical studies of Acitretin loaded nanostructured lipid carriers for topical treatment of psoriasis. *Int J Pharm* 2010, 401:93–102.

101. Raza K, Singh B, Lohan S, Sharma G, Negi P, Yachha Y, Katare OP: Nano-lipoidal carriers of tretinoin with enhanced percutaneous absorption, photostability, biocompatibility and anti-psoriatic activity. *Int J Pharm* 2013, 456:65–72.

102. Lin Y-K, Huang Z-R, Zhuo R-Z, Fang J-Y: Combination of calcipotriol and methotrexate in nanostructured lipid carriers for topical delivery. *Int J Nanomedicine* 2010, 5:117–28.

103. Agrawal U, Gupta M, Vyas SP: Capsaicin delivery into the skin with lipidic nanoparticles for the treatment of psoriasis. *Artif Cells Nanomed Biotechnol* 2013(August):1–7.

104. Pradhan M, Singh D, Singh MR: Novel colloidal carriers for psoriasis: current issues, mechanistic insight and novel delivery approaches. *J Control release* 2013, 170:380–95.

105. SASOL. (2014). Excipients for pharmaceuticals. [Online] Available: http://www.sasoltechdata.com/MarketingBrochures/Excipients_Pharmaceuticals.pdf (Accessed: 11-06-2014).

106. 2: Final Report on the Safety Assessment of Glyceryl Ricinoleate. *Int J Toxicol* 1988, 7:721–739.

107. World of Molecules. (2014). Oleic Acid Molecule. [Online]. Available: http://www.worldofmolecules.com/foods/oleic.htm (Accessed: 11-06-2014)

108. World Health Organization. (2013) Monographs: Pharmaceutical substances: Polysorbata 20, 60, 80 - Polysorbates 20, 60, 80. [Online] Available: http://apps.who.int/phint/en/p/docf/ (Accessed: 11-06-2014)

109. chemBlink. (2014). CAS # 9005-67-8, Tween 60, Polyethylene glycol sorbitan monostearate, Polyoxyethylene sorbitan monostearate. [Online] Available: http://www.chemblink.com/products/9005-67-8.htm (Accessed: 11-06-2014)

110. chemBlink. (2014). CAS # 9005-65-6, Tween 80, Polyoxyethylenesorbitan monooleate, Sorbitan monooleate ethoxylate. [Online] Available: http://www.chemblink.com/products/9005-65-6.htm (Accessed: 11-06-2014)

111. MALVERN INSTRUMENTS: Dynamic Light Scattering: An Introduction in 30 Minutes. 2014.

112. Sartor M: Dynamic Light Scattering. .

113. MALVERN INSTRUMENTS: Dynamic Light Scattering Common Terms Defined. 2011.

114. MALVERN INSTRUMENTS: Zeta Potential An Introduction in 30 Minutes. 2014.

115. Egerton RF: *Physical Principles of Electron Microscopy*. New York, USA: Springer Science+Business Media, Inc.; 2005.

116. Radboud University Nijmegen. (2014) SEM samples. [Online] Available: http://www.vcbio.science.ru.nl/en/fesem/info/preparatie/ (Accessed: 09-06-2014)

117. Radboud University Nijmegen. (2014). Cryo SEM. [Online] Available: http://www.vcbio.science.ru.nl/en/fesem/info/cryosem/ (Accessed: 09-06-2014)

118. Thermo Nicolet Corporation: Introduction to Fourier Transform Infrared Spectrometry. 2001.

119. Zhang K, Lv S, Li X, Feng Y, Li X, Liu L, Li S, Li Y: Preparation, characterization, and in vivo pharmacokinetics of nanostructured lipid carriers loaded with oleanolic acid and gentiopicrin. *Int J Nanomedicine* 2013, 8:3227–39.

120. Abdelbary G, Haider M: In vitro characterization and growth inhibition effect of nanostructured lipid carriers for controlled delivery of methotrexate. *Pharm Dev Technol* 2011, 18:1159–68.

121. ChemicalBook. (2014). Methotrexate CAS#: 59-05-02. [Online] Available: http://www.chemicalbook.com/ProductChemicalPropertiesCB2739302_EN.htm (Accessed: 09-06-2014)

122. PermeGear, Inc. (2014). DIFFUSION TESTING FUNDAMENTALS. [Online] Available: http://www.permegear.com/primer.pdf (Accessed: 20-03-2014)

123. Gomes MJ, Martins S, Ferreira D, Segundo M a, Reis S: Lipid nanoparticles for topical and transdermal application for alopecia treatment: development, physicochemical characterization, and in vitro release and penetration studies. *Int J Nanomedicine* 2014, 9:1231–42.

124. Tsuchiya S, Yamabe M, Yamaguchi Y, Kobayashi Y, Konno T, Tada K: Establishment and characterization of a human acute monocytic leukemia cell line (THP-1). *Int J Cancer* 1980, 26:171–6.

125. Meerloo J Van, Kaspers GJL, Cloos J: Cell Sensitivity Assays: The MTT Assay Johan. In *Cancer Cell Cult Methods Mol Biol*. *Volume 731*. 2nd edition. Edited by Cree IA. Springer Science+Business Media; 2011:237–245. [*Methods in Molecular Biology*]

126. Neves AR, Lúcio M, Martins S, Lima JLC, Reis S: Novel resveratrol nanodelivery systems based on lipid nanoparticles to enhance its oral bioavailability. *Int J Nanomedicine* 2013, 8:177–87.

127. NCBI. (2014). Methotrexate - PubChem. [Online] Available: http://pubchem.ncbi.nlm.nih.gov/summary/summary.cgi?cid=126941 (Accessed: 05-06-2014)

128. Kumari SDC, Tharani CB, Narayanan N, Kumar CS: Formulation and characterization of Methotrexate loaded sodium alginate chitosan Nanoparticles. *Indian J Res Pharm Biotechnol* 2013, 5674(December):915–921.

129. Beck P, Scherer D, Kreuter J: Separation of drug-loaded nanoparticles from free drug by gel filtration. *J Microencapsul* 1990, 7:491–6.

130. Healthcare GE: Gel filtration - Principles and Methods. 2014.

131. Santa Cruz Biotech. (2014). Methotrexate | CAS 59-05-2 | Santa Cruz Biotech. [Online] Available: http://www.scbt.com/datasheet-3507-methotrexate.html (Accessed: 09-06-2014)

132. Misra A, Kalariya M, Padhi BK, Chougule M: Methotrexate-Loaded Solid Lipid Nanoparticles for Topical Treatment of Psoriasis : Formulation & Clinical Implications. *Indian J Dermatology, Venereol an Leprol* 2004, 4.

133. Peppas N a, Bures P, Leobandung W, Ichikawa H: Hydrogels in pharmaceutical formulations. *Eur J Pharm Biopharm* 2000, 50:27–46.

134. Nagle A, Goyal AK, Kesarla R, Murthy RR: Efficacy study of vesicular gel containing methotrexate and menthol combination on parakeratotic rat skin model. *J Liposome Res* 2011, 21:134–40.

135. U.S. Department of Health and Human Serivices (National Toxicology Program). (2014). ChemIDPlus/HSDB 9005-65-6 Toxicity - National Toxicology Program. [Online] Available: http://ntp.niehs.nih.gov/?objectid=E8841408-BDB5-82F8-FC7F7D3E0F941C7E (Accessed: 13-06-2014)

136. Park EK, Jung HS, Yang HI, Yoo MC, Kim C, Kim KS: Optimized THP-1 differentiation is required for the detection of responses to weak stimuli. *Inflamm Res* 2007, 56:45–50.

137. Ridolfi DM, Marcato PD, Justo GZ, Cordi L, Machado D, Durán N: Chitosan-solid lipid nanoparticles as carriers for topical delivery of tretinoin. *Colloids Surf B Biointerfaces* 2012, 93:36–40.

138. Müller-Goymann CC: Physicochemical characterization of colloidal drug delivery systems such as reverse micelles, vesicles, liquid crystals and nanoparticles for topical administration. *Eur J Pharm Biopharm* 2004, 58:343–56.

7. Supplementary Figures

Figure A1. Sephadex column utilized for the separation of NLCs from unincorporated drug by gel filtration.

Figure A2. Experimental setup of *in vitro* drug release assays.

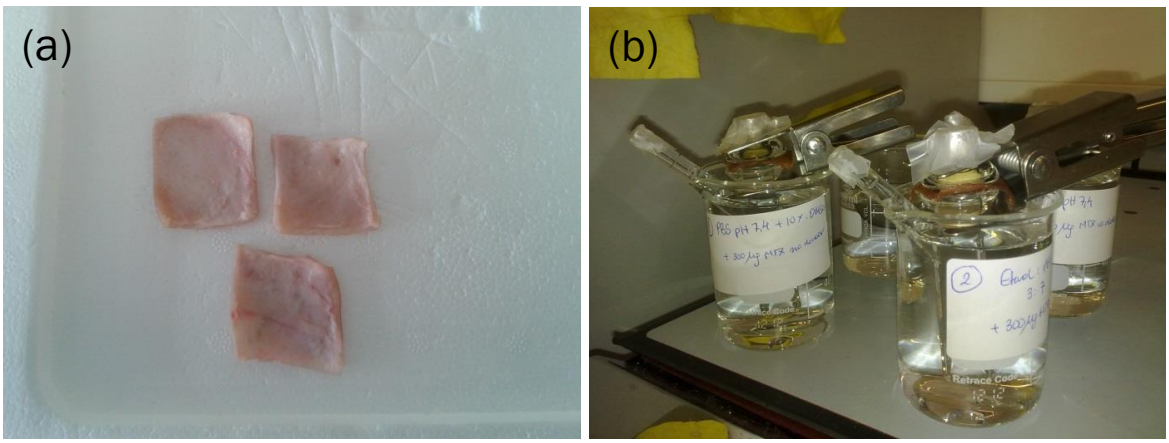

Figure A3. (a) Example of pig ear skin fragments after cartilage detachment and fat removal and (a) Franz Cell experimental setup utilized for *in vitro* permeation assays.

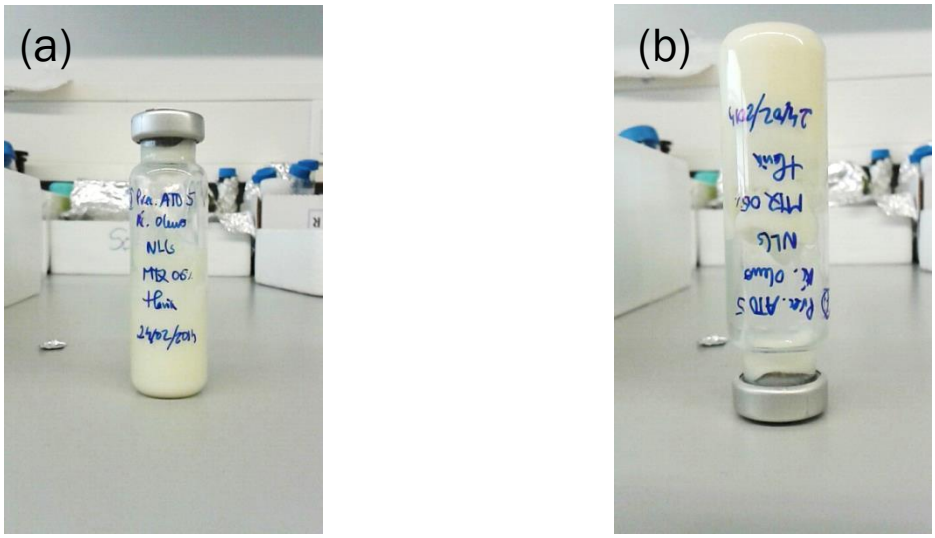

Figure A4. Aspect of NLCs formulation G.1.2. (a) siding up and (b) upside-down, to show its gelatinous consistence.

Figure A5. Aspect of the NLCs formulations D.1.2.7., D.1.2-ALT and D.1.2.8. with polysorbate 60 as the surfactant, and D.1.2.9.-D.1.2.11. with polysorbate 80.

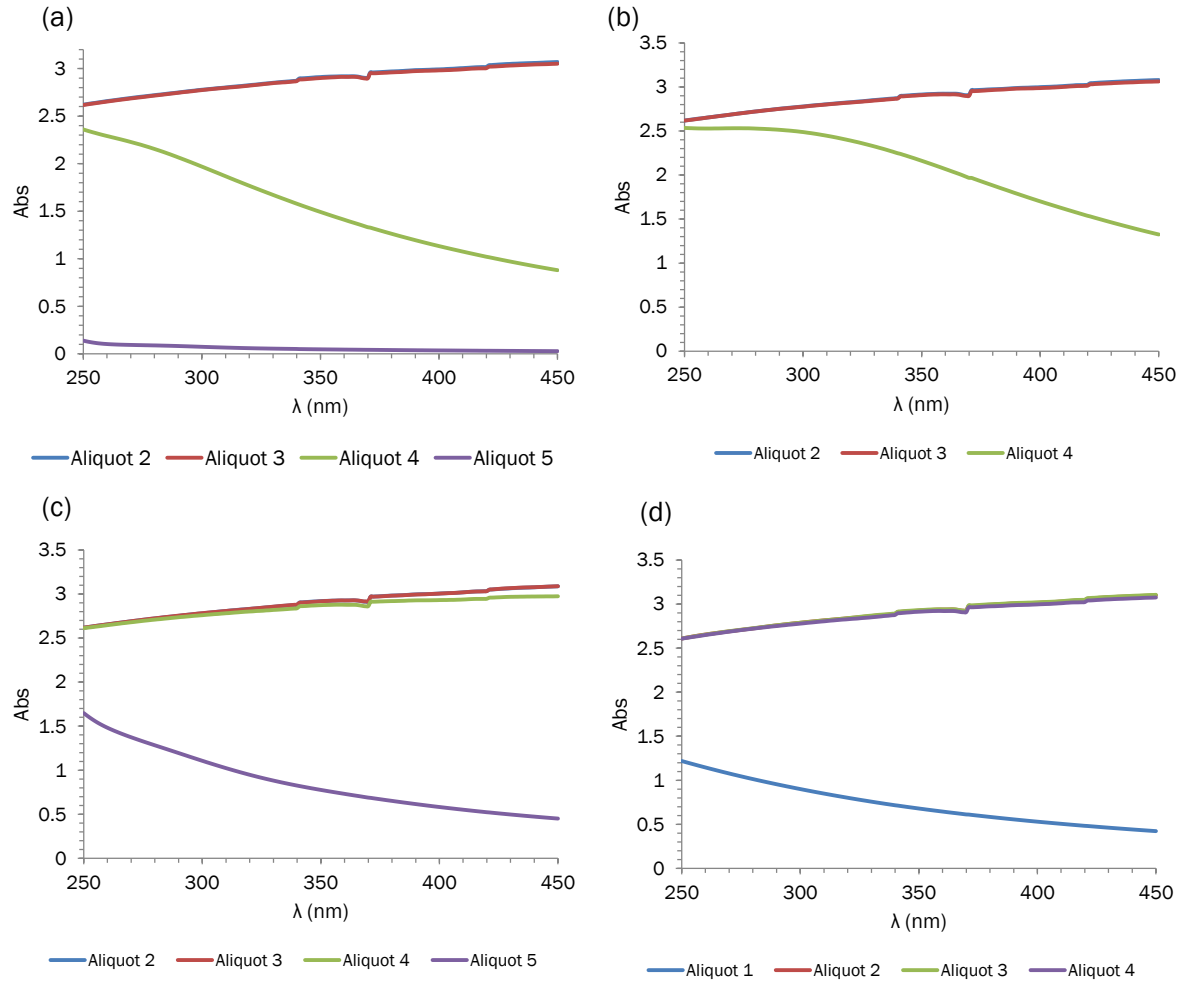

Figure A6. UV-VIS spectra measured for (a) Aliquots 2-5 obtained for the separation of 200 µL of the NLCs formulation NLC-P60, (b) Aliquots 2-4 obtained for the separation of 200 µL of the NLCs formulation NLC-P80, (c) Aliquots 2-5 obtained for the separation of 500 µL of the NLCs formulation NLC-P60, (d) Aliquots 1-4 obtained for the separation of 1 mL of the NLCs formulation NLC-P60 from unincorporated drug (2 mL per aliquot) in a Sephadex G-50 column with a moving phase composed of PBS pH 7.4 buffer. Data points are correspondent to one absorbance measurement for each sample. Some of the presented spectra are partially superimposed due to similarity.

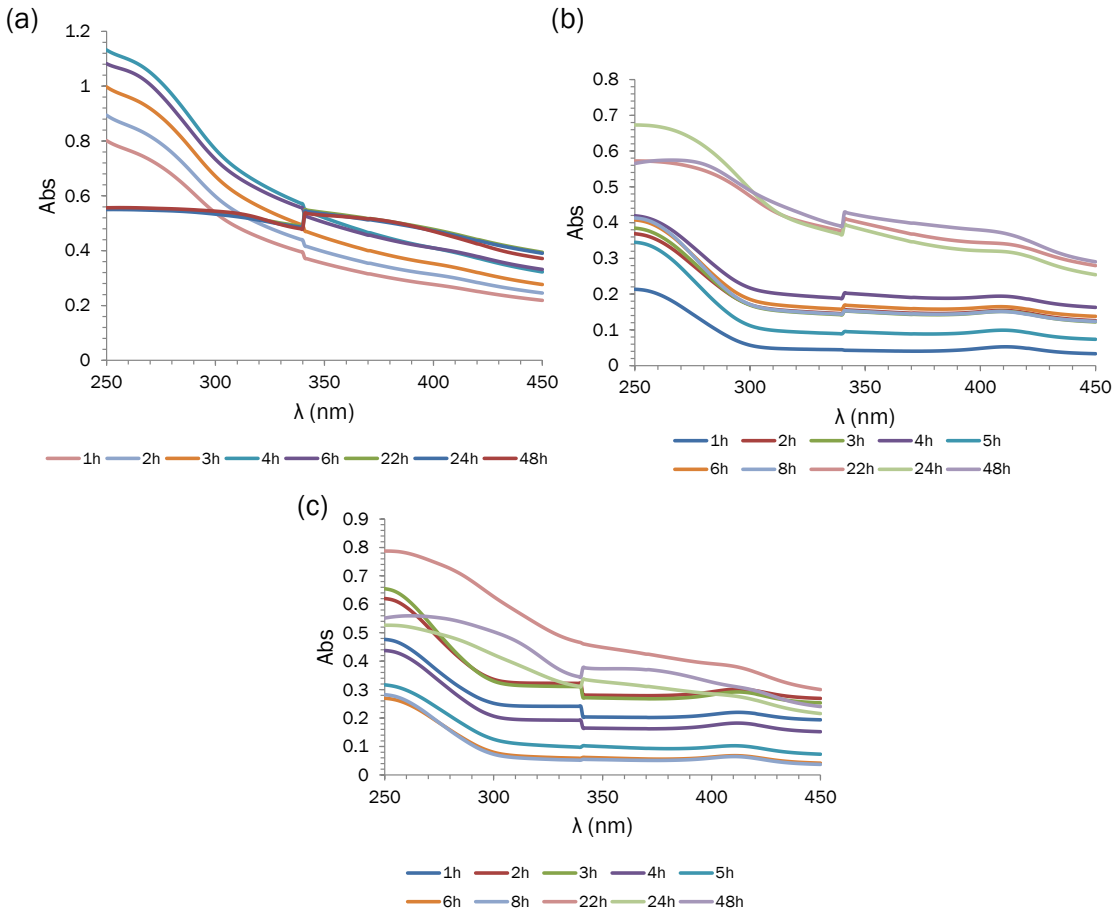

Figure A7. UV-VIS spectra obtained for samples collected overtime for preliminary *in vitro* skin permeation assays performed at 37ºC with donor volume corresponding to (a) MTX-loaded NLCs formulation NLC-P60 containing 300 µg of total MTX (encapsulated and non-encapsulated), (b) volume of the drug-free NLCs formulation NLC-P60 corresponding to the added volume of MTX-loaded formulation NLC-P60 (equivalent in terms of excipient mass) and (c) 300 µg of free MTX in PBS pH 7.4 (1 mg/mL). The receptor medium consisted of PBS pH 7.4 buffer (5 mL). Data points are correspondent to the mean of n=3 absorbance measurements for each sample, with one replicate per assay.